Tissue Engineering Approach To Anterior Cruciate Ligament Reconstruction

GE ZIGANG

NATIONAL UNIVERSITY OF SINGAPORE

2005

Tissue Engineering Approach To Anterior Cruciate Ligament Reconstruction

GE ZIGANG

A THESIS SUBMITTED

FOR THE DEGREE OF Ph.D. OF MEDICAL RESEARCH

DEPARTMENT OF ORTHOPEDIC SURGERY

NATIONAL UNIVERSITY OF SINGAPORE

2005

ACKNOWLEDGEMENTS

I would like to express my sincerest appreciation and gratitude to my supervisors, Associate Professors Goh Cho Hong, James and Professor Lee Eng Hin, for their advice, help, patience and guidance throughout my project.

I would like to express my sincere thanks to my colleagues; it is difficult to imagine that I could have completed this thesis without their continuous support. I also thank them for making my stay enjoyable and fun, their help in many ways, friendship and encouragement: Chong Sue Wee, Tan Boon Kiat, Lee Grace, Tan Jessie, Ouyang Hongwei, Wang Zhuo, Shao Xinxin, Ameer, Chan Julee, Tan Bee Leng, Tan Wei Liang William and Abel Damien Ang.

I would like to thank National University of Singapore for the use of facilities. I would also appreciate the support and understanding from my family, which is crucial for the completion of my PhD study.

Ge Zigang

January 2005

Summary

Anterior cruciate ligament (ACL) injuries may result in significant disability and the poor healing capacity of the ACL has led orthopedic surgeons to perform ACL reconstructions in most of the cases. In current clinical practice, autografts, including the bone-patellar tendon-bone grafts and hamstring tendons, are the most popular and successful surgical replacements for the ACL due to their potential for graft remodeling and integration with bone in the knee joint. Allografts and artificial ligaments have also been used for ACL reconstruction. All these methods have their individual drawbacks, such as donor site morbidity, postoperative pain, deterioration in tensile properties as well as inflammatory reaction. Tissue engineered anterior cruciate ligaments have the potential to overcome these drawbacks by using principles of life science and engineering to provide structural and mechanical support essential for ligament regeneration. The objective of my current research is to evaluate two hypotheses, (1) that knitted biphasic scaffolds can provide enough mechanical strength before ligament regeneration and (2) that mesenchymal stem cells (MSCs) and fascia wrap can promote anterior cruciate ligament regeneration when used on biphasic scaffolds followed by implantation in knee joints. Three stages of experiments were designed, firstly, to select the optimal cell source for ACL tissue engineering from MSCs, anterior cruciate ligament (ACL) fibroblasts and medial collateral ligament (MCL) fibroblasts; secondly, to design and characterize the knitted scaffolds for ACL tissue engineering; and lastly, to test the *in vivo* effects of knitted scaffolds in a rabbit model as well as to evaluate the effects of MSC seeding and fascia wrap application. In the first stage, MSCs, ACL fibroblasts and MCL fibroblasts were compared, with regards to the rate of proliferation, collagen excretion, expression of

collagen type I and III as well as alpha smooth muscle actin. MSCs were found to be a better cell source than the other two regarding proliferation and collagen excretion. In the second stage, biocompatibility, cell adhesion, degradation and mechanical properties of knitted scaffolds were evaluated as potential tissue engineered prostheses. After knitted scaffolds were found to be suitable for this purpose, they were further tested in a rabbit model for ACL reconstruction. Histological assessment was carried out at 4 and 20 weeks post operatively. Furthermore, immunohistochemistry, western blot of collagen type I and III as well as mechanical properties were examined 20 weeks after implantation. Ingrowth of a large amount of fibroblasts was found to surround the knitted scaffolds, which showed little sign of inflammation and foreign body reaction at the 4 and 20 weeks time points. Ligament explants were positively stained with antibodies for collagen type I and III. Tissue engineered ligaments remained intact after 20 weeks' implantation in most of the cases, though maximal loads and stiffness of them were still lower than normal ACL. Both the amount of collagen type I and collagen type III in group III (MSC seeding/fascia wrap) and IV (fascia wrap) were significantly higher than that in group II (MSC seeding), which was much higher than that in group I (scaffold only). Results showed that MSC seeding could promote synthesis of collagen type I and collagen type III, while fascia wraps have even stronger effects than MSC seeding. Both MSC seeding and fascia wrap did not further enhance ultimate tensile load and stiffness. For future work, the use of scaffolds with improved mechanical properties in combination with MSC seeding, fascia wrap, and growth factors may improve ACL reconstructions.

TABLE OF CONTENTS

TABLE OF FIGURES

TABLE OF TABLES

1 INTRODUCTION

The incidence of anterior cruciate ligament (ACL) injuries has increased with increasing popularity in sport activities over the years. The prevalence of anterior cruciate ligament injuries is about 1 per 3,000 Americans [1]. About 200,000 Americans required reconstructive surgery of ligaments in 2002 with total expenditure exceeding five billion dollars [2, 3], with even higher costs incurred in loss of man-hours of work, healthcare and social benefits. Anterior cruciate ligament injuries may result in significant disability and joint dysfunction, which may consequently lead to injury of other tissues, such as the meniscus with subsequent development of degenerative joint disease [4]. The poor healing capacity of the ACL has led orthopedic surgeons to perform ACL reconstructions in most of the cases. In current clinical practice, autografts, including the bone-patellar tendon-bone grafts and hamstring tendons [5], have been the most popular and successful surgical replacements for the ACL for their potential for graft remodeling and integration into the joint [6]. Nevertheless, donor site morbidity is a major concern when utilizing autografts. Autografts are occasionally not available for use for repeat surgery or infection. The use of allograft avoids donor site morbidity, reduces surgical time and minimizes postoperative pain. However, the decrease in tensile properties during sterilization and preservation as well as risk of inflammatory reaction has been a concern [1]. The use of synthetic ligament replacements has gained some popularity in limited conditions in the late 1980s, because they do not involve the sacrifice of autogenous tissues and as such, minimize the associated morbidity and risk of disease transmission. At the same time, they permit a simpler and easier reconstructive technique as well as a more rapid rehabilitation,

as they do not lose their strength during tissue revascularization and reorganization. For artificial ligament prostheses, the results of ACL reconstruction deteriorate with time, due to material degradation, foreign body reaction and related inflammation. Furthermore ACL prostheses that do not induce tissue ingrowths will shield mechanical loading and are prone to fail in the long run, due to synovitis, effusion, arthritis, or mechanical deterioration of the prosthesis [7]. These grafts have yet to display the strength or performance of human tissue, which is another important hurdle for broad usage in clinical practice.

Research for a potential tissue engineered anterior cruciate ligament has been going on for some time, with the hope of overcoming the present problems. This revolutionary approach requires the use of biocompatible and biodegradable scaffolds, which provide structural and mechanical support essential for ligament regeneration. Our two hypotheses for this study are; first, knitted biphasic scaffolds can provide enough mechanical strength before ligament regeneration; second, mesenchymal stem cells (MSC) and fascia wrap can promote anterior cruciate ligament regeneration when used on knitted biphasic scaffolds followed by implantation in the knee joint.

1.1 Anterior cruciate ligament

1.1.1 Knee Anatomy

The knee joint is made of bony structures, cartilage surfaces, meniscus, synovium, capsule, ligaments and surrounding muscles (Fig 1). The knee consists of the distal femur, the proximal tibia and the patella. As the fibula has migrated distally during embryologic

development, it is not part of the joint. The distal femur takes the form of two condyles, which are separated by the intercondylar fossa. The intercondylar fossa is the proximal attachment site for the anterior cruciate ligament and posterior cruciate ligament. Like the distal femur, the proximal tibia consists of two condyles (also known as tibial plateau), the medial condyle and lateral condyle. The meniscus found on the proximal tibia serves as a cushion between tibia and femur. The patella protects the femoral condyles in flexion, transmits force from quadriceps across the femur, and increases stability of the knee [8]. The knee joint is covered by a capsule starting from femur to tibia, some of which becomes the arcuate ligament [8]. Five peripheral ligaments (medial collateral ligament, the posterior oblique ligament, the arcuate-popliteus corner, the lateral collateral ligament and the anterolateral femorotibial ligament), together with the two cruciate ligaments, stabilize the knee passively [9].

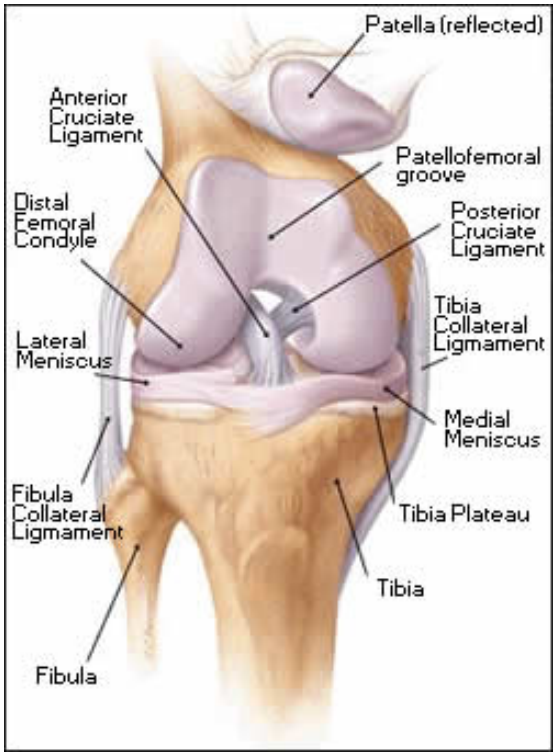

Figure 1 Frontal view of knee joint

(Source: http://www.orthopaedics.co.uk/boc/patients/patella_tendonitis_indications.htm)

1.1.2 ACL anatomy

The cruciate ligaments are parallel bands of regularly oriented, dense connective tissue that connect the femur and tibia. They are surrounded by a mesentery-like fold of synovium that originates from the posterior intercondylar area of the knee and completely envelopes the ligaments. Hence, while the anterior cruciate ligaments are intraarticular, they are also extrasynovial. The ACL starts from a fossa on the posterior aspect of the medial surface of the lateral femoral condyle and terminates at another fossa in front of and lateral to the anterior tibial spine of the tibia (Fig 2) [10]. The cruciate ligaments are attached to the femur and tibia, not as a singular cord but as a collection of individual

fascicles that fan out over a broad flattened area. The ACL is made of two bands, the anoteromedial band and posterolateral bund. The anteromedial band is primarily tight throughout flexion and extension, which makes it even tighter as the knee is flexed. The posterolateral band is tight in extension and becomes quite relaxed as the knee is flexed [11].

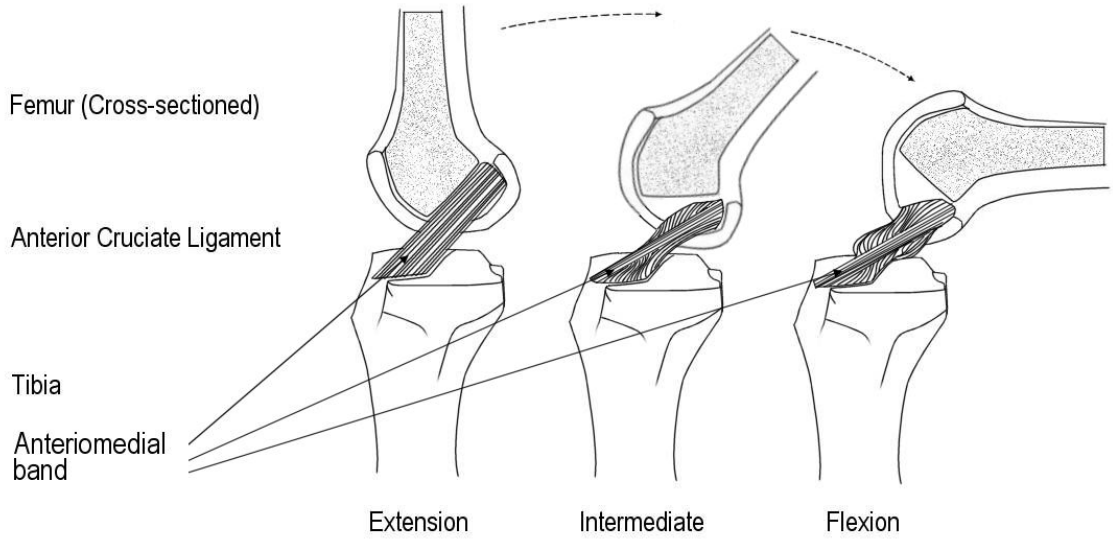

Figure 2 Side view of ACL in flexion and extension

The cruciate ligaments are made up of multiple collagen fascicles [12]. Fibrillar collagen that gives the ligament its high tensile strength is synthesized by fibroblasts. The collagen molecule is a glycine-rich triple helix. They assemble sequentially into microfibrils, subfibrils, and fibrils (20 to 150nm in diameter) before forming fibers (1-20μm in diameter) with cross-links to each others and further make up a subfascicular unit (100-250μm in diameter). These subfascicular units are surrounded by a loose band of connective tissue known as the endotenon. Three to twenty subfasciculi subsequently form a fasciculus, (from 250μm to several millimeters in diameter), which are surrounded

by an epitenon. This interfascicular connective tissue also supports the neurovascular elements of the ligament [13]. These individual fascicles are either oriented in a spiral fashion around the long axis of the ligament or they pass directly from the femur to the tibial attachment. The entire continuum of fascicles is surrounded by the paratenon, a connective tissue cover similar to but much thicker than the epitenon [10]. Fibroblasts also enzymatically break down and remove old collagen as part of a renewal process.

ACLs attach to the femur and tibia via collagen fibers [14]. The abrupt change from flexible ligamentous tissue to rigid bone is mediated by a transitional zone of fibrocartilage and mineralized fibrocartilage. This alteration in microstructure from ligament to bone, allows a gradual change in even distribution of stress [13].

The major blood supply to the ACLs arises from the ligamentous branches of the middle genicular artery as well as some terminal branches of the medial and lateral inferior genicular arteries [15]. ACLs are innervated by branches of the tibial nerve (posterior articular branch of the posterior tibial nerve) [16].

In order to successfully reconstruct an ACL, it is necessary to understand the anatomy, orientation and attachment sites of the normal ligament. In the reconstruction of the ACL, the graft must be positioned so as to minimize the length changes within the ligament, which occurs as the knee is flexed and extended [10].

As ACL fibroblasts do not have unique markers, ligaments have been evaluated on the presence of a combination of factors, such as the extracellular matrix components (collagen I and III, elastin, fibronectin, decorin, and biglycan), relative ratio of collagen type I to type III (6-8 folds), types and amounts of reducible cross-links, cell morphology and ultrastructure of collagen network [3].

1.1.3 ACL Kinematics and Mechanics

The basic movement between the femur and tibia is a combination of rolling and gliding, as well as automatic and voluntary rotation. With the loss of cruciate integrity, as well as combined lesion of three or more of these ligaments, which often happens simultaneously in an injury, complex pathologic instability is inevitable and without surgical intervention disability will probably ensue [9]. A good understanding about kinematics of the cruciate ligaments is essential for surgeons performing the reconstruction.

Fiber recruitment of the cruciate ligaments involves the relative constant tension of the fibers spanning the isometric points and progressive recruiting of the non-isometric bulk of ligament fibers [9]. The fiber crimps in the ACL allow for 7% to 16% of creep prior to permanent deformation and ligament damage. The ACL can withstand cyclic loads of approximately 300 N for about 1.5 million times per year. It is also regularly exposed to tensile forces ranging from 67 N (for ascending stairs) to 630 N (for jogging) [17], while its maximal tensile load is 1,730 N [18]. In general, the Young's modulus value for human anterior cruciate ligament is 111MPa, ultimate tensile strength is at least 38MPa [18], while ultimate mechanical properties of ligaments generally increase during development

and eventually diminish with aging [19]. The maximum strain that a ligament can endure before failure is between 12-15% strains [20].

1.1.4 Current therapies

As mentioned earlier, ruptures of the ACL and associated ligaments will lead to degenerative changes in knee joints. However, it does not mean that all the ACL ruptures have to be reconstructed, as features such as patient age and activity level are quite important. One third of the cruciate lesions are only partial tears, with some of the functional bands of that ligament being left intact. Almost half of the patients with ACL ruptures could be treated adequately by conservative therapies with results equivalent to those obtained by surgical measures. Lifestyle, age, instability and cooperation are to be considered before therapy [21]. Usually isolated and partial lesions of the ACL are amenable to conservative treatment, but total ruptures of the ACL and severe associated injuries within the knee joint should be treated surgically, mainly with ACL reconstruction, with ligament repaired, capsule sutured, and/or broken meniscus removed [11].

In current clinical practice, the most popular and successful surgical replacements for the ACL have been autografts, including the bone-patellar tendon-bone graft [22] and hamstring tendon [5], because of their potential for graft remodeling and integration into the joint [6]. Donor site morbidity is a major concern when utilizing autografts and autografts are occasionally not available for use as a result of repeat surgery or infection. The use of allograft avoids donor site morbidity, shortens surgical time and diminishes

postoperative pain. However, the deterioration in tensile properties with sterilization and preservation as well as risk of inflammatory and disease reaction has been a concern [1].

The use of synthetic ligament replacements had gained some popularity in late 1980's, but in limited conditions only. They do not involve the sacrifice of autogenous tissues and as such minimizes the associated morbidity and risk of disease transmission. At the same time, they permit a simpler, easier reconstructive technique and a more rapid rehabilitation, as they do not lose their strength during tissue revascularization and reorganization. Both braided polytetrafluoroethylene fibers (Gore-Tex) ligament and knitted polyethylene terephthalate (Stryker Dacron) ligament prostheses have received general device releases from the Food and Drug administration (FDA) as permanent prosthetic devices, but they have not been used for a long time [7]. For both Gore-Tex and Dacron ligament prostheses, the results of ACL reconstruction deteriorate with time, due to material degradation, foreign body reaction and related inflammation. Furthermore, ACL prostheses that do not induce tissue ingrowth will shield mechanical loading and are prone to fail in the long run, due to synovitis, effusion, arthritis, or mechanical deterioration of the prosthesis [7]. The Leeds-Keio prosthesis, which is composed of polyester with an open-weave tube to promote fibrous growth, has been popular outside the United States. This device has been shown to host collagenous tissue ingrowths and improves mechanical properties after implantation [7]. The usage of Leeds-Keio prosthesis is limited due to the high incidence of chronic foreign body inflammation, particulate-induced synovitis, some particle shedding into lymph nodes, and complete graft rupture [23]. Of 855 prosthetic ligaments tracked for 15 years, 40%-78% failed owing to wear

debris, tissue reactions, and mechanical limitations [24]. Except for their own drawbacks and subsequent changes after implantation, these grafts have yet to display the strength or performance of human tissue, which is another important hurdle for broad usage in clinical practice (Table 1).

Table 1 Mechanical properties of materials used in ACL reconstruction

	Ultimate Tensile load (N)	Stiffness (N/mm)	Elongation at break (%)	Young's Modulus (MPa)
Human ACL	2160 ± 157 [18]	306 [25] 242 ± 28 [26]	~ 33 [26]	111MPa [18]
Human hamstring graft	3790 – 4140 [25]	776 [25]		
Human patellar-tendon graft		685 ± 86 [26]		
Gore-Tex Prosthesis	5300 [3] 4830 [27]	322 [3]	9	
Dacron	3631	420	18.7	
Kennedy ligament augmentation device	1500 [27]	36 [27]		

1.1.5 Requirements of scaffolds for ACL reconstruction

The ideal scaffolds for ACL reconstruction should meet several requirements

a. Biocompatible and biodegradable
b. Similar initial strength with normal ACL

c. Controlled and gradual mechanical strength loss in degradation with simultaneously increased strength from regenerated tissue
d. Young's modules matched with normal
e. Not to disrupt the potential ACL regeneration

It is a pity that there is no satisfactory prosthesis at present, though much work has been done on it.

1.2 Tissue engineering

1.2.1 Definition

Tissue engineering is an interdisciplinary field that applies principles of engineering and the life sciences toward the development of biological substitutes that restore, maintain, and improve the function of damaged tissues and organs [28]. Since the early 1990s, much development has been achieved in this popular field, especially in tissue-engineered bone, cartilage, liver, kidney, etc. Tissue engineering uses the techniques of cell biology, engineering, materials science and surgery to fabricate new functional tissues using cells and a matrix or scaffold which can be natural, man-made or a composite of both. Tissue engineering has the chance to achieve more progress with the help of newly developed techniques and concepts from many scientific fields, especially cell biology and materials science. Today, a lot of effort has been made to generate new, natural, permanent tissue replacements by creating implantable devices composed of tissue-specific cells on synthetic biodegradable polymer scaffolds [29].

1.2.2 Functional Tissue Engineering

The ideal matrix should essentially be biocompatible, and is completely absorbable while leaving behind a totally natural tissue replacement following degradation of the polymer [30]{Guilak, 2002 512 /id}. Furthermore, the matrix should be easily and reliably reproduced into a variety of shapes and structures that retain its shape when implanted. As a vehicle for cell delivery, the matrix should provide mechanical support for a duration so as to maintain a space for tissue to form [29].

Tissue engineering often uses cells, biomaterial scaffolds, biochemical and physical regulatory signals in various ways to engineer tissues *in vitro* and *in vivo*. The most often used strategy is to mimic the *in vivo* normal healing process or embryonic process to fabricate a new tissue [3]. The essential components are the presence of reparative cells, a structural template, facilitated transport of nutrients and metabolites, a provision of molecular and mechanical regulatory factors. An envisioned scenario of clinically relevant tissue engineering involves the use of autologous cells, biodegradable scaffolds (Designed to serve as a temporary structural and logistic template of tissue development) and bioreactors (designed to control the cellular environment) [3].

1.2.3 Progresses and challenges in tissue engineering

In recent years there has been remarkable progress in tissue engineering, not only in regeneration of nerve [31], liver, myocardium, pancreas, bone, cartilage, skin and laminin as well as myocardial revascularization, but also in the understanding of biological principles, such as cell division, cytology, metabolism, stem cells and even in human

cloning [31]. Research on biodegradable prostheses for ACL ligament reconstruction has been going on for some time, with the hope of overcoming the present problems. Most of them have been with the use of biological and synthetic polymers which are biocompatible and degradable. Though there are many reports on tissue engineered ACLs, only a few of them have been used *in vivo* for ACL reconstruction (Table 2). Collagen and polylactic acid (PLA) are the most often used. Fibroin (silk) ACL scaffold have shown promising results [26], but no further *in vivo* test has been reported. Conceptually *in vitro* cultured tissue engineered ligament with two bone ends would be ideal, as what has been reported [32], but there is little further progress reported.

Table 2 In Vivo studies of tissue engineered ACLs

	Materials	Structure	In Vivo model /duration	Ultimate Tensile load (% normal)	Ultimate Tensile strength (% normal)	Author/year of publication
Biological polymers	Collagen fiber	Cross-linked	Rabbit 20w	32N (12.7%)	10MPa (20.4%)	Dunn, M.G. 1992 [33]
	Collagen fiber	PLA matrix	Rabbit 4w	40N	13MPa (34.2%)	Dunn, M.G. 1995 [34]
	Collagen matrix from bone	Block	Goat 1 year	474N (18.7%)	49MPa (28.7%)	Jackson, D.W. 1996 [35]
	Collagen fiber	Braided /Cross-linked	Goat 6m	102N (6.9%)		Chvapil, M. 1992 [36]
Synthetic polymers	PLLA fiber	Braided	Sheep 48w	175N (12.3%) 295N (20.7%, fascia wrap)		Laitinen, O. 1993 [37]

In general, progress in ligament tissue engineering has been rather slow. This can be attributed to several factors: 1) ACLs have to undergo complex and multidirectional mechanical forces *in-situ*, to date no scaffold has been reported to be able to reconstruct ACL to handle similar mechanical loadings *in vivo*; 2) following ACL rupture the blood supply will be disrupted, this will impede the regeneration of ACLs; 3) the transitional fibrocartilage zone between bone and ligament poses a great challenge to reconstitute with current techniques; 4) significant changes of cytokine profiles after ACL injuries could lead to the difficulties in ACL regeneration [38]; 5) inability in current tissue engineering techniques to restore the stretch-sensitive mechanoreceptors in ACL that trigger muscle contractions that protect the knee from extremes of motion [39].

Currently, most of all attention is paid to the first difficulty mentioned above, i.e. to improve the mechanical properties of scaffolds to match that of the ACL. Except for biocompatibility, there are several technical hurdles to overcome before we can get scaffolds with good mechanical properties:

a. initial mechanical properties of scaffolds should match to ACL, in terms of ultimate tensile load and strength, linear stiffness, visco-elasticity, Young's modulus, etc.
b. TE ACL structures should withstand multi-directional stresses without deforming *in vivo*, while *in vitro* tests only evaluate the tissues along the direction of loading.
c. The mechanical properties of scaffolds will change dramatically with enlarged cross-section area after tissue ingrowth and material degradation in a way not well controlled.

d. Mechanics of tissue engineered ACLs often drops before mass degradation and leads to quick loss of initial properties
e. Creeping (Visco-elasticity) is common for polymers and textile structures, which would lead to laxity of scaffolds and loss of their initial functionality.

1.2.4 Cell sources

1.2.4.1 Selection of cell sources for ligament reconstructions

As mentioned earlier, cells are essential to fabricate tissues *in vitro* and *in vivo*. The potential cell sources for use in the development of a tissue engineered anterior cruciate ligament are as follows: ACL fibroblasts, medial collateral ligament (MCL) fibroblasts [40], mesenchymal stem cells (MSCs) and embryonic stem cells (ESC). While the ethical debate on embryonic stem cells continues [41], the use of ESCs still harbors unresolved issues, such as animal feeder layers, potential for uncontrolled differentiation and difficulty in *in vitro* expansion has restricted their use in tissue engineering applications [42]. On the other hand, adult MSCs and other tissue-specific stem cells are present in large quantities in the human body; hence, there are lesser ethical and technical issues involved. Apart from that they have the potential to differentiate into a variety of mesenchymal cell phenotypes, including osteoblasts, chondroblasts, myoblasts and fibroblasts [43]. MSCs can also be easily obtained just by a simple aspiration procedure of the iliac crests, followed by in vitro expansion to large quantities [44, 45]. MSCs have been successfully used to promote the repair of a number of tissues, including tendon [46], bone [47] and possibly muscle [48]. Woo et al (1999) reported that MSCs can promote ligament regeneration and as such play an active role in ACL regeneration [49].

Ligament healing may be accelerated secondary to the cellular interaction between local tissue host cells and donor cells, while extracellular matrix is being excreted [50]. To our knowledge, there is little published data comparing these three cell types, which are of fundamental importance to tissue engineering applications. Previous studies on these three types have been based on different species at different ages, cultured with different protocols and as such it would be very difficult to compare the results. In this current study, it is important to compare the three cells types harvested from the same donors, prior to usage in tissue engineering studies. The objective of the current study was to evaluate the rate of cell proliferation and collagen expression of ACL fibroblasts, MCL fibroblasts and MSCs. Subsequently, after the identification of the optimal cell source, the goal was to examine its role as a donor cell and its survivability in the knee joint, particularly in an anterior cruciate ligament construct. The longer the donor cells are able to survive, the more effective it would be in contributing to tissue repair and regeneration.

1.2.4.2 Mesenchymal stem cells (MSCs)

Mesenchymal stem cells are a group of pluripotent progenitor cells in the embryo whose progeny eventually gives rise to skeletal tissues: cartilage, bone, tendon, ligament, marrow stroma and connective tissue [51]. Unmanipulated bone marrow contains mixtures of mesenchymal progenitors, some possessing an unrestricted potential for mesenchymal differentiation with others showing commitment to one or perhaps two lineages. Both intrinsic and extrinsic factors control their developmental pathways to different mesenchymal tissues. MSCs also exist broadly in adult mesenchymal tissues, such as bone

marrow, periosteum, fat, muscle, etc [52]. Bone marrow derived MSCs were initially isolated by their adhesive properties to tissue culture surfaces [53] and since then, many protocols on isolation and purification have been proposed [54]. Mesenchymal stem cells used in tissue engineering are usually groups of heterogeneous cells, with different morphologies, proliferation rates, and differentiation abilities [55-57]. As there are lots of concerns about the use of embryonic stem cells (ESCs) in both clinical practice and research [41], the use of MSCs could effectively circumvent the current ethical concerns about human embryo research. Another advantage of the use of MSCs over ESCs is that MSCs could only differentiate into mesenchymal lineages, thus minimizing the concerns about unclear pathways and uncontrolled endpoints with ESCs, though there is still a controversy about the possibility for MSCs to cross lineage boundaries [58].

1.2.4.3 Allogeneic VS autologous

Main considerations of cell seeding are seeding efficiency, convenience, immunological response and potential future human application. While there is no report about seeding efficiency between allogeneic and autologous cell seeding, allogeneic cell seeding is more convenient than autologous seeding. For potential future application, allogeneic cell seeding could provide a more abundant source of younger cells with shorter preparation times. Bone marrow mesenchymal stem cells also incur little immuno-response by inhibiting the response of naive and memory antigen-specific T cells to their cognate peptide [59]. Some clinical applications have been reported without immunological response [60]. In general, allogeneic MSC seeding is preferred.

1.2.5 Materials for tissue engineering

1.2.5.1 Requirement for tissue engineering

Tissue engineering generally requires the use of a porous biodegradable scaffolds, which serve as three-dimensional templates for initial cell attachment and subsequent tissue formation both in vitro and in vivo [29]. The biodegradability of the scaffolds allows them to be totally replaced by new synthesized functional tissues. Ideal scaffolds used in tissue engineering should meet five requirements: (i) high porosity and optimal pore sizes with interconnection among individual pores for cell growth and transmission of nutrients and metabolic waste; (ii) biocompatible and biodegradable with controlled degradation mode and rate to match tissue regeneration; (iii) suitable surface properties for cell adhesion, proliferation, and differentiation, as well as extracellular matrix maturity: (iv) mechanical properties to match target tissues; (v) ease of processing into various shapes and sizes by solid free form fabrication [61].

1.2.5.2 Biological polymer

Materials which could meet the requirements mentioned above are mainly from polymer, either natural or synthetic. Much attention has been paid to biological polymers in the past decades, including collagen, silk, polysaccharides, such as alginate, agarose, chitin/chitosan, hyaluronan, etc.

1.2.5.2.1 Collagen

Collagen forms the most substantial group of structural proteins in connective tissues and represents about one third of total body proteins with more than 27 sub-types [62]. Collagen is made of highly repetitive triple helices leading to significant homogeneity in secondary structure. So far, collagen is the most intensely studied biological polymer with potential biomedical usage [63]. Since collagen accounts for more than 80% of the dry weight of a normal ligament [64, 65], it is reasonable to reconstruct ACL with it. There are many reports on ACL reconstruction and tendon repair with collagen-based constructs [35, 66, 67]. In general, collagen used in laboratories is derived from the bovine submucosa and intestine [63, 65], as well as mouse tails in small quantities. Naturally derived collagen has to be processed so as to improve its mechanical strength and to slow down the degradation rate by cross-linking and the removal of antigenic response. Chemical cross-linking is often used, including immersion in aldehyde solution and chromium trioxide [63, 65]. Collagen is degraded mainly by lysosomal enzymes [68] while collagenase also participates to some extent [63]. The pure triple helical collagen molecule does not elicit a strong antigenic response when compared with associated cellular debris, ground substance, or the associated nonhelical telopeptide region of the collagen molecule [63]. Many methods have been reported to dissociate, purify and reconstitute collagen to achieve this aim [69, 70]. Gelatin is a degradation product of collagen and has similar properties with collagen. In general, good biocompatibility and ease of processing are advantages, while low mechanical strength, shrinkage, possibility of pathogen transfer and batch to batch variation are disadvantages.

1.2.5.2.2 Silk

Silks are generally defined as protein polymers that are spun into fibers by silkworms, as well as spiders, scorpions, mites and even flies. Silks from different sources have different amino acid composition and mechanical properties. Similar to collagen with repeated triple helices, silk is characterized by a highly repetitive β-sheet that leads to significant homogeneity in secondary structure [71]. Silk from *B. mori* silkworm is the largest and most stable source that has been commercialized for a long time. Silk comprises of a fibroin core and a glue-like sericin cover. Unique mechanical properties, as well as biocompatibility, slow degradation time and options for genetic control, make it suitable for ligament tissue engineering [72]. The extraordinatory mechanical properties and enhanced environmental stability of silk fibers are due to the high homogeneity in secondary structure (β-sheet), extensive hydrogen bonding, the hydrophobic nature of much of the protein, and the crystallinity. Silk undergoes proteolytic degradation at a variable rate dependent on the environmental conditions. Silk fibers lose the majority of their tensile strength within 1 year in vivo, and fail to be recognized in 2 years [73-75]. Encouraging results from silk-based ACL tissue engineering constructs have been reported [76]. Usually the glue-like sericin in silk is the major cause of adverse problems with biocompatibility and hypersensitivity [77-79]. Though many successful clinical applications have been reported, it is still difficult to assess the biological responses with the absence of detailed characterization of the fibers used including the extent of extraction of the sericin, the chemical nature of wax-like coatings and related processing factors.

1.2.5.2.3 Polysaccharides

Polysaccharides are polymers of monosaccharide units. The monomers of a polysaccharide are usually all the same (called homopolysaccharides), though there are exceptions (called heteropolysaccharides). In some cases, the monomeric units are modified monosaccharides. Polysaccharides differ in the composition of the monomeric unit, the linkages between them, and the ways in which branches from the chains occur. Except for the demand from tissue engineering for new scaffolds materials with controllable biological activity and different degradation kinetics factors, two other factors have contributed to growing usage of polysaccharide based tissue engineering scaffolds [80]: first is the large information on the critical role of saccharide moieties in cell signaling schemes and in the area of immune recognition; second has been the recent development of new synthetic techniques with the potential for automated synthesis of biologically active oligosaccharides, which may eventually allow us to decode and exploit the language of oligosaccharide signaling [63]. Polysaccharides could form gels with hydrogen-bond and/or iron through a number of mechanisms influenced by the monosaccharides as well as the presence and nature of substitute groups. The gel forming abilities also contribute to their growing tissue engineering applications.

1.2.5.2.4 Alginate

Alginate, a polysaccharide, produced from seaweed in 1940, is a product of a neutralizing reaction between alginic acid and caustic soda [81]. Calcium, sodium, and ammonium alginates have long been used as foams, clots or gauzes for absorbable surgical dressings, however, impuries of alginate have been a pertinent hurdle related to biocompatibility.

Despite a handful of purification procedures including filtration, precipitation and extraction have effectively removed most of impurities [82], the duration of graft function and the fibrous tissue overgrowth are two main concerns for further applications [83].

1.2.5.2.5 Agarose

Agarose, a polysaccharide composed of alternating units of galactopyranosyl and 3,6-anhydrogalactopyranosyl units, is created by purifying agar. When heated and cooled, it forms a gel that is used as a support for many types of electrophoresis and immuno-diffusion. It is porous and solid in different grades. Its gel forming ability has been well used to entrap tissue engineering endocrine cells and cell injection [84]. Agarose has also been used to study the effects of dynamics on cells, mainly on chondrocyte culture [85, 86], but the Young's modulus usually are not good enough for ligament tissue engineering [87-89].

1.2.5.2.6 Chitin

Chitin, poly [ß- (1–4)-2-acetamido-2-deoxy-D-glucopyranose], is one of the most abundant natural polymers. It occurs in animals, particularly in crustacea, molluscs and insects as an important constituent of the exoskeleton and in certain fungi as the principal fibrillar polymer in the cell wall [90]. The main sources of material for the laboratory preparation of chitin are the exoskeletons from various crustacea, principally crab and shrimp. Various procedures have been adopted to remove the impurities in raw chitins and no standard process has been developed. HCl is most frequently used for demineralization

while NaOH is for deproteinization. However, other methods can be used and the order in which these two steps are carried out has varied between different works, although in most instances, deproteinization has been carried out prior to demineralization.

Currently, chitin has a diverse usage in health care, particularly, in wound care [91], cartilage tissue engineering [92], bone tissue engineering [93] and drug delivery [94]. Chitin sutures have been reported biocompatible [95, 96] and lost 45% of its tensile strength by 14 days [97]. When braided chitin scaffolds were used for tendon repair, they lost their tensile strength more rapidly than those from poly-caprolactone and Poly-lactic acid [98].

1.2.5.2.7 Chitosan

Chitosan, a derivative of chitin, is obtained by the partial deacetylation of chitin. Chitosan comprises a series of polymers varying in their degree of deacetylation, molecular weight, viscosity, pKa etc. It has been widely used in wound dressing [99], controlled release of drugs [100-102], nerve regeneration [103], disc regeneration [104], bone tissue engineering [105], cartilage tissue engineering [106-108] and skin tissue engineering [109]. Chitosan fiber could be made by wet-spinning process, but no mechanical properties has been reported [110].

1.2.5.2.8 Hyaluronan

Hyaluronan (HA), also known as hyaluronic acid, is a polysaccharide of the extra cellular matrix (ECM). As a glycosaminoglycan (GAG), it has many structural, rheological, physiological and biological functions in the body, and is well distributed in various soft tissues [63]. Hyaluronan forms highly viscous solutions in water and interacts with binding proteins, proteoglycans and growth factors, while actively contributing to the regulation of the water balance, acting on the osmotic pressure and low resistance and selectively sieving the diffusion of plasma and matrix proteins. Due to its good biocompatibility and controlled biodegradability [80], hyaluronan has been used in joint surgery, corneal transplantation, cataract treatment, wound healing and angiogenesis. It has been well used in cartilage tissue engineering [111, 112], osteochondral defects repair [113] and cell-carrying medium [114]. However, water solubility and rapid in vivo degradation are disadvantages in making HA a potential material for ligament tissue engineering. Though several attempts have been made to fabricate a scaffold material with sufficient physical properties by cross-linking and coupling reactions, potential toxicity of some cross-linking agents, including gluteraldehyde, formaldehyde and isocyanates, continues to restrict its usage [63].

1.2.5.3 Synthetic polymer

For non-naturals, polymers in the group of polyesters, the family of polylactic acid (PLA), polyglycolic acid (PGA), polycaprolactone (PCL) and copolymers of lactic and glycolic acids (PLGA) could fulfill the criteria mentioned earlier to certain extent, including biocompatibility, processibility and controlled degradation [29]. Synthetic polymers also offer several advantages over natural polymers. Their chemical and physical properties,

including scaffold shape and porosity, degradation rate, cell adhesion ability and mechanical properties are easily modified by the processing and chemical modification. It leads to broad usages in recent tissue engineering [115].

1.2.5.3.1 Poly-glycolic acid (PGA)

PGA is highly crystalline, hydrophilic, linear aliphatic polyester with a high melting point (210ºC at a molecular weight of 50,000) and a relatively low solubility in most common organic solvents [116]. PGA degrades through hydrolysis and the degradation rate of PGA depends on the crystallinity, which is usually between 46-52% [117]. It usually loses most of its mechanical strength over the first 2-4 weeks of degradation in a fluid with pH 7, at 37ºC in vitro [118]. Though there are a lot of reports on application of PGA in tissue engineering [119, 120], it has seldom been used directly in vivo due to limitation such as mechanical strength and quick degradation. It was usually used either as a scaffold for in vitro 3-D cell culture before implantation [120], or used as a template for further modification [121].

1.2.5.3.2 Poly-lactic acid (PLA)

PLA is also a polyester and is more hydrophobic and amorphous than PGA, with an increased solubility to organic solvents compared to PGA [116]. Due to an extra methyl group compared with PGA, PLA usually has two isoform, L- and D- forms, while L-form PLA, also known as PLLA, is most often found. PLLA has a lower melting point than PGA (159ºC at a molecular weight of 100,000). It degrades into lactic acid by de-

esterification and degrades completely within a period of between 10 months to 4 years depending on its molecular weight, crystallinity, shape and implantation site [116, 119]. PLA has been widely used in cartilage tissue engineering [122, 123], bone tissue engineering [124], controlled release of growth factors [125], as well as ligament reconstruction [37, 126]. Due to its mechanical properties, it has also been used in combination with other polymers, as reinforcement or as modification reagent for other polymers [127, 128].

1.2.5.3.3 Poly-caprolactone (PCL)

Polycaprolactone is a biodegradable thermoplastic polymer derived from the chemical synthesis of crude oil. As a semicrystalline polymer, its crystallinity tends to decrease with increasing molecular weight. Its high solubility in organic solvents, low melting point (59-64ºC), slow degradation rate and exceptional ability to formulate blends have lead to many biomedical applications, such as drug delivery [129], cartilage tissue engineering [130, 131] and bone tissue engineering [132, 133]. PCL sutures were reported to keep 90% of original strength after 18 weeks' implantation [134]. It has also been used in fabrication of potential ACL prosthesis [135]. Unfortunately, there is no subsequent report on in vivo experiments.

1.2.5.3.4 Co-polymers

Copolymer is a polymer consisting of two or more different monomers. Copolymers of polyesters are currently often used in tissue engineering, such as PLGA (copolymer of

PGA and PLA at different ratios), tricalcium phosphate and poly (l-lactide-co-glycolide-co -caprolactone) composites [133], poly(epsilon-caprolactone)-silica sol-gels [136] and hydroxyapatite/poly(epsilon-caprolactone) composite [137] for bone tissue engineering, since advantages or properties from different polymers could be effectively combined to achieve the specially designed purposes. Sometimes, surface modification of one polymer with another polymer could be done to achieve a special aim, to improve mechanical properties, or to improve cell adherence [138-140].

1.2.5.4 Biocompatibility and Degradation

Biocompatibility, defined as "acceptance of an artificial implant by the surrounding biological tissue and by the body as a whole" [141], is an important factor for all implantable biomaterials. In vitro characterization of materials and the functional performance of prototypes are usually prerequisites that must be met successfully, prior to evaluation of their biocompatibility [142]. Though PLLA and PGLA have long been regarded as biocompatible biomaterials, the knitted scaffolds made of these biomaterials have to be tested again due to potential contamination during fiber production and knitting procedure.

Controlled degradation of biomaterials in tissue engineered constructs is important and difficult to achieve. An ideal tissue engineered composite should maintain a stable mechanical strength matching the original target tissue while degrading. In other words, increased mechanical strength from regenerated tissue should make up the loss of mechanical strength caused by degradation of biomaterials (Fig 3) [61]. Though there is

more knowledge about degradation mechanisms of different biomaterials, most of them are based on in vitro degradation or in vivo muscle implantation. From our experience, even the same material undergoes different degradation rates when implanted in knee joints, bone tunnels or onto periosteums. In addition, differences in composition, molecular weight, crystallinity, mechanical stimulus and processing of biomaterials will also add more variation to the degradation rate.

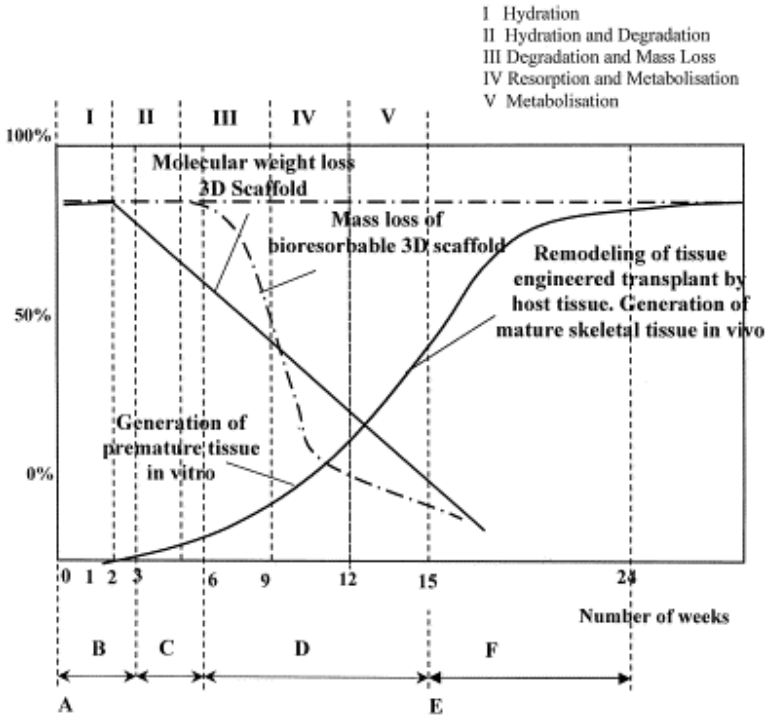

Figure 3 Degradation of polymer

Graphical illustration of the complex interdependence of molecular weight loss and mass loss of a 3D scaffold matrix plotted against the time frame for tissue engineering a cartilage/bone transplant [61].

(A) Fabrication of bioresorbable scaffold;

(B) Seeding of the osteoblast/cartilage populations into the polymeric scaffold in a static culture (petri dish);

(C) growth of premature tissue in a dynamic environment (spinner flask);

(D) growth of mature tissue in a physiologic environment (bioreactor);

(E) surgical transplantation;

(F) tissue-engineered transplant assimilation/remodeling.

1.2.5.5 Cell- surface interactions

As both cells and materials are essential components in ligament tissue engineering, the interactions between them are important. Materials could affect cell adhesion, proliferation and differentiation [127, 140] while cell adhesion and subsequent functionality also affect properties of surrounding materials. The cells include potential seeding cells, regenerative cells as well as inflammatory cells, such as macrophages, lymphocytes, neutrophils, etc. As ligament fibroblasts and their precursors have to attach before being functional, cell attachment is an important stage. Usually cells adhere to the material surface either by direct adhesion or by pre-absorbed proteins [143].

In direct adhesion, cells first attach to a surface by pseudopodial extensions and then form focal contacts while they probe the surface for protein ligands [144]. The physical properties of cell adhesion are governed by both non-specific and specific interactions. Specific interactions refer to receptor-ligand bond formation, while non-specific interactions include electrostatic forces, steric stabilization and Van Der Waal's forces. According to the fluid-mosaic model, the surface of an animal cell comprises a lipid bilayer composed of phospholipids, cholesterol and glycolipids [145]. Four major superfamilies of adhesion receptors have been identified in animal cells, including integrins, cadherins, immunoglobulins and the selectins. Among them, integrins are the most well studied and play an important role in cell-material interactions. Many integrin receptors recognize the specific peptide sequence Arg-gly-Asp (RGD), which is present in many adhesive proteins such as fibronectin, fibrinogen and vitronectin [146]. As transmembrane proteins, integrins are found to be involved in adhesion by linking

extracellular matrix proteins to the cytoskeleton. RGD peptide sequences have been immobilized onto synthetic surfaces to promote cell adhesion in a similar manner to fibronectin [147]. Some factors also affect cell adhesion, especially non-specific interactions, including temperature, medium concentration, small ion concentration and pH value of the surrounding medium, etc.

On the other hand, cells also attach to materials through proteins which have been absorbed to material surface. Proteins contain regions of differing polarity, charge and hydrophilicity. The precise structures are not only determined by the specific amino acid sequence, but also by the secondary and tertiary structure that determines the conformation of the molecule, the distribution and orientation of the side groups. When a protein solution comes in contact with another phase, there is a tendency for the protein molecules to accumulate at the interface [143]. As nearly all interactions between mammalian cells and artificial surfaces are mediated by a layer of adsorbed protein [148], many proteins have been coated on surfaces of target materials when adhesion or improved biocompatibility is expected, for examples, fibrinogen [149], collagen [150], hyaluronan [151, 152], etc.

1.2.5.6 Structures

As we know that the ACL is a load-bearing tissue, which plays an important role in providing stability during the movement of the joints, e.g. extension and flexion. From a mechanical point of view, the ACL is an anisotropic structure which mainly bears the extension force in its axial direction. To restore ACL function, the ACL reconstruction

should functionally mimic all the characteristics of a normal ACL in terms of strength, compliance, elasticity, and durability without any side effects. Therefore, the mechanical properties of the ACL scaffold are of critical importance during regeneration or remodeling.

Anatomically, the ACL is comprised of bands of dense collagen fibers. A fiber is a simple element of anisotropic structure. All the ACL scaffolds and synthetic prostheses are practically composed of fibers. The differences are the way to organize the fibers, i.e. their textile structures. Parallel structure is the simplest way to organize the fibers. However, the lack of interaction between fibers restricts its application. Twisting fiber bundles is an elegant way to solve the problem [26]. Twisting grafts are morphologically closer copies of the normal ACL and can eventually reduce and fine-tune the peak forces in extension [153]. Due the complexity of the ACL mechanical environment, researchers are keen to adopt more complex textile structures in ACL reconstruction, including all four textile categories: woven, non-woven, knitted and braided.

The properties of textile grafts depend on the characteristics of the constituent yarns or fibers and on the geometry of the formed structure. In general, grafts that are braided are usually dimensionally very stable, but less extensible and porous than the other structures. A good example is the Gore-Tex ligament prosthesis composed of braided bundles of polytetrafluroethylene (PTFE) [27]. This graft has high strength and fatigue life, but limited tissue ingrowth due to the low porosity [3]. However, the pore size of the braided structures can be regulated by yarn bundle size and braiding angles [154]. Compared with

braided fabrics, knitted structures are highly porous, which supports tissue ingrowth. It has been reported that the Dacron's knitted construction promotes good ingrowth of fibrous tissue [155]. Textile materials for tissue engineering applications typically have specific performance requirements relating to porosity and mechanical properties.

Porosity

It is known that a highly porous scaffold is desirable to allow cell seeding or migration throughout the materials. Pore size is important for tissue ingrowth and determines the internal surface area available for cell attachment. A large surface area is required so that a large number of cells, sufficient to replace or restore organ function, can be cultured [156]. The fabric structures are hierarchically opened porous structures. Their pore porosities can be considered from three aspects [157]. One is the open space inside created by the loops for a knitted fabric or the pores between yarns in other fabric structures, which may range from tens to hundreds of microns. The other is the distance between filaments or fibers, which is about a few microns. A third kind of porosity can be induced by the method of assembling the fabrics by folding, rolling, etc.

Mechanical properties

The mechanical properties of the scaffold are often of critical importance especially when regenerating tissues such as ligament, tendon, cartilage and bone. The ideal artificial ACL perfectly mimics all the characteristics of a normal ACL in terms of strength, compliance, elasticity, and durability without any side effects. Unfortunately, none of the synthetic grafts have met the qualifications needed for a lasting ACL substitute (Table 3). Usually,

synthetic grafts are too rigid and begin to fragment gradually due to repeated cycling of the knee and probably some chafing at the edges of the bone tunnels, which leads to particles of prosthetic materials shedding and distributing throughout the joints, even occasionally spreading into the lymphatic system.

Table 3 Properties of textile structures

	Woven	Knitted	Braided	Nonwoven
Composition[158]	Yarn	Yarn	Yarn	Fiber
Formation [158]	Interlace	Interloop	Interwine	Bond or entangled
Geometry [158]	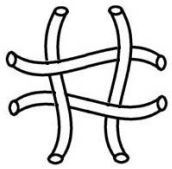			
Cell model [158]	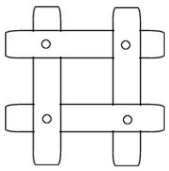	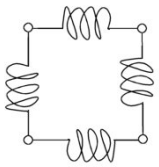	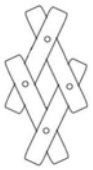	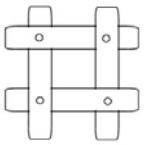
Mobility [158]	Limited	Tremendous	Limited	Very slight
Porosity	High	Very high	High	High
Examples	Leeds-Keio PET graft [159, 160]	Stryker-Dacron PET graft [161-163] Biodegradable scaffold [164]	Gore-Tex PTFE graft [27, 161, 165] Biodegradable scaffold [166, 167]	Fiber bonding [168] Electrospinning [166, 169]

Regardless of their initial mechanical properties, a loss of them occurs after transplantation due to the processes of ischemic necrosis and remodeling. Strength and stiffness of the grafts are also lowered by adding fixation [25].

If the stiffness of the implant greatly exceeds that of the ingrown host tissue, the implant will bear most of the mechanical load and the load-deprived host tissue will not remodel or mature. To address this problem of stress-shielding, a ligament augmentation device

(LAD) is needed to protect biological grafts from high loads in the early postoperative period, in addition to being used as a permanent prostheses [170]. The Kennedy LAD was a braided polypropylene yarn attached to bone on only one end of the autogenous repair. Due to the low stiffness of the device, stress-shielding of the graft is reduced, thus normal neoligament remodeling should occur [27]. However, long-term maintenance of the mechanical properties of the device is not necessary or even desirable. Therefore, an ideal ligament augmentation device should be biodegradable, gradually transferring mechanical loads completely to the biological graft. The tissue engineering approach provides optimism by using biodegradable scaffolds combined with appropriate cell sources to create mechanically and biologically functional substitutes. In contrast to the permanent synthetic prostheses losing strength with time, the mechanical behavior of the tissue engineering grafts should improve with time due to neoligament tissue development and remodeling [27].

1.2.6 Regeneration and functionalilty

As dense and well organized connective tissue, ligament attributes much of its function to its specific structures, cross-linked collagen bundles and crimps [12]. Though there are no unique cell markers for ACL, it still can be evaluated and distinguished by its specific expression of different factors and their relative ratios [3],

- Specific expression of extracellular matrix components of collagen types I, III, V and their ratios, for example, collagen amount: 80.3mg collagen/g dry tissue and ratio of collagen types I and III, 7.3 (both lower than tendon) [171]

- Different type and higher amount of reducible cross-links compared with MCL and tendon [172]
- Different cell morphology and function with distinct regions [171]
- Special ultrastructure of collagen network (collagen pattern, collagen fibril diameter) [172]
- Higher metabolical rate than tendons [171]
- Specific expression of ground substances, elastin, fibronectin, decorin, and biglycan,
- Specific expression of glycoaminoglycans (GAG), such as hyaluronic acid, chondroitin sulfate [172]
- Furthermore, the composition of individual component changes in regeneration, while some of them promote functionality and the others may not or impede it [173].

All these characteristics could give clues for future scaffolds for ligament tissue engineering.

As degradation of scaffolds is inevitable, it is important to promote rapid functionality of regenerated collagen fibers. Except for seeding cells, enhancing the growth factors which have been implicated in regeneration, have all shown promise [174]. Blocking decorin formation by antisense gene therapy could increase diameter and maximal tensile strength of regenerated ligament [173]. Blocking Collagen V formation may have a similar positive effect [175]. Scaffolds carrying antisense gene therapy could be helpful.

Collagen fibers and "crimp-like structures" with different maturities have been reported after ACL reconstruction with tissue engineered ligaments, for examples, from carbodiimide but not glutaraldehyde cross-linked collagen fibers after 20 weeks [128], from hexamethylenediisocyanate (HMDIC) cross-linked collagen after 3 months [176], so far the relatively most matured collagen fibers from demineralized bone [35], and from fascia lata wrapped braided PLLA yarns after 48 weeks [177]. However, the unsatisfactory mechanical results showed that the regenerated collagen were unable to demonstrate original mechanical properties. Three reasons could be attributed to it; 1) the reported relatively mature and well orientated collagen fibers reside only in some areas of the grafts, but not homogenously; 2) they were only immature collagen with small diameters; 3) collagen fibers were not well oriented and lacked cross-linkages.

1.2.7 Bioreactors

There are three main strategies to engineer tissues clinically and scientifically, (a) direct cells to form specialized tissues, (b) provide and characterize the specific regulatory signals (biochemical, physical) that are known to modulate cell function and tissue development, (c) precisely control the environmental conditions (e.g. pH value, temperature) and mass transport of chemical components (e.g. nutrients, oxygen, metabolites, growth factors) to and from the cells. Bioreactors are essential to meet these requirements and to further study the exact role of each factor [3]. Currently tissue engineering depends on two approaches to succeed: one is to implant tissue engineered constructs directly into the injured sites to use an in vivo environment as "bioreactors"; or

to culture the constructs *in vitro* under well controlled conditions to promote tissue regeneration [178]. Sometimes, it is necessary to combine the two ways. Potential tissue engineered ACLs would not only face harsh environments, such as complex mechanical and enzymatic attacks, but also lack of blood supply at the initial stage. All these factors contribute to usage of bioreactors before in vivo implantations.

While knowledge about embryo development and adult regeneration develops, bioreactors could employ more controlled conditions to fabricate desired tissues. Much attention has recently been focused on the development of bioreactors. Though many results support the notion that bioreactors providing dynamic loading are essential for meeting the complex requirements of *in vitro* engineering of functional skeletal tissues [3, 179], few of them has been specially designed for ligament tissue engineering. Ligament-like tissue have been made in bioreactors [180, 181] in some general bioreactors, as well as in ligament designed bioreactors [76]. However, all of them could not induce mature collagen cross-link and bundle formation, which symbolize the functional ligaments.

1.2.8 Regulatory factors and controlled release

Lots of biochemical factors, including growth factors, could promote or disturb tissue regeneration. Oxygen can markedly affect extracellular matrix (ECM) synthesis rates and the *in vitro* development of engineered tissues [182-184]. High oxygen tensions (21%) supported optimal ACL fibroblast proliferation, whereas lower tensions (10%) enhanced ECM collagen synthesis [185]. Ascorbate-2-phosphate (a long-acting derivative of vitamin C) could enhance cell growth and collagen excretion [186, 187]. Growth factors

are polypeptides that transmit signals to modulate cellular activities, stimulate or inhibit cellular proliferation, differentiation, migration and gene expression [188]. A lot of growth factors have the capacity to increase cell proliferation, including epidermal growth factor (EGF), platelet-derived growth factor (PDGF), basic fibroblast growth factor (bFGF), insulin-like growth factor II (IGF-II) and transforming growth factor-beta (TGF-β) [189-195]. Insulin, TGF- β, and IGF-II promote protein expression and ECM generation in soft connective tissue [192, 193, 196]. TGF- β and EGF (or insulin) act in concert to stimulate normal proliferation of fibroblasts and mesenchymal cells [193, 197, 198]. PDGF, FGF, cartilage-derived morphogenetic protein (CDMP) and growth and differentiation factor (GDF) also could promote functionalities in tendon and ligament regeneration [199-202]. Bone morphologic protein (BMP)-12 has also been reported to promote proliferation and collagen expression of tendon fibroblasts *in vitro* and functionality *in vivo* [203, 204].

The main concerns to use growth factors are cost and controlled release. As mentioned earlier in the section on bioreactors, tissue engineering may have to culture its products *in vitro* or *in vivo*, and sometimes both. Growth factors could be incorporated into the scaffold either during or after scaffold fabrication [205-207] (or added when cultured in vitro sometimes), as well as be co-transplanted through natural growth factor-secreting cells or genetically engineered cells within the tissue engineering constructs [208]. Two hurdles currently hamper clinical usages of growth factors: firstly, the exact role as well as necessary dose and duration of a growth factor have not been fully understood;

secondly, the technical profile for individual growth factor has not been fully established, though much progress has been made.

1.3 Animal model

The use of animals in orthopedic research has played a vital role in the numerous medical advances, though public controversy regarding animal experimentation still exists. Most people however support animal experimentation, emphasizing the need to pay particular attention to animal welfare and animal rights [209].

1.3.1 Experimental design, evaluation and data analysis

Each experiment is designed to answer one hypothesis, an unproven theory as well as a specific, logical and scientific form of a thought. After serious review on previous studies, an experimental design including number of animals used, consideration of animal variance, evaluation methods, randomization and sampling error and controls should be well stated [210]. The most often used evaluation methods in orthopaedic animal research are: clinical observation, radiography, macro-observation at necropsy, histological evaluation, and mechanical testing. Sometimes, electron microscopy, computed tomography (CT) and magnetic resonance imaging (MRI) are used. Data analysis is often necessary for a conclusion, which includes descriptive statistics, one-way sample analysis, paired/unpaired comparisons, analysis of variance, correlation and regression analysis and nonparametric data [210].

1.3.2 Animal model of ligament

As animal research acts as the bridge between *in vitro* studies and human clinical trials, the ideal way is to choose primate models, as the results from them are easily extrapolated to human conditions. However, when ethics, availability, housing requirements, ease of handling, costs as well as susceptibility to disease are considered as a group, the choices of animal species are usually compromised [211].

To investigate ligament regeneration and reconstruction, it is prudent to choose animal models in which the type and degree of ligament injury is similar to that in humans, and to realize that the results from animal research may be species and ligament specific and may not necessarily simulate that of humans [64]. Most often used animal models in ligament research are dogs, rabbits, goats and sheep. The reasons to use dogs are due to ease in handling, receptiveness to various exercise regimens as well as well published information [64]. Goats and sheep are broadly used for ACL reconstruction using biological grafts and ligament prostheses [212, 213] because of larger knee joint size and less degree of flexion. Rabbits are widely used in biomedical research due to their docile nature and relatively inexpensive purchasing cost and maintenance as well as well-documented biochemical and functional properties of rabbit knee ligaments [64]. However, their rather small joint size limits accuracy of ACL operations and obesity during long-term caging leads to high loads in the knee joints [64]. After the consideration of all these factors, the rabbit model was chosen to evaluate the performance of our knitted scaffolds for ACL reconstruction.

1.4 Hypothesis & objective ACL

The hypotheses of this study are as follows:

a. knitted biphasic scaffolds can provide enough mechanical strength before ligament regeneration;
b. mesenchymal stem cells (MSC) and fascia wrap can promote anterior cruciate ligament repair when used on knitted biphasic scaffolds followed by implantation in the knee joint.

In view of these two hypotheses, the specific objectives of this project are designed as such:

1. to select optimal cell source for ACL tissue engineering regarding proliferation, collagen excretion and collagen expression profiles.
2. to design and characterize the knitted scaffolds for ACL tissue engineering on their mechanical properties and degradation.
3. to test *in vivo* effects of knitted scaffolds used in a rabbit ACL reconstruction model, as well as MSC loading and fascia wrap.

---------- *CHAPTER 2* ----------

2 Materials and Methods

2.1 Cell selection

2.1.1 Harvest and Culture of ACL fibroblasts, MCL fibroblasts and MSC

All the animal experiments have been ethically approved by the Animal Holding Unit, National University of Singapore. In this study, 12 male NZW rabbits weighing between 2.2-2.5kg were used. The ACL and MCL were harvested from the rabbits under sterile conditions according to the method described by Kobayashi et al [214] and Nagineni et al [215]. The anesthesia technique used was as follows: 0.3ml/kg hyponym was administrated intra-muscularly to tranquilize the animal; this was followed by intra-venous 0.3ml/kg Valium for induction. Then, 1% halothane inhalation was used for maintenance. 0.3ml/per animal of cephacexin was given subcutaneously as antibiotics. Briefly, after the femoral and tibial insertions of the ligaments were resected, the synovial sheath and periligamentous tissue were stripped away from each ligament. Immediately following the isolation of the ACL and MCL, each ligament was carefully cut into 1mm×1mm indices and digested with 5ml 0.25% collagenase (Gibco) in 37ºC shaking water bath for 10 hours followed by twice DMEM rinse. The isolated ligament cells from the two ACL of the same rabbit were cultured in one 25cm^2 flask (Corning) with DMEM (Sigma, pH 7.4) supplemented with 10% FBS (GIBCO, 10270-106), 10,000U/ml penicillin/10,000µl/ml streptomycin and 2mM L-Glutamine (Gibco). Then the cell-medium system was incubated at 37ºC with 5% CO_2 until 80% confluence. It is important to note that the medium was changed at three days' interval until 80% confluence was achieved.

The MSCs were isolated by using the short-term adherence to plastic method as described by Friedenstein [53]. Briefly, the procedure is as follows: the rabbit was put under general anesthesia and 2-ml of bone marrow was aspirated from iliac crest (Fig 4) and subjected to centrifugation. After centrifugation and wash, the cells were cultured in DMEM (Sigma, ph 7.4) supplemented with 10% FBS (GIBCO, 10270-106), 10,000U/ml penicillin/10,000µl/ml streptomycin and 2mM L-Glutamine (Gibco). The cells were cultured in 75cm^2 flask (Corning) at 37º with 5% CO_2 until 80% confluence. The medium was changed at every three-day's interval. Hemopoietic cells were removed at each change of medium. Subsequently, the cells were trypsinized with 1ml of 0.25% trypsin-EDTA (Gibco) and sub-cultured before use in the evaluation protocol and follow-up experiments.

Figure 4 Aspiration of bone marrow

2.1.2 Proliferation Assay

Cell proliferation assessment of the three cell types, ie ACL fibroblasts, MCL

fibroblasts and MSC were performed after passage 1, with an initial cell number of 0.2 million of each cell type. The cells were cultured in 5ml of DMEM medium (with the same supplement as described previously) in a 25cm^2 flask until 80% confluence. Once reached, the cells were trypsinized and counted again. The cell doubling times (TD) were calculated from the following equation:

$$TD = t \cdot lg2 / (lgN_t - lgN_0) \quad \text{----------Equation 1}$$

where N_0 and N_t are the primary cell number and acquired cell number respectively [216].

2.1.3 Collagen Assay

In order to carry out the collagen assay, 50,000 cells of each cell types were loaded in one of the wells of a 24-well plate. After 24hrs, the medium was changed to 0.8ml of DMEM supplemented with 5% FBS, 10,000U/ml penicillin/10,000µl/ml streptomycin and 2mM L-Glutamine (Gibco). Collagen assays were performed strictly according to the Sircol collagen assay kit protocol (Biocolor, UK). Briefly, the collected supernatant from the culture well was centrifuged at 1,500rpm for 4 min to drop the extracellular matrix (ECM), this was followed by mixing 100µl supernatant with 1ml of Sircol dye for 30 min and centrifuging at 10,000rpm for 5min to drop the formed collagen-dye complex. After decanting the suspension, droplets were dissolved in 1ml Sircol alkali reagent and vortexed. Subsequently, 100µl of the acquired solution was read at 540nm.

2.1.4 Immunohistochemistry

The immunohistochemistry evaluation was carried out on the three cell types; 10,000

cells of each cell types were cultured on each well of the 4-well chamber slide (Iwaki, Japan). The four wells were stained respectively with antibodies of monoclonal anti-collagen type I (Sigma, C2456), monoclonal anti-collagen type II (Ab-3, NeoMarkers), monoclonal anti-collagen type III (63172, Chemical Credential, USA) and monoclonal anti-α smooth muscle actin (1A4, Sigma, A2547). The UltraVision Detection system (TP-015-HD, Lab Vision Corporation) was used in this study. Pre-dilution of type I, type II and type III antibody was 1:4,000 while α smooth muscle actin antibody was diluted with 1:400. A brief description of the procedure is as follows: after one week of cell culture, the cells were fixed in 2% paraformaldehyde for 10min. The cells were then incubated with six drops of hydrogen peroxide and block for 15min, followed by Ultra V Block for 5 min. Then, the cells were stained with the prepared primary antibody for 3 hour, biotinylated Goat anti-polyvalent for 10min, streptavidin peroxidase for 10min and finally with the freshly prepared DAB solution for 10min. The cells were washed before each step with PBS.

2.2 Characterization of knitted scaffolds

2.2.1 Fabrication of Scaffold

The scaffolds were knitted out of two poly-L-lactic acid (PLLA) yarns (multifilament, nonbraided, 30 filaments, each filament between 15-20 microns in diameter, denier, 83, Scaffix International, USA, Fig 5) and 1 poly-lactic and glycolic acid (PLGA, the ratio of PLA and PGA in the co-polymer is 10:9, 12 filaments in one yarn and each filament between 15-35um in diameter, denier 50-60, Shanghai Tianqing Biomaterial, China,

Fig 6) in knitting machine (SK270, Silver Reed, Suzhou Harisa Machinery Co., China, Fig 7) with four-needle mode. The two ends of each 5cm long knitted structure were sealed with heat. In order to sterilize the scaffolds, they were immersed in 70% alcohol for 30min after being washed with PBS twice. Subsequently, the scaffolds were immersed in 3 changes of PBS for 15min before use.

Figure 5 PLLA yarn (white)

Figure 6 PLGA yarn (blue)

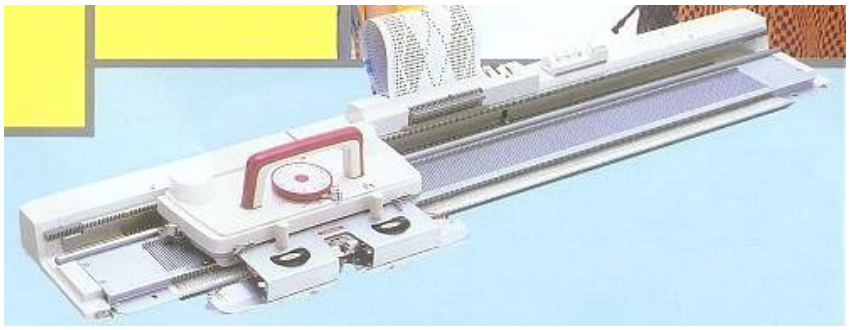

Figure 7 Knitting machine

2.2.2 Tetrazolium-based colorimetric assay (MTT)

The test scaffolds were cut into 5mm long strips and sterilized by above mentioned methods. One well of 96-well plate was filled with 100µl of 5×10^5cell/ml of cell suspension. The test scaffolds, as well as positive controls (rubbers) and negative controls (high density polyethylene, 54670, USP, US) were placed in the wells (4 replicates) while another 4 wells were maintained free of sample as control. The system was incubated at 37°C, 5% CO_2 and the percentage of viable cells was determined after 24 hrs. Twenty microliters of MTT solution (5mg/ml) was added in each well and after 3h of incubation at 37°C, 5% CO_2 the wells were emptied and 150µl of DMSO was added to each well and the optical density at 540nm wavelength measured to determined the percentage of viable cells.

2.2.3 *In vitro* cell loading on scaffold

Two centimeter long knitted scaffolds were folded back before two loose ends were sealed. After sterilizing with the above mentioned method, 2 million MSCs in 30µl tisseel were loaded onto scaffolds, followed by 30µl thrombin (Tisseel Kit, Baxter, Austria). After 20min of incubation at 37°C, 5% CO_2, 1ml of above mentioned DMEM was added to each well in 24-well plate containing the scaffold. Medium was changed at two-day intervals. Ten days later, scaffolds were incubated with 10ng/ml FDA (Fluorescein diacetate, F1303,molecular Probes, Oregon, USA) for 2 min just before being examined by Laser Scanning Confocol Microscope (TCSSP2, Leica, Germany) at 490nm.

2.2.4 Characterization of the knitted structures

2.2.4.1 Porosity

The porosity of the knitted scaffolds was estimated by deduction of cross-section areas of individual PLLA yarns and PGLA yarns from gross cross-section of scaffolds. Knitted scaffolds, PLLA yarns and PGLA yarns were fixed under slight tension (approximately 5N) before the diameter was measured under phase contrast microscope. The following formula was used to calculate the porosity of the scaffolds:

Porosity= 1-(PLLA area +PLGA area)/scaffold area

PLLA area: the sum of all cross section areas of PLLA yarns

PLGA area: the sum of all cross section areas of PLGA yarns

Scaffold area: the cross section area of entire scaffold

After immersion for scheduled time, the scaffolds were fixed in paraffin under little tension. Then the specimens were cut to 6μm with microtome, before cross-sections were examined under microscope (Olympus BX51) and counted with Olympus Microimage 4.5.1.

2.2.4.2 Molecular weight

One microgram of samples was dissolved in 2ml chloroform (i.e. concentration of sample is around 0.05%) before molecular weights were determined by Gel Permeation Chromatography (GPC, Waters, USA) at an elution rate of 1ml/min at 25°C with a column (Shodex K-806M, Japan). 100ul was analyzed each time while polystyrene was used as the standard. Mean values at each time points were compared with one way ANOVA (LSD, $P<0.05$).

2.2.4.3 Mechanical properties of the scaffolds

The two ends of the scaffolds were sandwiched between sand papers and secured by super glue (Alteco 110, Alteco Chemical, Singapore, Fig 8) to prevent slippage of the scaffolds between the pneumatic grips used in the tensile test. The scaffolds had a gauge length of 20mm. The tensile properties were measured with the Instron 5848 Micro Tester at a constant strain rate of 0.8%/s (Fig 9). The cross-sectional area of the scaffold was taken to be the sum of cross-sectional areas of the individual filaments measured under an optical microscope. The values of stress were obtained by dividing the load by the cross-sectional

area of the scaffold. The strain values were obtained by dividing the elongation by the gauge length of the specimen. The first linear region (i.e. at lower strain levels) after "toe" region was used for determination of modulus. The percentage changes in gradients before and after every ten points were obtained. The region with the smallest fluctuation in percentage change was picked. From this selected region, a tangent line was drawn, which gradient gave Young's Modulus.

The viscoelastic properties were studied by carrying out relaxation and creep tests. In both viscoelastic tests, a pre-load of 0.2N was first applied before pre-conditioning the scaffolds for 10 cycles at a frequency of 0.1Hz and amplitude of 2% gauge length. The scaffolds were then stretched to 2.5% strain for relaxation tests and 1.5N load for creep test and held at the strain and load values respectively for 900s. The strain and load levels selected for the viscoelastic tests correspond to the range of strain experienced *in vivo* **[20]**.

The normalized stress relaxation rate is obtained by finding the slope of the normalized stress vs ln(t) strain plot. The normalized stress is obtained by dividing the stress values by the initial stress immediately after the initial 2.5% strain has been applied (i.e. stress at time zero). The logarithmic operation on the time axis transformed the inherently nonlinear relation in load decay vs time into a linear relation such that a simple linear regression could be used to determine the rates of relaxation [217].

Similarly, the normalised creep rate is obtained using the same method. For creep test, the normalised strain is obtained by dividing the strain values by the initial strain immediately after the initial 1.5N load has been applied (i.e. strain at time zero). The logarithmic

operation of the time axis transformed the inherently nonlinear relation in strain vs time into a linear relation such that a simple linear regression could be used to determine the creep rates.

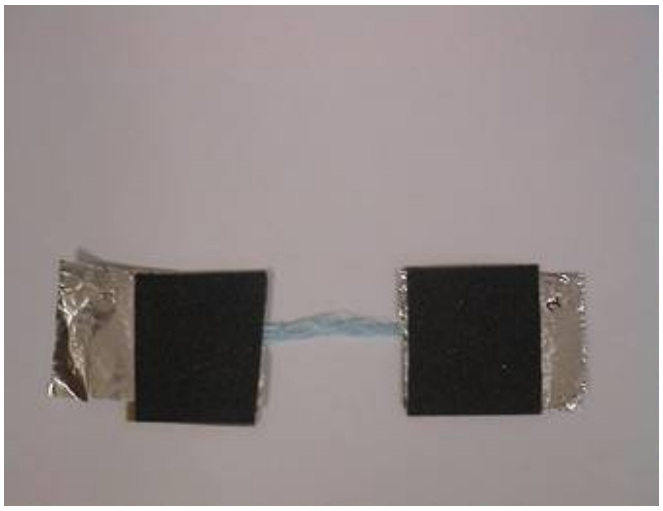

Figure 8 Specimen preparation

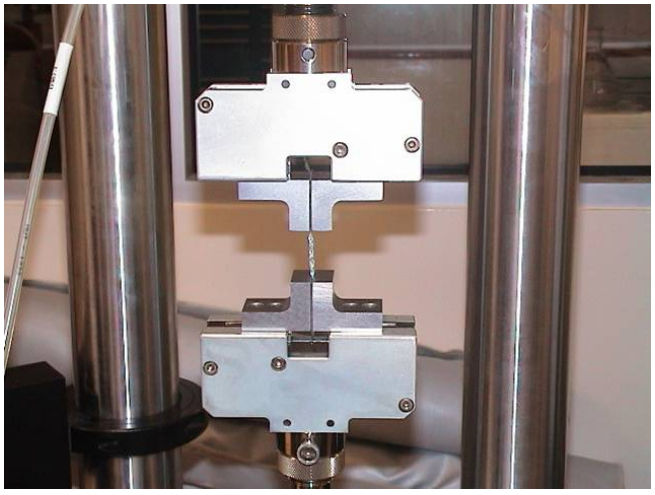

Figure 9 Instron 5548 microtester

2.2.4.4 *In vitro* degradation

Knitted scaffolds were immersed in1ml of above mentioned DMEM in15ml centrifuge tubes. The systems were incubated at 37°C, 5% CO_2 while medium was changed weekly. PH values from three centrifuge tubes were measured as a group by using a pH meter (Coring PH meter 430). The scaffolds were immersed for 4, 8, 12, 16, and 20 weeks before weighing; GPC and mechanical tests were done according to previous methods. 9 replicates were used at each time point (3 for mass loss followed by GPC and 5 for mechanical testing). After immersion for the scheduled time, the scaffolds were fixed in paraffin under little tension. Then the specimens were cut to 6μm with a microtome, before cross-sections were examined under the microscope (Olympus BX51) and counted with Olympus Microimage 4.5.1.

2.3 ACL reconstruction in Rabbit Model

2.3.1 Reconstruction

Animal experiments were ethically approved by the Animal Holding Unit, National University of Singapore. Forty-eight skeletally-matured male New Zealand White rabbits weighing 3.0 - 3.4 kg were divided into four groups, with 12 rabbits in each group, while 4 additional rabbits were used for cell survival test (Table 4). The anesthesia technique used was as follow: 0.3 mL/kg hyponym was administrated intra-muscularly to tranquilize the animal; this was followed by intra-venous 0.3 mL/kg Valium for induction. Subsequently, 1% halothane inhalation was used for maintenance. 0.3 mL/per animal of cephacexin was given subcutaneously as antibiotics during post-operation.

Table 4 Grouping of experimental rabbits

	Rabbits, (N)	Scaffolds / Rabbit	Cells	Fascia cover
Group I	14	2	-	-
Group II	14 + 2	2	+	-
Group III	14 + 2	2	+	+
Group IV	14	2	-	+

The operations were performed under aseptic conditions. The right knee joint of the rabbit was exposed using a midline skin incision and lateral parapatellar arthrotomy. The patella was dislocated medially with the knee extended. With the knee placed in hyperflexion state, normal ACL was removed by sharp dissection at the tibial and femoral attachment sites, while the fat pad was left intact. Using a 2-mm diameter drill bit and a gas–driven drill (K 100 Air Powered Mini Driver, 3M, USA), bone tunnels were made from the anatomic ACL femur attachment site to lateral femoral condyle (Fig 10), as well as from the anatomic ACL tibial attachment site to medial tibia, which is distal and medial to the tibial tubercle. Each end of the sterile knitted scaffold was sutured with 4-0 Vicryl suture (Ethicon, NJ), to facilitate the ease of threading the scaffold through the tibial and femoral bone tunnels. For group I, two scaffolds were combined and passed through the femoral bone tunnel, into the intraarticular space, and through the tibial bone tunnel separately (normal procedure). For group II, 3 million MSCs in 60µl of Tisseel fibrin glue (Baxter Healthcare Corporation, Glendale, CA) were loaded on the two scaffolds before normal procedure. For group III, firstly, a 0.5 cm wide and 5 cm long fascia lata at lateral

part of femoral condyle was carefully dissected, while keeping the pedicle near the femur bone tunnel connected. After 3 million MSCs in 60 μL of Tisseel fibrin glue were loaded (Fig 11), the scaffolds were wrapped with pedicle fascia lata (Fig 12) and sutured with 4-0 Vicryl suture just before normal procedure. For group IV, the scaffolds were wrapped and sutured with same fascia lata as in group III prior normal procedure. The two ends of the construct in each group were then sutured to the periosteum with 2-0 Ethibond non-absorbed suture (Johnson &Johnson, USA). This was done with the knee at 45º of flexion with the constructs in slight tension. The experimental rabbits were left in cage without immobilization. After twenty weeks, the rabbits were euthanized by 1 mL (400mg) /2.5kg body weight of pentobabitone sodium (Euthanasia Fort Solution, Apex Laboratories, Australia) and knee joints were dissected for histology and mechanical test.

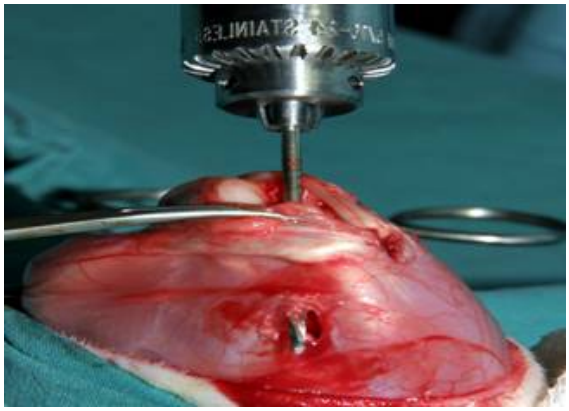

Figure 10 Drilling bone tunnel at femur

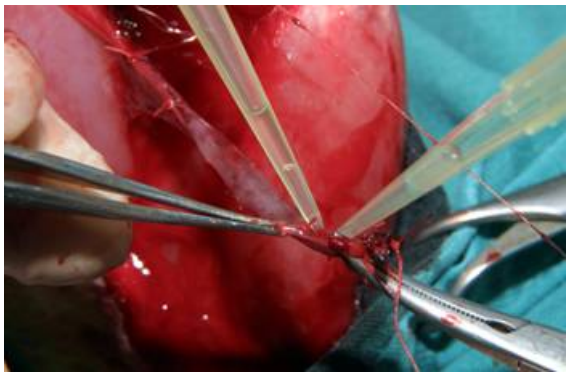

Figure 11 Cell loading on the scaffold

Figure 12 Fascia lata dissection

2.3.2 Histology and Immunohistochemistry

Two rabbits from each group were sacrificed at 4 weeks for histological study and the remainings were sacrificed at 20 weeks for histology, immunohistochemistry, western blot analysis and mechanical testing. All connective tissues and other ligaments in the knee joints were removed except for the ACL. For histology, the harvested specimens were immersed in 10% formalin for one week prior to decalcification in 30% formic acid for three weeks, followed by normal paraffin-embedding for hematoxylin- and eosin-staining procedure.

For immunohistochemistry, the harvested ACLs were cryo-sectioned to 6μm and placed on Saline-PREP™ slides (s4651, Sigma Diagnostics, MO, USA) before fixation with acetone for 4 min. Slides were stained with anti-collagen type I (Sigma, C2456) and anti-collagen type III monoclonal antibodies (63172, Chemical Credential, USA). The UltraVision ™ Detection system (TP-015-HD, Lab Vision Corporation) was used in this study. Pre-dilution of type I and type III antibody was 1:2,000. A brief description of the procedure is as follows: Slides with harvested specimens were incubated with hydrogen peroxide for 15min, followed by Ultra V Block for 5 min. Cells were then stained with the prepared primary antibody for 3 hour, followed by biotinylated goat anti-polyvalent for 10 min, streptavidin peroxidase for 10 min and finally with freshly prepared DAB solution for 10 min. The slides were washed in between steps with PBS.

2.3.3 Mechanical testing

Five rabbits from each group were used for mechanical testing (tensile test) while five randomly chosen left knees were used as controls. The knee joints with intact capsules and 4 cm of femurs and tibias were harvested. The specimens were sealed and kept in -80 ºC until they were tested. The specimens were thawed at room temperature for 24 hours and were dissected free of all connectives tissue and other ligaments except for the ACL. The knee joints of the specimens were covered with saline wet gauze to keep the samples moist at all times (Fig 13). The knees were mounted with Meliodent (CE 0044, Heraeus Kulzer GmbH, Germany) in the proximal femur and distal tibia, clamped at 45º

flexion in a Instron 5543 material testing system (Instron, Canton, MA)(Fig 14). Cross-sectional areas were determined by assuming an elliptical cross-section and measuring the minor and major axes of the ligament midsubstance using Vernier calipers with minimal compressive force. The maximal load and elongation were measured at a constant speed of 2 cm/min. The specimens were sprayed with saline from time to time (Fig 15). Stiffness was determined by calculating the slope of the load versus displacement plot. The first linear region (i.e. at lower strain levels) after "toe" region was used for determination of stiffness. The percentage changes in gradients before and after every ten points were obtained. The region with the smallest fluctuation in percentage change was picked. From this selected region, a tangent line was drawn, which gradient gave Young's Modulus.

Figure 13 ACL preparation for mechanical test

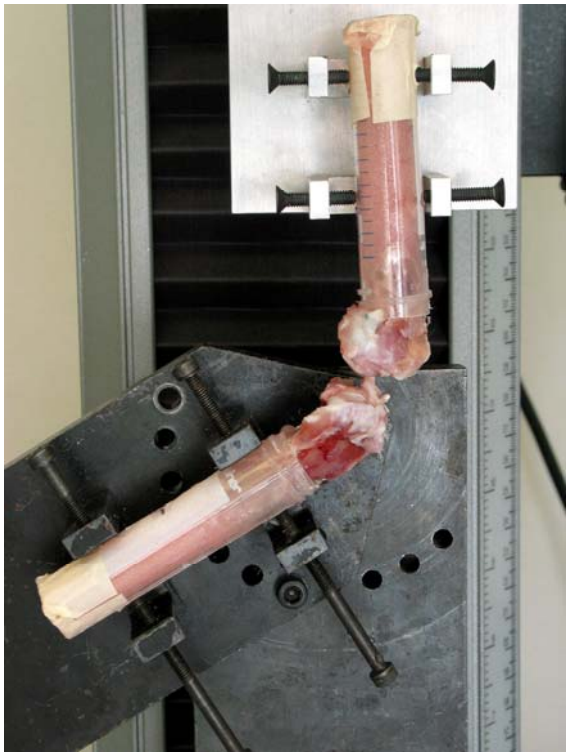

Figure 14 Knee joint mounted in dental cement and fixed in Instron machine

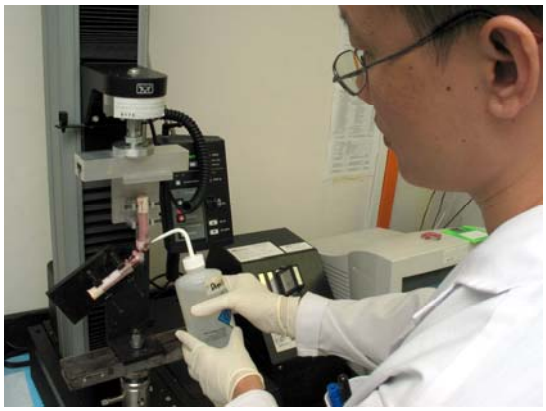

Figure 15 Mechanical testing with saline spray

2.3.4 Western blot

ACL specimens after mechanical testing were used for western blot analysis. Ten pieces of 10μm slices were cut from each explant and extract in buffer (pH 6.8) consisting: 48% (w/v) high-purity urea (Gibco BRL, #15505-050), 15.2% (w/v) thiourea (Bio-Rad, highest purity), 0.075M dithiothreitol (Bio-Rad), 0.0498M Trizma base (Fluka, high purity), 3% (w/v) SDS (Bio-Rad) and 0.004% bromophenol blue.

Calibration curve was made with Bio-Rad Protein Assay (Bio-Rad Laboratories, CA, USA) according to protocol. Briefly, 20mg of lyophilized bovine serum albumin (BSA) standard was reconstituted with 20ml of deionized water and mixed until totally solved. 1 part Dye Reagent concentrate was diluted with 4 parts distilled deionized water before filtered with Whatman #1 filter to remove particulates. BSA standard was further diluted to different concentrations between 0-250μg/mL. 10μl of standard at different concentration was added into one of 96-well plate with 200μl diluted dye reagent solution. After totally mixing with microplate mixer and incubating for 10 min, absorbance was read at 595nm with SUNRISE microplate reader (TECAN, Au). Duplicate standard was examined.

Equal amounts of total proteins (10ug) were loaded to 7% SDS-minigels at 15m Amps per gel until the marker dye reached the bottom of the gel. The protein was transferred to the nitrocellulose membrane by electrophoretic blotting from the gel using the Trans-blot Electrophoretic Transfer cell (Bio-Rad). The transfer was run overnight at 29V. The membrane was immersed in blocking solution (6% non-fat dry milk in TBS). The

solution was then placed on an orbital shaker for one hour at room temperature. The blocking solution was poured out and TTBS was added to wash the membrane. The membrane was washed for 5-10 minutes while gently agitating the solution at room temperature. After removing the TTBS, the primary antibody solution (Anti-collagen type I, human (mouse), Calbiochem) or (collagen type III, oncogene) prepared in 1% skimmed milk was add to the membrane and shaken for 1-2 hours at room temperature. The membrane was again washed in TTBS as described above. After repeating the wash cycle, the TTBS decanted and the second antibody, the horseradish peroxidase–conjugated anti-mouse IgG Ab 6789 (Abcam Ltd) was added to the membrane. Once again, the membrane was incubated with gentle agitation for 1 hour at room temperature. The membrane was washed using TTBS as described previously, and repeated four times. At the same time the chemiluminescence reagent (Perkin-elmer) was prepared by mixing an equal volume of the enhanced Luminol Reagent and the Oxidizing Reagent and added to the membrane for 1 min. Exposion to Kodak X-OMAT was for 30 sec. Then the acquired results were scanned and analyzed with gel pro analyzer (MediaCybernetics) software.

2.3.5 Cell survival-labeling-CFDA

Four additional rabbits were used for cell survival tests. Two of them were treated according to procedures in group II while group III rabbits respectively. Three million of P1 MSCs were stained with 15mM of Vybrant^{TM} CFDA SE Cell Tracer Kit (V-12883, Molecular Probes, Oregon) for 15 min and cultured for 24 hours prior to loading on scaffolds for ACL reconstruction, in group II (scaffolds plus cells) and group III (Scaffolds plus cells and fascia cover) . The cell-loaded constructs in the knee joints

were dissected and cryo-sectioned at 8 μm before examination under a confocal laser microscope (TCS SP2, Leica, Germany) at 488 nm.

3 Results and discussion

3.1 Cell selection for ligament tissue engineering

3.1.1 Cell Proliferation Study

The ACL fibroblasts (Fig 16) and MCL fibroblasts (Fig 17) acquired from digestion were anchorage dependent and well distributed in the flasks, although they occasionally showed "clone-like" growth. They grew in monolayer and showed typical fibroblast-like morphology either with spindle shapes (bipolar) or stellate (multipolar) patterns. However, cell morphology varied a little between different areas and with the time of the culture. The total numbers of acquired cells were not stable from batch to batch, ranging from 200,000 to 500,000 fibroblasts after 10-14 days' culture with the current technique. It was also observed that some of the cells started to show senescence with fatty morphology.

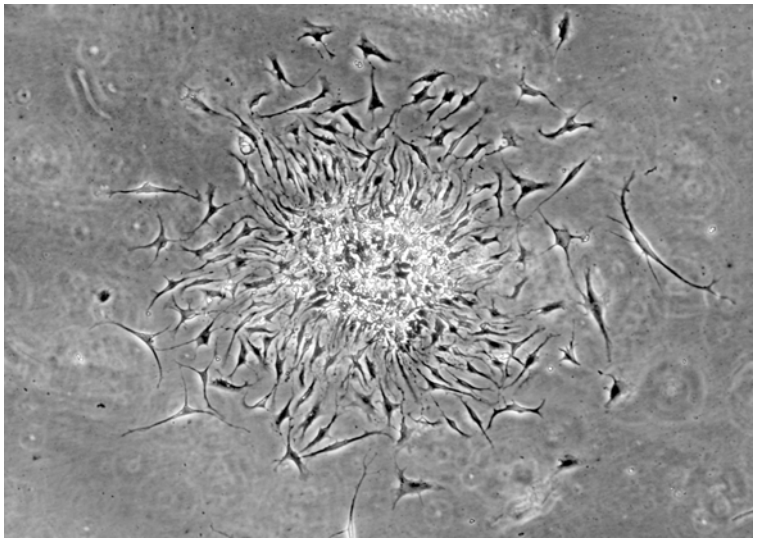

Figure 16 ACL fibroblasts (40x)

Figure 17 MCL fibroblasts (40x)

One and a half million to three million MSCs were acquired with typical colony forming property and fibroblast-like morphology after 18-20 days of cell culture (Fig 18). They were also anchorage dependant and grew in monolayer. In general, they were larger than ACL and MCL fibroblasts and with visible nucleus and nucleolus. After the first passage (P1), it was observed that the MSCs kept the previous fibroblast-like morphology and proliferated well, but after the second passage (P2) at 25 days (Fig 19) as well as the third passage (P3) at 30days (Fig 20), the MSCs stopped proliferation while they increased in size and had irregular morphology. MSCs at P3 were even larger than MSCs at P2. The difference in size was obvious when MSCs were trypsinized.

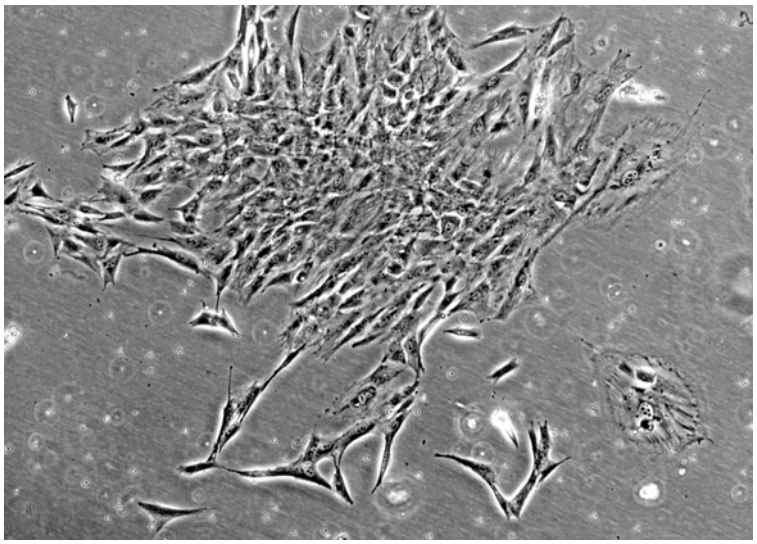

Figure 18 Primary mesenchymal stem cells (MSCs, 40x)

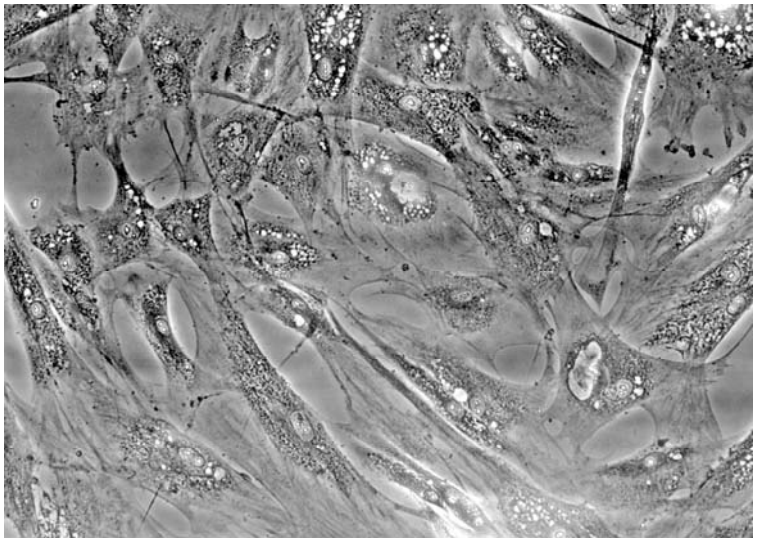

Figure 19 Passage 2 of MSCs (100x)

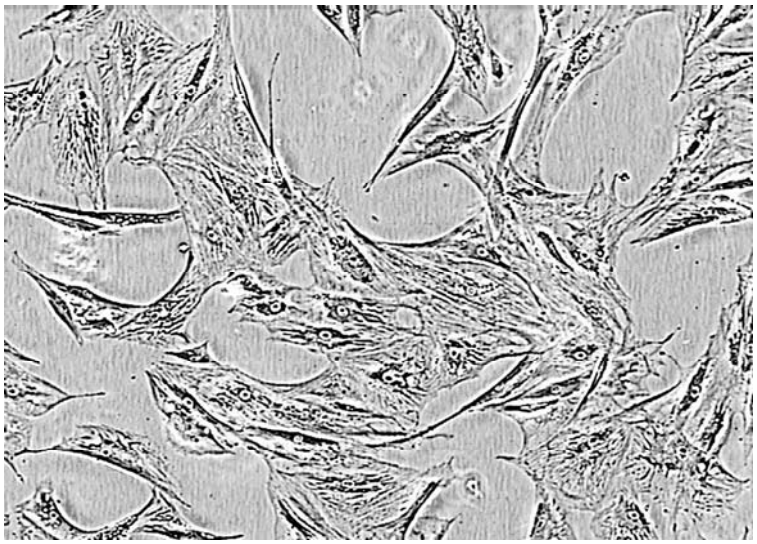

Figure 20 Passage 3 of MSCs (100x)

From equation 1 (given in the preceding section), the MSC at P1 were estimated to double in number at an average of 55.6h (±14h, n=4) while the number of dead P1 MSC was too small to quantify. The total number of MSCs at P2 and P3 dropped after 44 hours in current culture condition, while some of them became detached and died. This was demonstrated by using trypan blue (Sigma, T8154, USA) (Table 5). As for the ACL and MCL fibroblasts, after the first passage, the cells stopped proliferating as a whole and started to deteriorate with obvious morphological changes, ie increase in size and shape irregularily.

Table 5 Proliferation of MSCs

	Cell No at 44h	*No. of dead cells at 44h*	*Cell No. at 168h*	*No. of dead cells at 168h*
P1 MSC	362k ±65.6k	--	--	--
P2 MSC	160k ±15.4k	20k ±5.6k	92k ±23.6k	13k ±2.2k
P3 MSC	134k ±35.5k	18k ±3.1k	97k ±11k	15k ±5k

After 44h proliferation, the number of dead P1 MSC was too small to quantify. As for the ACL and MCL fibroblasts, after the first passage, the cells stopped proliferation as a whole and started to deteriorate with obvious morphological changes, i.e. increase in size and irregular shape formation.

Proliferation, protein synthesis and deposition of extracellular matrix components have been shown to play crucial roles in the repair and remodeling of ligaments [218]. In addition, the survival of loading cells is crucial in tissue engineering experiments. It has been found that the rate of proliferation and collagen excretion of MSCs were higher than that of ACL and MCL fibroblasts, while all of them expressed collagen I, III and α-smooth muscle actin, but not collagen II.

MSC could be harvested from periosteum [219], muscle connective tissues [220] and adipose tissues [221], however, the most accessible and reliable source is the bone marrow. Since Friedenstein et al reported the initial isolation of bone marrow MSCs through

their adherence to tissue culture surfaces [53], the methods for MSC isolation have not been well developed. Several research groups have developed protocols to prepare more homogeneous populations [43, 55, 222], including the use of density gradients in an attempt to further separate sub-populations of adherent cells [223], but none of these protocols has gained wide acceptance. In this study, the most common protocol, ie direct plating [53] was used to culture the MSC due to the ease of the procedure and wide acceptance in most MSC related works. Phenotype of the acquired MSCs has been testified by their potential to differentiate into osteo-lineage, chondro-lineage and adipo-lineage [224], as well as the typical well-spread morphology [43].

Previous studies had reported that sub-populations of human MSC could be amplified by about 20 to 120 population doublings [43, 45] and even up to one giga fold [44] in defined conditions before growth arrest and terminal differentiation was observed. However, to the authors' knowledge no similar report has been made in rabbit MSC. One of the key factors in reduced number of mesenchymal progenitor cells in isolation and culture is age. This had been reported in both human [56] and rabbit [55] studies. Though rabbit MSC as a whole could not proliferate well after passage 2 (i.e. 25days) in current culture conditions, it was not necessary for all sub-populations to stop proliferation, especially when high variability existed in rabbit MSCs [225]. The proliferation rate of ACL and MCL fibroblasts were slightly lower than those reported in a previous study [215], possibly due to difference in age of rabbits.

In considering the use of ACL fibroblasts, it is possible that after rupture, the stump

of the ACL could still possibly serve as potential cell source for further tissue engineering repair and regeneration, although inflammatory reactions may distort and impede the proliferation of fibroblasts [226]. The potential of MCL to heal without intervention [227, 228] also makes the MCL a potential cell source for ACL repair and regeneration. In this study, it was found that the proliferation rate of ACL fibroblasts and MCL fibroblasts were slightly lower than those reported in previous studies [215]. In comparison between the proliferation rates of MSCs, the proliferation rates of ACL fibroblasts and MCL fibroblasts were much lower. The cultured ACL and MCL fibroblasts could not be expanded to large amounts and exhibited senescence after 14 days.

3.1.2 Collagen assay

MSCs, ACL fibroblasts and MCL fibroblasts all actively excreted collagen. Collagen excretion of P1 MSCs and P2 MSCs were 37.1mg/ml and 36.4mg/ml respectively, which were higher than ACL fibroblasts (23.2mg/ml) and MCL fibroblasts (19.8mg/ml). There was no significant difference either between P1 and P2 MSC or between ACL fibroblasts and MCL fibroblasts, while collagen excretion of P1 MSCs and P2 MSCs are significantly higher than ACL and MCL fibroblasts [one-way ANOVA, LCD, $p<0.05$] (Fig 21 and Fig 22) [One-way ANOVA, LSD, $p<0.05$] (Table 6). Since P2 MSCs had already stopped proliferation, therefore it was not necessary to measure P3 MSCs' collagen excretion.

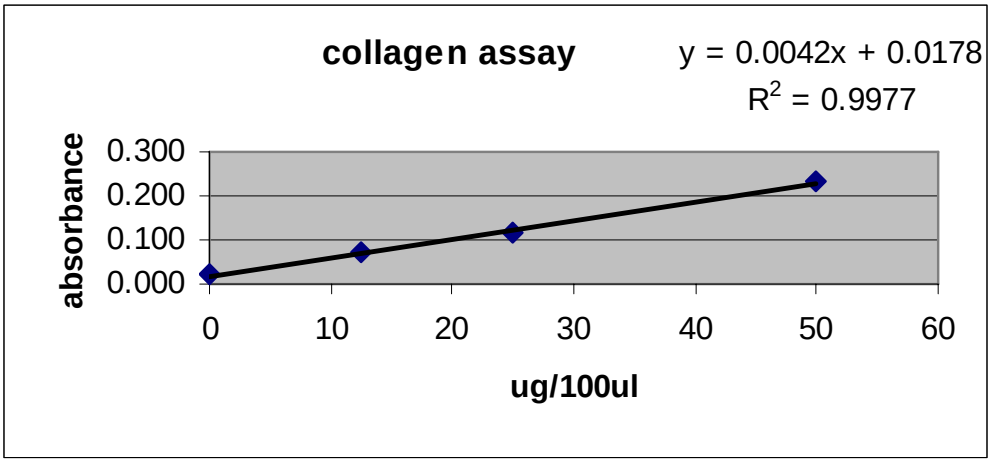

Figure 21 Calibration curve of collagen

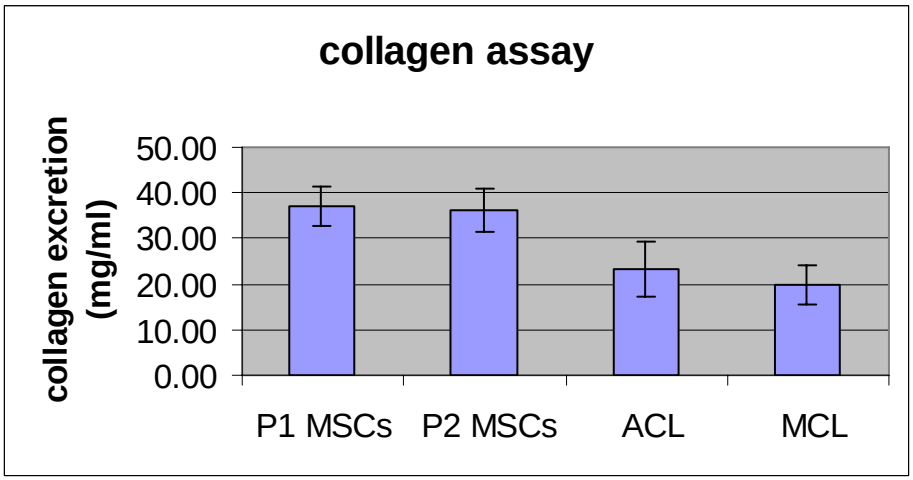

Figure 22 Collagen assay of P1 MSCs, P2 MSCs, ACL fibroblasts and MCL fibroblasts

Table 6 Multiple comparisons of collagen excretion of MSCs, ACL and MCL fibroblasts

(I) GROUP	(J) GROUP	Mean Difference (I-J)	Std. Error	Sig.	95% Confidence Interval	
					Lower Bound	Upper Bound
P1 MSC (37.1mg/ml)	P2 MSC	0.76	1.64	0.65	-2.55	4.06
	ACL	13.94	1.78	*0.00*	10.37	17.51
	MCL	17.30	2.09	*0.00*	13.11	21.49
P2 MSC (36.4mg/ml)	P1 MSC	-0.76	1.64	0.65	-4.06	2.55
	ACL	13.18	1.94	*0.00*	9.29	17.08
	MCL	16.54	2.23	*0.00*	12.07	21.01
ACL (23.2mg/ml)	P1 MSC	-13.94	1.78	*0.00*	-17.51	-10.37
	P2 MSC	-13.18	1.94	*0.00*	-17.08	-9.29
	MCL	3.36	2.33	0.16	-1.31	8.03
MCL (19.8mg/ml)	P1 MSC	-17.30	2.09	*0.00*	-21.49	-13.11
	P2 MSC	-16.54	2.23	*0.00*	-21.01	-12.07
	ACL	-3.36	2.33	0.16	-8.03	1.31

LSD, the mean difference is significant at the 0.05 level.

Collagen is the most abundant protein in mammals, constituting 25% of the total protein mass [229]. The individual collagen polypeptide chains are synthesized on membrane-bound ribosomes and injected into the lumen of the endoplasmic reticulum (ER) as larger precursors procollagen. After secretion of procollagen, the propeptides are removed by specific proteolytic enzymes outside the cell. This converts the procollagen molecules to collagen molecules, which assemble in the extracellular space to form much larger collagen fibrils. Procollagen is usually 1,000 fold more soluble that collagen molecules [229]. Though serial extraction of collagen have been used to examine the total collagen content in extracellular matrix [230], it is also reasonable to measure the level of collagen excretion ability of cells by determining the procollagen as reported [231, 232], as

procollagen propeptides and mature collagen are synthesized in a ratio of 1:1. It was observed that the level of collagen excretion of MSCs was more than 40% higher than that of ACL fibroblasts and MCL fibroblasts. Based on the results of the proliferation and collagen excretion studies, MSCs clearly exhibited distinct advantages over ACL fibroblasts and MCL fibroblasts, as a potential cell source for tissue engineering repair and regeneration of ligaments. From our knowledge, no previous study has shown the identical result.

3.1.3 Immunohistochemistry

MSCs were positively stained with collagen type I, III and α-smooth muscle actin while negatively stained with collagen type II (Fig 23, 24, 25). The staining densities of collagen I and III for individual MSC varied while more than 90% of MSCs were well stained. The staining densities of alpha smooth muscle actin for individual MSC were more homogenous and well distributed in cytoplasma.

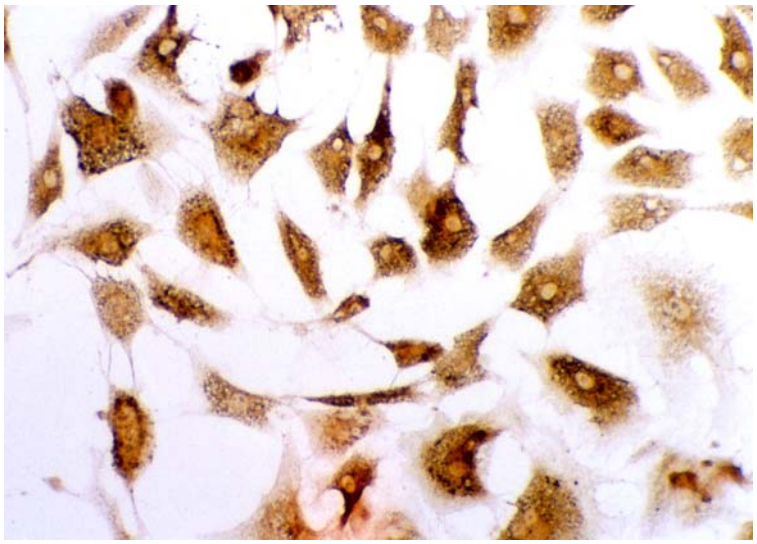

Figure 23 Collagen type I staining of MSCs (100x)

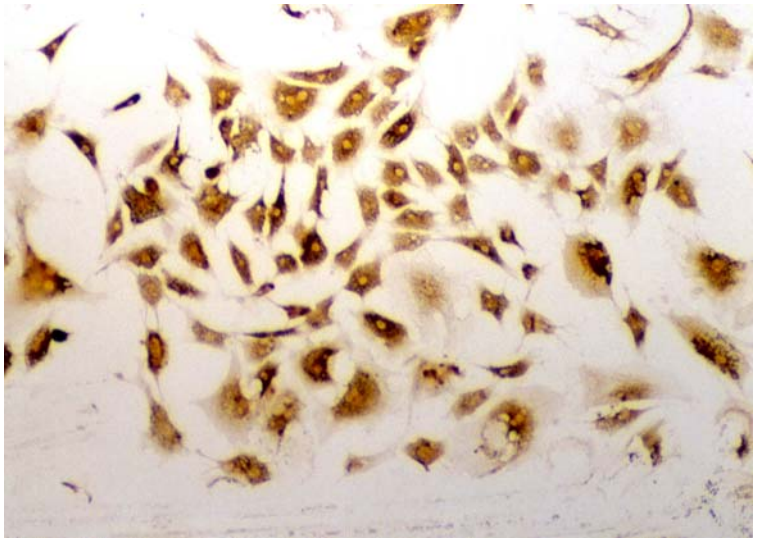

Figure 24 Collagen type III staining of MSCs (100x)

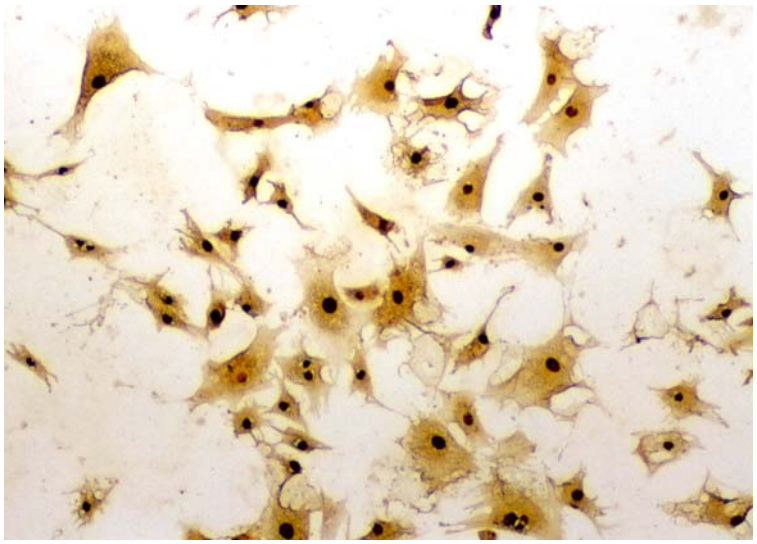

Figure 25 Alpha smooth muscle action staining of MSCs (100x)

Both ACL and MCL fibroblasts were positively stained with collagen I, III and α-smooth muscle actin while negatively stained with collagen II (Fig 26-31). The staining densities of collagen I for ACL and MCL fibroblasts were lower than MSCs while there was no difference in density among collagen I, III and α-smooth muscle actin. The stained collagen I, III and α-smooth muscle actin were well distributed in the cytoplasma.

Figure 26 Collagen type I staining of ACL fibroblasts (100x)

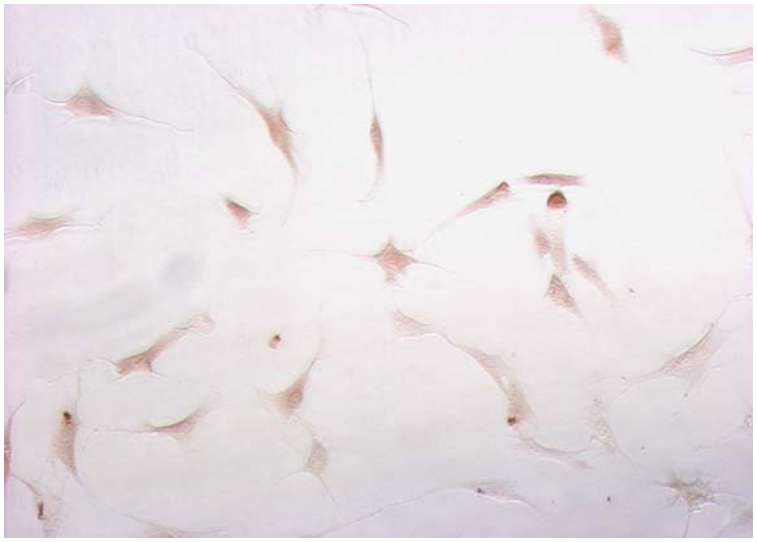

Figure 27 Collagen type III staining of ACL fibroblasts (100x)

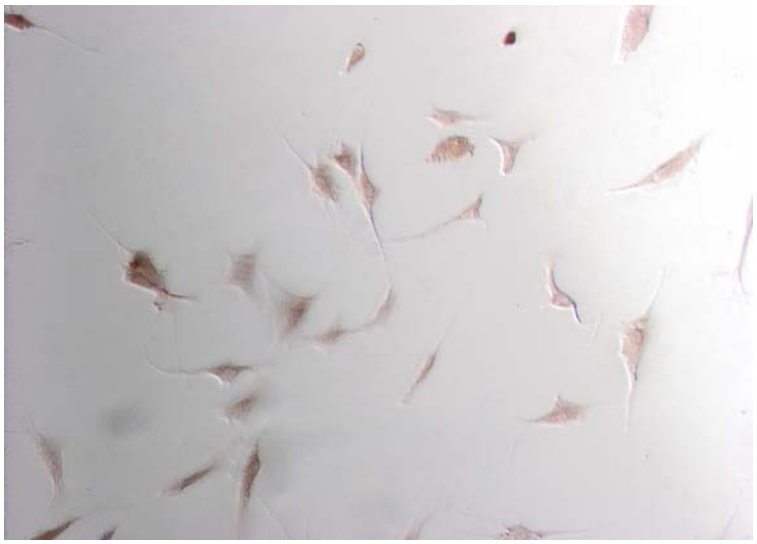

Figure 28 Alpha smooth muscle actin of ACL fibroblasts (100x)

Figure 29 Collagen type I staining of MCL fibroblasts (100x)

Figure 30 Collagen type III of MCL fibroblasts (100x)

Figure 31 Alpha smooth muscle of MCL fibroblasts (100x)

Various cells have been used in ligament tissue engineering and many of them have reported the fate of loaded cells in ACL reconstruction with tissue engineering methods [50, 233-235], but little has been discussed about the functionality of these cells. In previous studies, skin fibroblasts [236] has been identified as a potential candidate

for ligament tissue engineering primarily due to their abundance in the body. However, it may not be an appropriate choice for the following reasons: Firstly, harvesting of skin normally results in high morbidity. Secondly, the physiological environment of skin fibroblasts is distinctively different from that of the ACL, thus it may potentially affect their performance.

Type I collagen is about 6 to 8 times more abundant than type III collagen in ligamentous tissues, while other collagens such as types V, VI and XII occur in small amount. However, there was no visible difference in staining density between collagen I and III in the fibroblasts and the MSCs. A probable explanation for this phenomenon could be that the collagen III content was significantly increased during injury [237]. The quantitative ratio of collagen I to collagen III is important for the ultimate fibril diameter and functionality [238]. In the current study, the exact ratio was not determined and estimated less than its normal ratio. One potential concern is that the functionality of cells in 2D culture is different from 3D. However, we hope that our current study can provide a clue for better understanding.

The results from the immunohistochemistry assessment showed that the MSCs, as well as both the ACL fibroblasts and MCL fibroblasts, excreted type I and type III collagen, however, the amount of collagen from MSCs was about 40% more than that from ACL fibroblasts and MCL fibroblasts.

Fibroblasts play pivotal roles in connective tissue development, physiological

remodeling, and wound repair. These cells are likely to comprise heterogeneous populations [239]. Alpha-Smooth muscle actin is a functional marker for a fibroblast subtype (i.e. myofibroblast) that rapidly remodels the extracellular matrix [240]. Myofibroblasts containing α smooth muscle actin also play an important role in the healing process of rabbit medial collateral ligament [241] and maintaining human ACL [242]. Alpha-Smooth muscle actin also has been reported in rabbit, canine [243] and murine [244] MSC, but there is no report on rabbit ACL fibroblasts. As *in vitro* cell culture could increase α-smooth muscle actin expression [245, 246], there is still much to study in order to evaluate and quantify the content of α-smooth muscle actin expression *in vivo* as well as in tissue engineered ligaments.

This study has shown that rabbit MSCs have clear and distinct advantages over ACL fibroblasts and MCL fibroblasts, with respect to proliferation and collagen excretion rates. The cultured rabbit MSC were found to share the same collagen expression-types and α-smooth muscle actin as the ACL fibroblasts and MCL fibroblasts. Therefore, MSCs were shown to be a potentially a better cell source than ACL fibroblasts and MCL fibroblasts for tissue engineering repair and regeneration of ACL or any other ligamentous tissues.

3.2 Characterization of knitted scaffolds

3.2.1 Tetrazolium-based colorimetric assay (MTT)

PLLA and PLGA yarns were knitted into flat sheets before rolling up into tube-like scaffolds. In the current study, four needles were used to knit. Theoretically, more

needles (Up to 100) could be used to knit different sizes of knitted sheet and there is no limited length for the fabricated scaffolds. Current 6-cm yarns were designed for the ACL reconstruction in rabbits'. The acquired knitted scaffolds were blue porous scaffolds (Fig 32), while the porosity could decrease to some extent under slight tension (Fig 33).

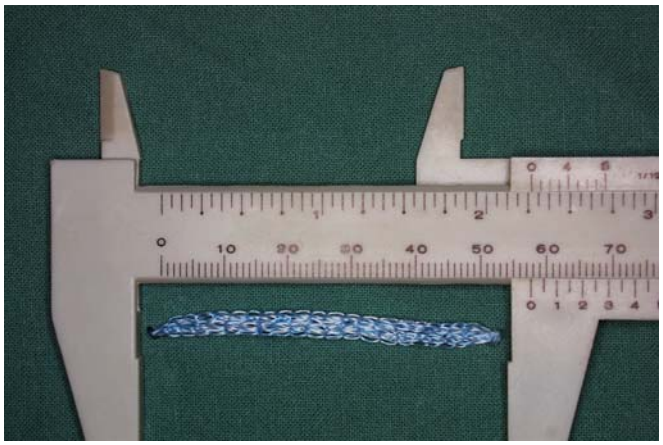

Figure 32 Knitted scaffolds

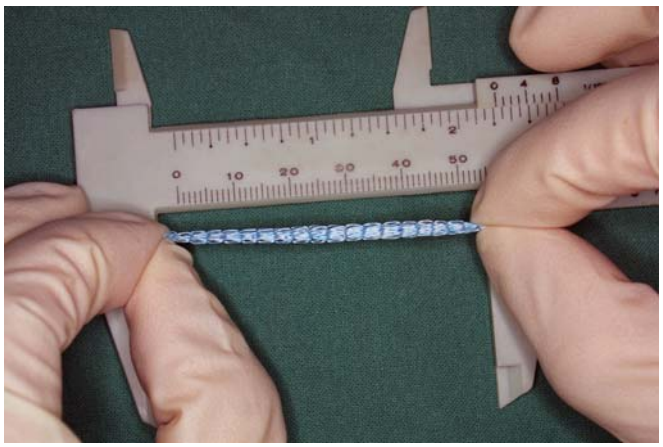

Figure 33 Knitted scaffold under slight tension

Current results showed that the knitted structures were free from contamination after sterilization (Fig 34), which was important for future tissue engineering applications.

The tetrazolium-based colorimetric assay (MTT) is a quantitative method for evaluating the biological response of cells to a foreign body in order to determine the sterility of the structures. Mesenchymal stem cells were used instead of characterized cell lines, which were more commonly used, because mesenchymal stem cells were a better loading cell source, compared to ACL fibroblasts and MCL fibroblasts in ligament tissue engineering with regards to proliferation rate and collagen excretion. Phenotypic characterization of acquired MSCs were confirmed based on their typical morphology, as well as osteogenic, adipogenic and chondrogenic differentiation [224].

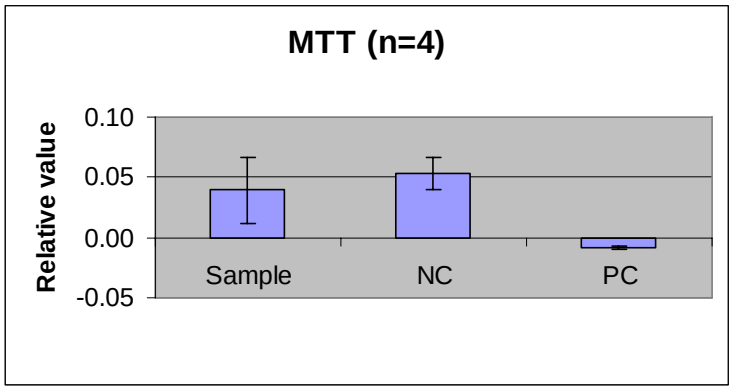

Figure 34 MTT results of the knitted structures

Sample: knitted structures, NC: negative control, PC: positive controls.

Biocompatibility, defined as "acceptance of an artificial implant by the surrounding biological tissue and by the body as a whole" [141], is an important factor for all implantable biomaterials. *In vitro* characterization of materials and the functional performance of prototypes are fundamental prerequisites prior to evaluation of their biocompatibility [142]. PLLA and PGLA have long been regarded as biocompatible

biomaterials, however, the knitted scaffolds made from these biomaterials need to be tested again due to potential contamination from fiber production and scaffold fabrication. It is also critical to ensure that no contaminant resides within the scaffold that can potentially aggravate the culture environment, while the scaffold degrades and becomes less compact.

3.2.2 *In vitro* cell loading on scaffold

MSCs adhered readily to the knitted structures and appeared elongated (Fig 35). As fibrin gel is a natural product, using it in the cell loading process could mimic in vivo interaction. The relationship between biomaterials and surrounding cells is an important factor, both *in vitro* and *in vivo*. Microfilaments in the cytoplasm can be connected with the cell membrane via intergrin structures, which can also bind to the RGD sequence of fibronectin or other adhesive proteins. These adhesive proteins can in turn bind to solid substrates such as the extracellular matrix components and other cells. This specific receptor is thus used to connect the cytoskeleton with extracellular adhesive sites via the intermediate fibronectin [247]. It is essential for structures used in ligament tissue engineering to allow easy adherence by surrounding cells, in vitro and in vivo. Though it has been reported that PLGA films could allow more MSCs to attach compared to PLLA films [248], there is still no report of cell attachments on fibrous scaffolds, as physical geometry could possibly affect migration, adhesion and attachment of the cells. However, MSCs which did not attach to fibers remained unpolarized (Fig 36).

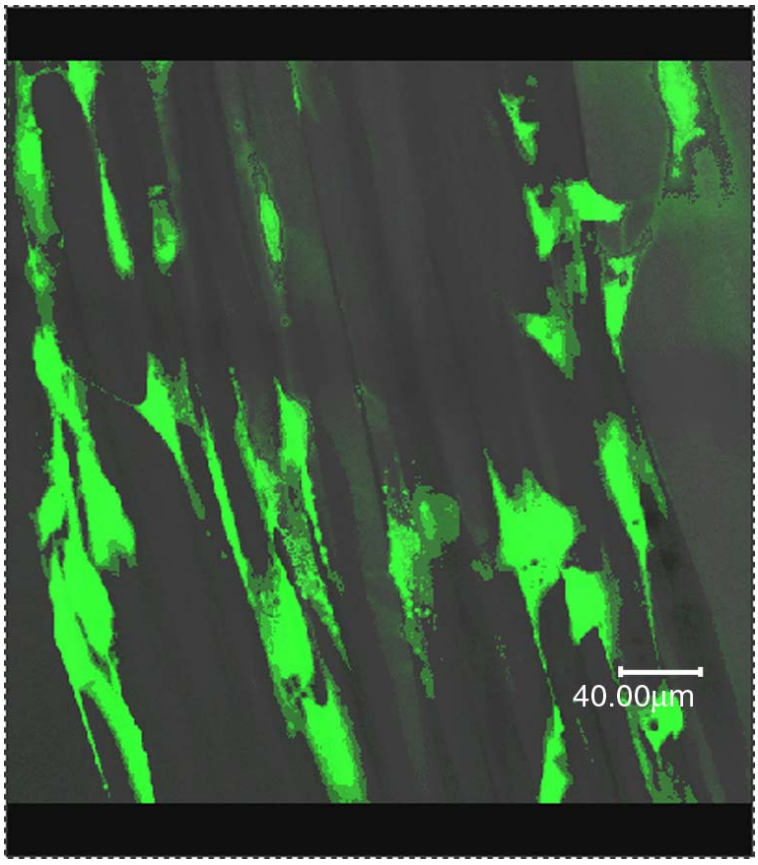

Figure 35 MSCs' attachment on knitted scaffolds

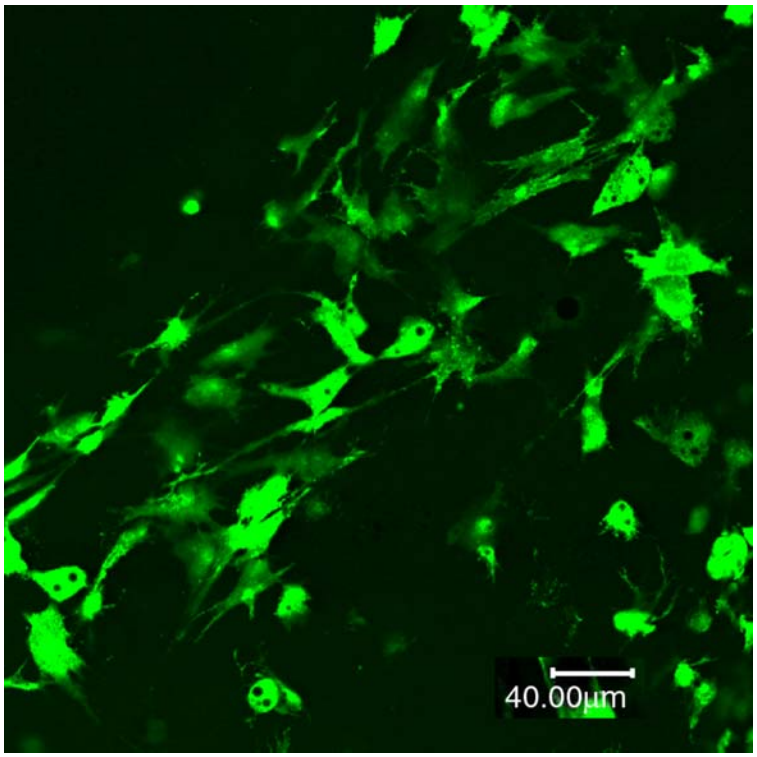

Figure 36 MSCs in fibrin glue

3.2.3 Porosity

The porosity of current knitted scaffolds was 44% (current knitted structures, table 7). It is important that tissue engineering scaffolds have sufficient porosity to accommodate tissue regeneration and nutrient exchange following implantation. Kim and Mooney (1996) pointed out that it is advantageous to have a polymer construct with a large surface area to volume ratio [249]. Such a construct provides a conduit for uniform cell delivery and development of high cell density. One of their criteria for an ideal scaffold was that the porosity should be at least 90% in order to provide a high surface area for cell-polymer interactions, sufficient space for extracellular matrix (ECM) regeneration, and minimal diffusion constraints during *in vitro* culture. However, when it came to considering *in*

vivo biodegradation, scaffolds with low porosity (relatively with low surface to volume ratio), could possibly be an advantage as the slow degradation would keep the integrity of the original constructs for a longer period of time, as hydrolysis of both PLLA and PLGA starts from surface [250]. To balance these two considerations, the porosity of 44% (current knitted structures) could possibly be a better combination of these two factors.

Table 7 Porosity of scaffolds

Diameter (μm)	Sample 1	Sample 2	Sample 3	Sample 4	Sample 5	Ave (μm)	Area (mm^2)	No. of yarns	Total areas (mm^2)
PLLA	166.3	178.2	173.2	178.2	187.0	176.6	0.0245	16	0.392
PLGA	126.9	119.7	122.0	124.6	124.4	123.5	0.012	8	0.096
Scaffold	1241.6	1091.5	1041.0	963.8	919.7	1051.5	0.87	24	0.87

3.2.4 *In vitro* degradation

During the 20 weeks of immersion, pH values of the immersing medium were always around 7.4, except for a minute decline below 7 at week 3 (Fig 37). In general, the trace amount of acidic degradation products, mainly from polymers of lactic acids and glycolic acids, will not interrupt the internal human environment by abrupt pH drop as they are rapidly cleared. Even at week 3, the low pH value may not happen in a real implantation scenario, as the degradation products will be continuously cleared in the living system,

unlike the situation in our experiment where the medium was changed once a week [251]. The drop in pH value at week 3 was possibly due to rapid degradation of PLGA.

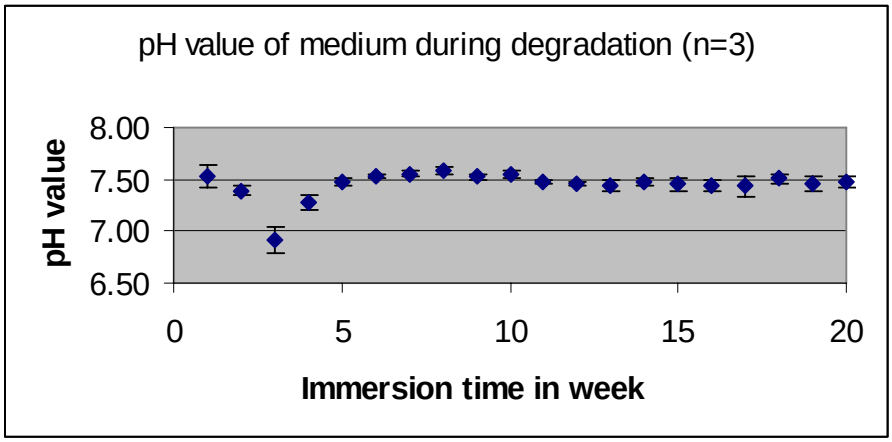

Figure 37 Change of pH value of immersion medium of PLLA/PLGA scaffolds

The mass of the knitted structures decreased with time following immersion as predicted (Fig 38). Two statistical significances have been observed, between initial weight and all remaining groups as well as between weight after 4 weeks and after 20 weeks (Table 8, One way ANOVA, LSD, $P< 0.05$). The first significance could possibly be attributed to relatively rapid degradation of PLGA, which could also be visually testified by loss of blue color of the scaffolds at initial stage (Fig 39) as well as the drop in pH value at week 3. The second significance is also reasonable. As mass loss of the scaffolds started gradually, it would become apparent after a certain time point, 20 weeks in this case. Blue PLGA yarns degraded faster than PLLA yarns as the knitted scaffolds almost lost their blue color after 8 weeks (Fig 39).

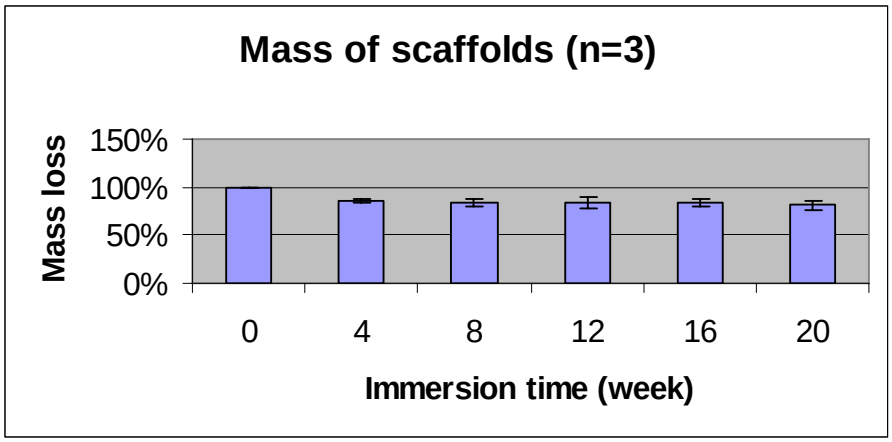

Figure 38 Mass losses of PLLA/PLGA scaffolds in in vitro degradation with time

Table 8 Mass loss percentage of knitted scaffolds after immersion **in medium**

(I) VAR	(J) VAR	Mean Difference (I-J)	Std. Error	Sig.	95% Confidence Interval	
					Lower Bound	Upper Bound
a.Original weight (100%)	b	.138(*)	.033	*.00*	.066	.210
	c	.166(*)	.033	*.00*	.095	.238
	d	.163(*)	.033	*.00*	.091	.235
	e	.160(*)	.033	*.00*	.088	.231
	f	.188(*)	.033	*.00*	.116	.259
b.weight at 4w (86.2%)	a	-.138(*)	.033	*.00*	-.210	-.066
	c	.028	.033	.40	-.043	.100
	d	.025	.033	.46	-.047	.097
	e	.022	.033	.52	-.050	.094
	f	.050	.033	.16	-.022	.122
c.weight at 8w (83.4%)	a	-.166(*)	.033	.00	-.238	-.095
	b	-.028	.033	.40	-.100	.043
	d	-.003	.033	.92	-.075	.068
	e	-.007	.033	.84	-.078	.065
	f	.021	.033	.53	-.050	.093
d. weight at 12w (83.7%)	a	-.163(*)	.033	.00	-.235	-.091
	b	-.025	.033	.46	-.097	.047
	c	.003	.033	.92	-.068	.075
	e	-.003	.033	.92	-.075	.068
	f	.025	.033	.47	-.047	.096
e. weight at 16w (84.0%)	a	-.160(*)	.033	.00	-.231	-.088
	b	-.022	.033	.52	-.094	.050
	c	.007	.033	.84	-.065	.078
	d	.003	.033	.92	-.068	.075
	f	.028	.033	.41	-.044	.100
f. weight at 20w (81.2%)	a	-.188(*)	.033	.00	-.259	-.116
	b	-.050	.033	.16	-.122	.022
	c	-.021	.033	.53	-.093	.050
	d	-.025	.033	.47	-.096	.047
	e	-.028	.033	.41	-.100	.044

*LSD, * the mean difference is significant at the .05 level*

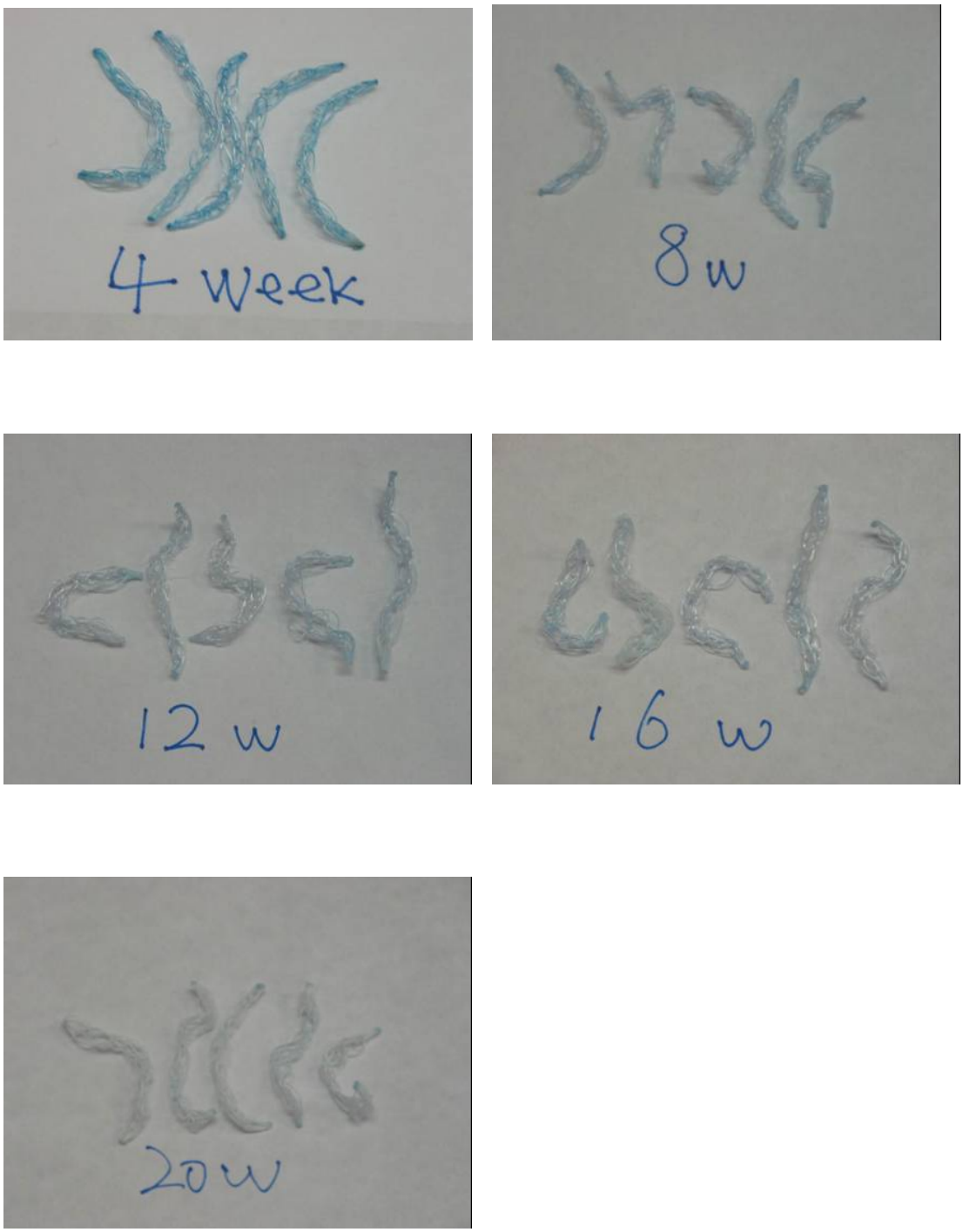

Figure 39 Macroscopic change of knitted PLLA/PLGA scaffolds immersed in medium

The molecular weights of PLLA at different immersion durations were measured. As the rapidly degradable PLGA was used to promote potential tissue ingrowth at a initial stage of implantation as well as to provide more space for regeneration at the later stage, its molecular weight was not examined. Their degradation could be identified by the loss of blue color in the knitted scaffolds. On the other hand, they did not dissolve in chloroform, which was used to dissolve PLLA for the GPC test (Fig 40). Hence, the existence of PLGA would not interrupt PLLA's molecular weight test. There was a descending trend in molecular weights of PLLA with time (Fig 41) as drop of molecular weight usually started earlier than mass loss [61]. However, there was no statistical significance until 12 weeks, possibly due to small differences between different groups. Further decline in molecular weight at 16 and 20 weeks was attributed to the statistical significance between them and other groups (Table 9 and 10, One Way ANOVA, LST, $P<0.05$).

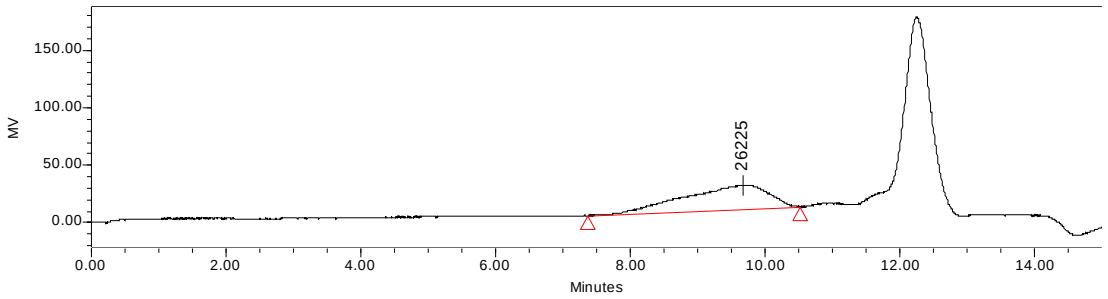

Figure 40 Graph from gel permission chromatography (GPC) of PLLA.

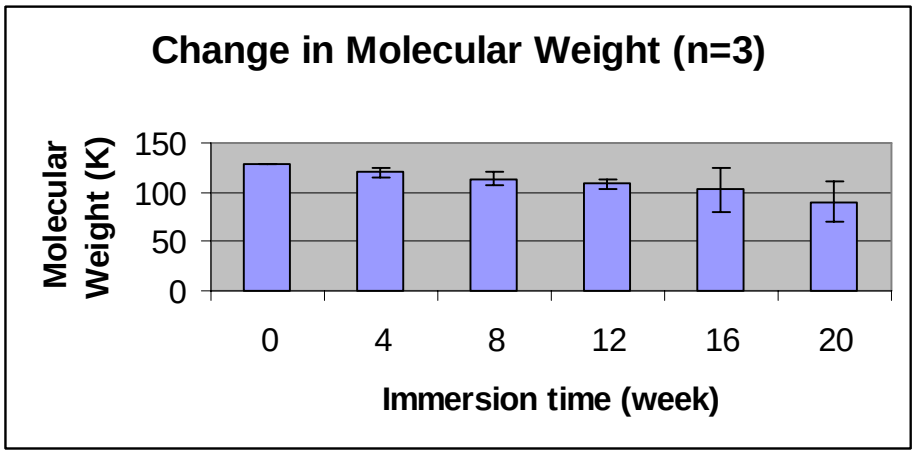

Figure 41 Changes in molecular weight

Table 9 Change of molecular weight during immersion

	original	4w	8w	12w	16w	20w
MW	127748	123491	107043	114139	127388	110760
	128381	122040	120637	107500	93486	89247
	128061	114775	113490	103580	86838	70020
average	128065	120102	113723	108406	102571	90009

Table 10 Multiple comparisons of molecular weights (MW)

(I) VAR	(J) VAR	Mean Difference	Std. Error	Sig.	95% Confidence Interval	
Molecular Weight					Lower Bound	Upper Bound
a. Original MW (128065)	b	7961	10461	.461	-14832	30755
	c	14340	10461	.196	-8454	37134
	d	19657	10461	.085	-3137	42451
	e	25493(*)	10461	.031	2699	48286
	f	38054(*)	10461	.003	15261	60848
b. MW at 4w (120102)	a	-7961	10461	.461	-30755	14833
	c	6379	10461	.553	-16415	29173
	d	11696	10461	.285	-11098	34489
	e	17531	10461	.120	-5262	40325
	f	30093(*)	10461	.014	7299	52887
c. MW at 8w (113723)	a	-14340	10461	.196	-37134	8454
	b	-6379	10461	.553	-29172	16415
	d	5317	10461	.620	-17477	28111
	e	11153	10461	.307	-11641	33946
	f	23714(*)	10461	.043	921	46508
d. MW at 12w (108406)	a	-19657	10461	.085	-42451	3137
	b	-11696	10461	.285	-34490	11098
	c	-5317	10461	.620	-28111	17477
	e	5836	10461	.587	-16958	28630
	f	18397	10461	.104	-4396	41191
e. MW at 16w (102571)	a	-25493(*)	10461	.031	-48286	-2699
	b	-17531	10461	.120	-40325	5262
	c	-11153	10461	.307	-33946	11641
	d	-5836	10461	.587	-28629	16958
	f	12562	10461	.253	-10232	35355
f. MW at 20w (90009)	a	-38054(*)	10461	.003	-60848	-15261
	b	-30093(*)	10461	.014	-52887	-7299
	c	-23714(*)	10461	.043	-46508	-921
	d	-18397	10461	.104	-41191	4396
	e	-12562	10461	.253	-35355	10232

- *LSD, The mean difference is significant at the .05 level.*

The main parameters which influence the polymer biodegradability are polymer

crystallinity, hydrophilicity, composition and form of the product. PLLA degraded by backbone breakage caused by water penetration. This can be rephrased “as the hydrophilicity of the polymer is increased so is its biodegradability,” because the solvent in the biological media is basically water with quite a high salt content [250]. Slow degradation of semicrystalline PLLA due to relatively hydrophobic property could be attributed to its usage in the potential ligament tissue engineered structures.

For tissue engineering, the ability to control the degradability of the biomaterials becomes critical for completion of the assigned function. The ideal rate of degradation should not exceed the rate of tissue regeneration, especially with regards to mechanical strength. In spite of the large number of investigations dealing with PLA, PGA and their copolymers, they still degrade at varying rates when implanted in various locations and under different mechanical stimuli. Recent data obtained from *in vitro* ageing experiments under physiological conditions showed that initial morphology and subsequent morphology changes were very important factors in determining the degradation behaviors of these polymers [252]. Thus current study of degradation of knitted structures remains meaningful after many related research investigations have been reported.

Design of the current *in vitro* degradation experiment was based on ISO standard 13781, “ Poly(L-lactide) resins an fabricated forms for surgical implants-*in vitro* degradation testing”, with small revisions. Cell culture medium was used instead of standard soaking solution, as the current structures could possibly be immersed in it during future *in vitro* and *in vivo* cell loading procedures and bioreactor incubation.

3.2.5 Mechanical properties

3.2.5.1 Tensile properties

Cross-sectional areas of knitted scaffolds (Fig 42) decreased sharply in the initial 4 weeks and then kept relatively stable until 20 weeks (Fig 43). The data showed that PLLA fibers almost kept their morphological integrity for the initial 20 weeks, after quick loss of PLGA fibers. It was also supported by morphological study. There was a significant difference between cross-sectional area at the initial stage and at subsequent time points, but there were no significant difference between those cross-sectional areas from 4 to 20 weeks (Table 11).

Figure 42 Image of transverse cross-section of scaffolds under microscope at 8 week (50x)

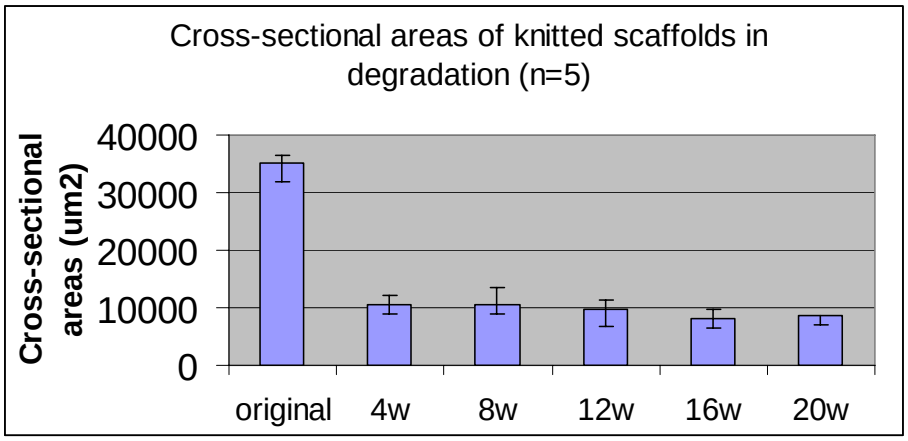

Figure 43 Cross-sectional areas of knitted scaffolds in degradation

Table 11 Cross-sectional areas of knitted scaffolds in degradation

(I) VAR (μm^2)	(J) VAR (μm^2)	Mean Difference (I-J)	Std. Error	Sig.	95% Confidence Interval	
					Lower Bound	Upper Bound
a. Areas at time 0 (35102)	b	24663(*)	1389	.000	21797	27529
	c	24496(*)	1389	.000	21630	27362
	d	25402(*)	1389	.000	22536	28268
	e	26914(*)	1389	.000	24048	29780
	f	26396(*)	1389	.000	23530	29262
b. Areas at week 4 (10439)	a	-24663(*)	1389	.000	-27529	-21797
	c	-167	1389	.906	-3033	2699
	d	739	1389	.599	-2127	3605
	e	2252	1389	.118	-614	5118
	f	1733	1389	.224	-1133	4599
c. Areas at week 8 (10606)	a	-24496(*)	1389	.000	-27362	-21630
	b	167	1389	.906	-2699	3033
	d	906	1389	.520	-1960	3772
	e	2418	1389	.094	-448	5284
	f	1900	1389	.184	-966	4766
d. Areas at week 12 (9700)	a	-25402(*)	1389	.000	-28268	-22536
	b	-739	1389	.599	-3605	2127
	c	-906	1389	.520	-3772	1960
	e	1512	1389	.287	-1354	4378
	f	994	1389	.481	-1872	3860
e. Areas at week 16 (8187)	a	-26914(*)	1389	.000	-29780	-24048
	b	-2252	1389	.118	-5118	614
	c	-2418	1389	.094	-5284	448
	d	-1512	1389	.287	-4378	1354
	f	-518	1389	.712	-3384	2348
f. Areas at week 20 (8706)	a	-26396(*)	1389	.000	-29262	-23530
	b	-1733	1389	.224	-4599	1133
	c	-1900	1389	.184	-4766	966
	d	-994	1389	.481	-3860	1872
	e	518	1389	.712	-2348	3384

LSD, The mean difference is significant at the .05 level.

The stress-strain behavior of the scaffold displays the characteristic toe, linear, yield and failure regions that are typically found in stress-strain curves of tendons and

ligaments [20] (Fig 44). The modulus generally increased with degradation time (Fig 45 and table 12). Similarly the ultimate tensile strength as well as strain generally decreased with degradation time (Fig 46 and 47, table 13). This trend has also been observed in other *in vitro* degradation studies [253, 254]. The increase in crystallinity during degradation at the amorphous regions are first hydrolyzed which resulted in a higher Young's modulus with degradation time. The simultaneous increase in mass loss and decrease in molecular weight at the same time resulted in more defects within the scaffold and thus reduced the ultimate tensile strength and strain [255].

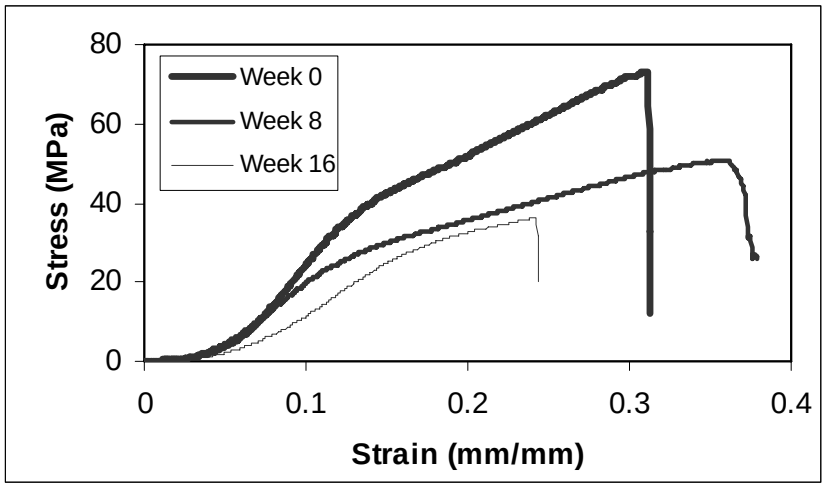

Figure 44 Typical stress-strain plots of PLLA/PGLA scaffolds at different duration of immersion

- *linear elastic region is from 0.07 to 0.14 strains in Figure 44.*

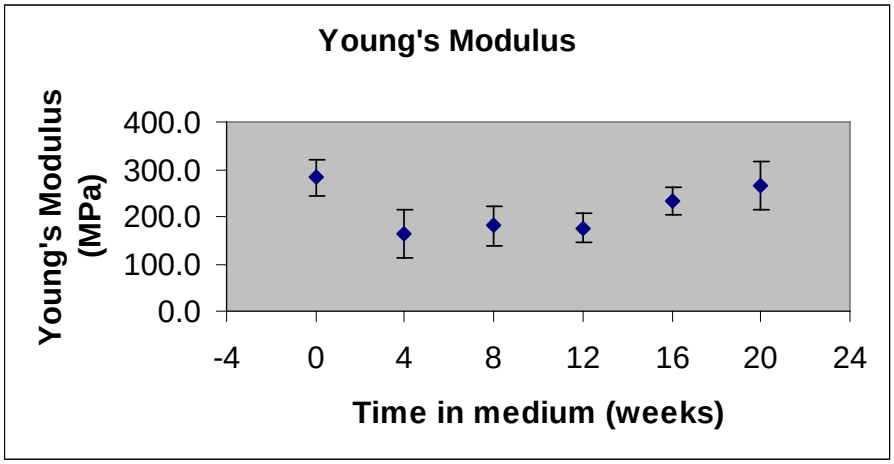

Figure 45 Young's modulus of the knitted scaffolds after immersion

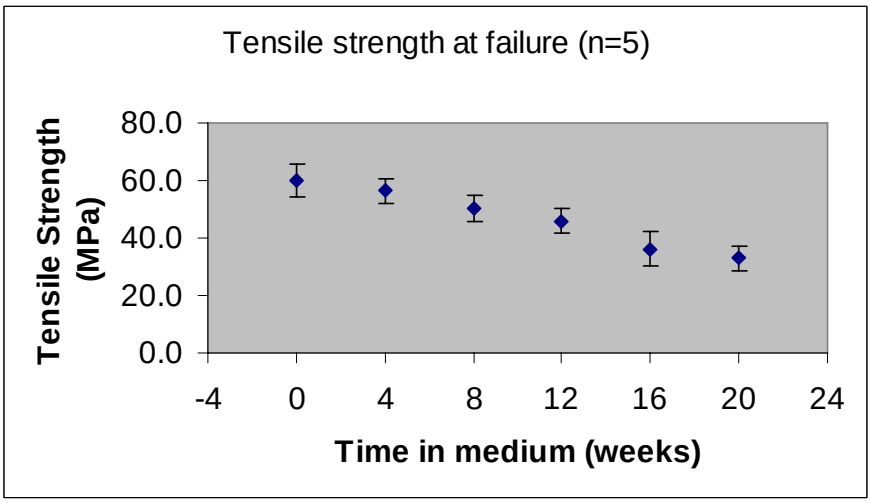

Figure 46 Tensile strength at failure of the knitted scaffolds after immersion

Table 12 Multiple comparisons of Young's Modulus in *in vitro* degradation

.

(I) VAR	(J) VAR	Mean Difference (I-J)	Std. Error	Sig.	95% Confidence Interval	
					Lower Bound	Upper Bound
a. Young's Modulus at time 0 (283 MPa)	b	119(*)	25	.000	67	171
	c	101(*)	25	.001	49	154
	d	106(*)	25	.000	53	158
	e	50	25	.059	-2	103
	f	17	25	.514	-36	69
b. Young's Modulus at week 4 (163 MPa)	a	-119(*)	25	.000	-171	-67
	c	-18	25	.494	-70	35
	d	-13	25	.608	-66	39
	e	-69(*)	25	.012	-121	-16
	f	-102(*)	25	.000	-155	-50
c. Young's Modulus at week 8 (181 MPa)	a	-101(*)	25	.001	-154	-49
	b	17	25	.494	-35	70
	d	4	25	.864	-48	57
	e	-51	25	.055	-104	1
	f	-85(*)	25	.003	-137	-32
d. Young's Modulus at week 12 (176 MPa)	a	-106(*)	25	.000	-158	-53
	b	13	25	.608	-39	66
	c	-4	25	.864	-57	48
	e	-56(*)	25	.038	-108	-3
	f	-89(*)	25	.002	-141	-37
e. Young's Modulus at week 16 (232 MPa)	a	-50	25	.059	-103	2
	b	69(*)	25	.012	16	121
	c	51	25	.055	-1	104
	d	56(*)	25	.038	3	108
	f	-33	25	.200	-86	19
f. Young's Modulus at week 20 (265 MPa)	a	-17	25	.514	-69	36
	b	102(*)	25	.000	50	155
	c	84(*)	25	.003	32	137
	d	89(*)	25	.002	37	141
	e	33	25	.200	-19	86

LSD, * The mean difference is significant at the .05 level. Multiple comparisons

Table 13 Multiple comparisons of tensile strength in *in vitro* degradation

(I) VAR	(J) VAR	Mean Difference (I-J)	Std. Error	Sig.	95% Confidence Interval	
					Lower Bound	Upper Bound
a. Strength at time 0 (60.2 MPa)	b	3.9	3.1	.227	-2.6	10.3
	c	9.8(*)	3.1	.004	3.4	16.2
	d	14.2(*)	3.1	.000	7.8	20.6
	e	23.9 (*)	3.1	.000	17.4	30.3
	f	27.2(*)	3.1	.000	20.8	33.6
b. Strength at week 4 (56.3MPa)	a	-3.9	3.1	.227	-10.3	2.6
	c	6.0	3.1	.067	-.5	12.4
	d	10.3 (*)	3.1	.003	3.9	16.7
	e	20.0 (*)	3.1	.000	13.6	26.5
	f	23.3 (*)	3.1	.000	16.9	29.7
c. Strength at week 8 (50.4 MPa)	a	-9.8 (*)	3.1	.004	-16.2	-3.4
	b	-6.0	3.1	.067	-12.4	.5
	d	4.4	3.1	.174	-2.1	10.8
	e	14.1(*)	3.1	.000	7.7	20.5
	f	17.4(*)	3.1	.000	10.9	23.8
d. Strength at week 12 (46.0 MPa)	a	-14.2(*)	3.1	.000	-20.6	-7.8
	b	-10.3 (*)	3.1	.003	-16.7	-3.9
	c	-4.4	3.1	.174	-10.8	2.1
	e	9.7 (*)	3.1	.005	3.3	16.1
	f	13.0 (*)	3.1	.000	6.6	19.4
e. Strength at week 16 (36.3 MPa)	a	-23.9 (*)	3.1	.000	-30.3	-17.5
	b	-20.0 (*)	3.1	.000	-26.5	-13.6
	c	-14.1(*)	3.1	.000	-20.5	-7.7
	d	-9.7 (*)	3.1	.005	-16.1	-3.3
	f	3.3	3.1	.302	-3.1	9.7
f. Strength at week 20 (33.0 MPa)	a	-27.2(*)	3.1	.000	-33.6	-20.8
	b	-23.3 (*)	3.1	.000	-29.7	-16.9
	c	-17.4(*)	3.1	.000	-23.8	-10.9
	d	-13.0 (*)	3.1	.000	-19.4	-6.6
	e	-3.3	3.1	.302	-9.7	3.1

* The mean difference is significant at the .05 level. Multiple comparisons, LSD

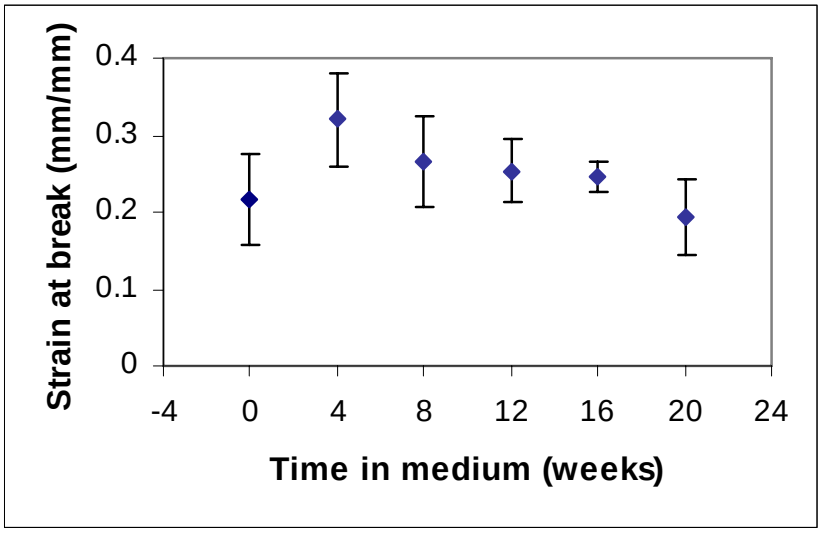

Figure 47 Tensile strain at break of the knitted scaffolds after immersion

The initial reduction in Young's modulus and increase in ultimate strain between week 0 and week 4, indicated that the scaffold became less stiff but more ductile. This trend is contrary to that observed at subsequent degradation times, as week 0 samples were not immersed in the medium at 37°C prior to tensile test, which was required by ISO standard 13781 that the initial values for all tests should be determined directly before starting the degradation test (time zero). The combined effect of immersion at an elevated temperature of 37°C in the medium could have resulted in some structural changes of the scaffold before the effects of hydrolysis became significant.

The Young's modulus of the scaffold at various durations of immersion in the medium range from 146% to 238% that of the value reported for human ACL [18]. In general, the Young's modulus value for human anterior cruciate ligament is 111MPa, ultimate

tensile strength is at least 38MPa [18], while ultimate mechanical properties of ligaments generally increase during development and then diminish with aging [19]. The ultimate tensile strength before 12 weeks of immersion in medium satisfies the minimum reported strength of 38MPa, while ultimate tensile strength at 16 weeks and 20 weeks account for 95% and 87% of it, respectively. It is possible that the new ligament tissue which regenerated within 12-16 weeks is sufficient to withstand the *in vivo* stresses as the tensile strength of the scaffold is reduced significantly after 16 weeks. Any compliance mismatch (difference in Young's modulus) between tissue and scaffold could result in failure of the implant [217, 256]. However, current structures should undergo more revisions before clinical application as tissue engineered ligaments, such as cell loading, extracellular matrix deposition and collagen cross-linking, pre-conditioning, influence of mechanical stimuli in bioreactors, biomembrane wrap. All these procedures would possibly alter the final Young's modulus and ultimate tensile strength. Hence, the results of the ultimate tensile strength and Young's modulus of current constructs being similar to that of human ACL, would definitely advocate their future applications.

The strains at failure fell between 19.4-32% after 20 weeks of immersion. There is much controversy about ACL strain at failure, due to the differences of mechanical procedures and standards of failure. Further loading beyond the toe region produces a nearly linear curve, when fibers lose their crimp and become parallel. The upper strain limit of this linear region is 2-5% and then collagen fiber failure begins at 7-8% strain—[257]. The maximum strain that a ligament can endure before failure is between12-15% strains [258]. A further 20-40% apparent linear region was reported after previous maximum strain

when the properties of whole ligaments were examined [259], while there were several possible artifacts in the testing technique. First, the initial failure of a small number of collagen fibers was not detected when it didn't decrease the load carrying ability of the ligament as a whole. Second, the measurement of the slippage between the grips provides an overestimation of the true tissue strain in the absence of high speed video recording. Third, preconditioning to align the individual fibers and different strain rates used in different experiments also contributed the differences [260, 261]. The current results almost match that of normal ACL, when ligaments were tested as a whole

3.2.5.2 Viscoelastic properties

The stress needed to sustain a constant elongation decreased with time (Fig.48) and the strain required to sustain a constant load increased with time (Fig.49) indicating that the scaffold behaves in a viscoelastic manner under mechanical loading, similar to normal ACLs [260-262]. Table 14 shows the viscoelastic properties of the scaffold obtained from the relaxation test. The data from the constant load creep test were analyzed in a similar manner to the relaxation test (Table 15). The purpose of using normalized stress and strain is to eliminate the effect of initial applied strain and stress in relaxation and creep tests respectively.

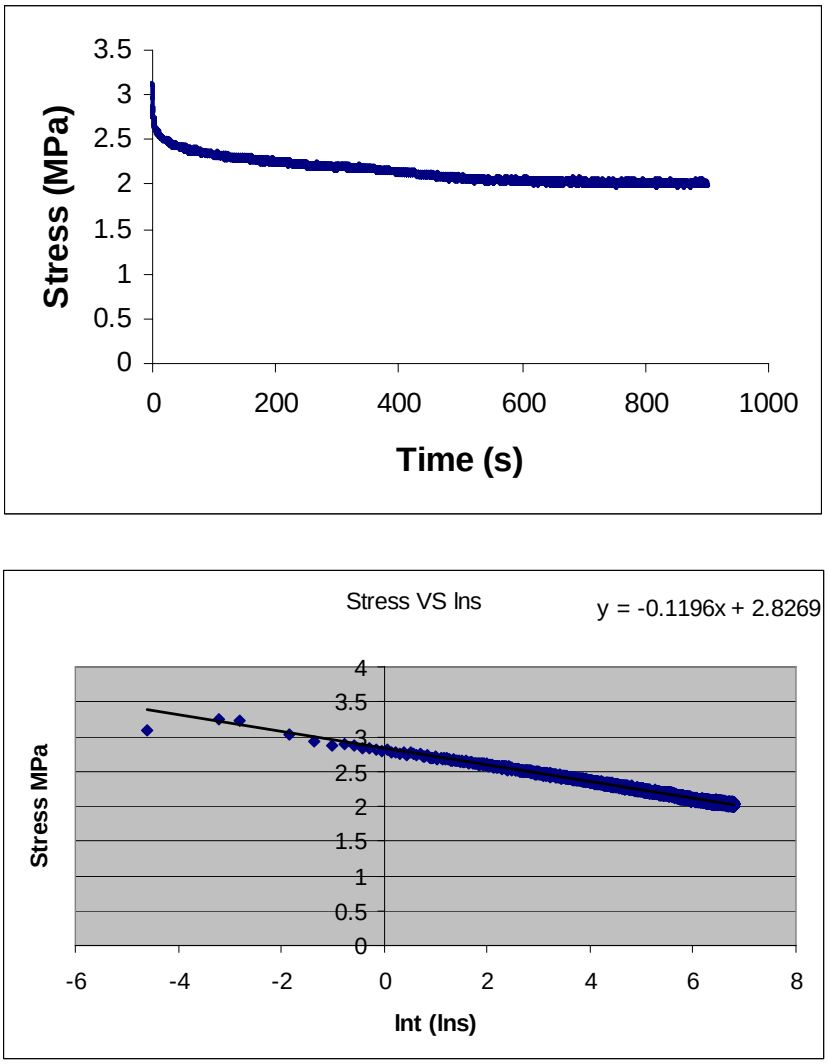

Figure 48 Stress relaxation curve of PLLA/PLGA scaffold with initial strain of 2.5%

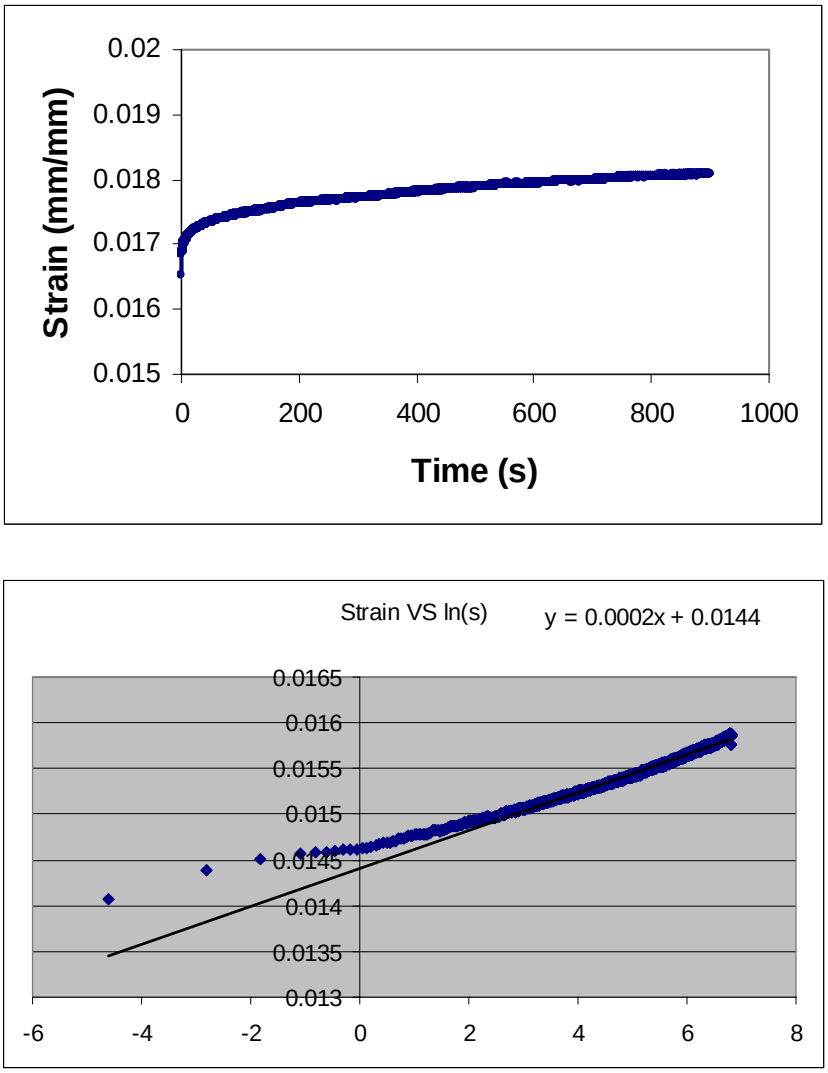

Figure 49 Creep curve of PLLA/PLGA scaffold with initial load of 1.5N

Table 14 Viscoelastic quantities from the relaxation test

Initial Stress	Final Stress	Normalized Stress

(MPa)	(MPa)	Relaxation Rate (1/ln(s))
3.4 ± 0.3	2.1 ± 0.3	-0.041 ± 0.009

Table 15 Viscoelastic quantities from the creep test

Initial Strain (mm/mm)	Final Strain (mm/mm)	Normalized Strain Creep Rate (1/ln(s))
0.016 ± 0.002	0.018 ± 0.002	0.013 ± 0.001

The normalized stress relaxation rate is obtained by finding the slope of the normalized stress vs ln(t) strain plot. The normalized stress is obtained by dividing the stress values by the initial stress immediately. The logarithmic operation on the time axis transformed the inherently nonlinear relation in load decay vs time into a linear relation such that a simple linear regression could be used to determine the rates of relaxation.

The normalized stress relaxation rate obtained (-0.041 /ln(s)) is comparable to that obtained by Donahue *et al* [263] in their study of anterior cruciate ligament (ACL) grafts made from bovine digital extensor (-0.038 /ln(s)) and human hamstring tendons (-0.036 /ln(s)). The normalized strain creep rate (0.013 /ln(s)), however, is lower than that obtained although it is of the same order of magnitude. Normalized strain creep rate for bovine digital extensor is 0.029 1/ln(s) and that for human hamstring tendons is 0.025 1/ln(s). The difference is probably due to the different testing methodologies and the fact that different materials are used (i.e. biological samples vs polymeric scaffold). However, the proximity of the values indicates that the PLLA/PLGA scaffold is possibly a

viable implant for ACL regeneration in terms of viscoelastic behavior.

Over the past 10 years, huge efforts were made to develop biomaterials that could be considered as "ideal" scaffolds for cell growth, however, few have reached clinical efficacy. Regardless of the source or type of biomaterials, they have to be biocompatible and mechanically compatible with native tissues to fulfill their desired role. A few of them have been reported suitable for ligament tissue engineering, when both appropriate mechanical properties and general requirements from tissue engineering are required [264].

The knitted PLLA/PLGA structures developed here can fulfill many of the requirements proposed for prospective candidates in ligament tissue engineering, with regards to porosity, cell attachment, degradation rate and mechanical properties. However, more research has to be carried out to improve and revise the mechanical properties of current knitted scaffolds before they can finally been used in clinical practice.

3.3 Rabbit ACL reconstruction

3.3.1 Fate of implanted cultured rabbit MSC

MSCs were fully stained and retained their previous morphology before transplantation (Fig 50). During the staining procedure, a small amount of MSCs (10-20%) detached. It was noticeable that not all MSCs were stained with the same intensity.

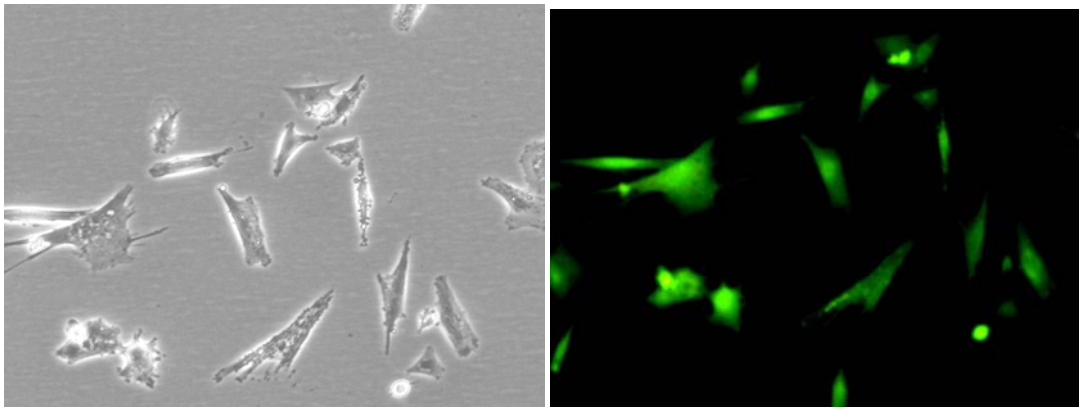

Figure 50 cFDA stained MSCs (100x)

Note: left pictures show normal morphology of MSC while fluorescence from cFDA stained MSC was found under fluorescent microscope.

Previous studies had reported the survivability of donor cells implanted in knee joints. These donor cells can survive for up to 4 to 6 weeks [234-236]. Unlike our study, these studies were performed with different cell sources, animal models and implantation sites. It would be difficult to make comparisons, as the donor cells may have differences in immunological response, potential blood supply and fascia protection, etc. Since our results showed that MSCs have the best potential as a cell source for tissue engineering applications, it was necessary to determine the fate of heterologous MSCs when used in the repair and regeneration of ACL. Implanted allogeneic MSC had been reported to play an essential role in graft facilitation in an allogeneic environment [265]. It has also been shown to exhibit a suppressive effect on T-lymphocyte responses in an *in vitro* study by Klyushnenkova *et al* (1998) [266]. Therefore, it is likely that implanted allogeneic MSCs should only face a mild immunological response and the probability of survival in an allogeneic environment should also be relatively good. This was demonstrated in this

study.

After eight weeks' implantation, the cFDA stained MSCs could still be found in both group II (MSC loading, Fig 51) and group III (MSC loading and fascia cover, Fig 52). The acquired results matched those of previous publications. In natural anatomy, the ACL is an intra-articular and extra-synovial structure, which is covered by a synovial membrane isolating it from the synovial fluid. A simple break in the synovial covering may lead to destruction of the ligament's integrity through exposure to the synovial fluid environment and also by compromising the vascular supply [267]. The pedicle fascia used in this study was supposed to provide the extra protective covering for loading MSCs while preventing the MSCs from diffusing into the knee joint as the fibrin glue usually degrades in one week [268].

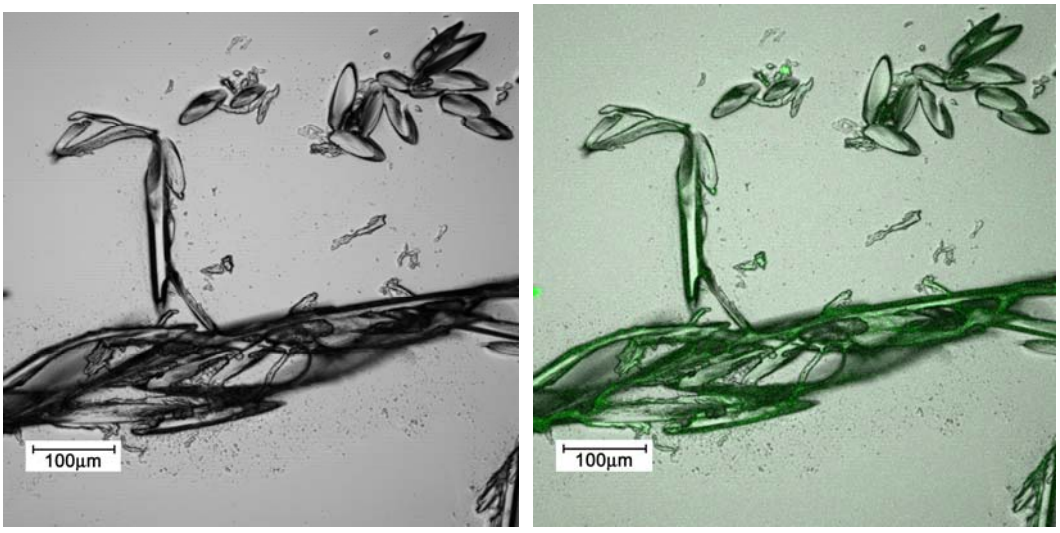

Figure 51 cFDA stained MSCs after 8 weeks' implantation from group II (MSCs)

Left picture shows section of scaffolds after 8 weeks' implantation. Note the varying

cross-sections of knitted scaffolds. In right picture, fluorescence denotes the cFDA stained MSCs around the scaffolds.

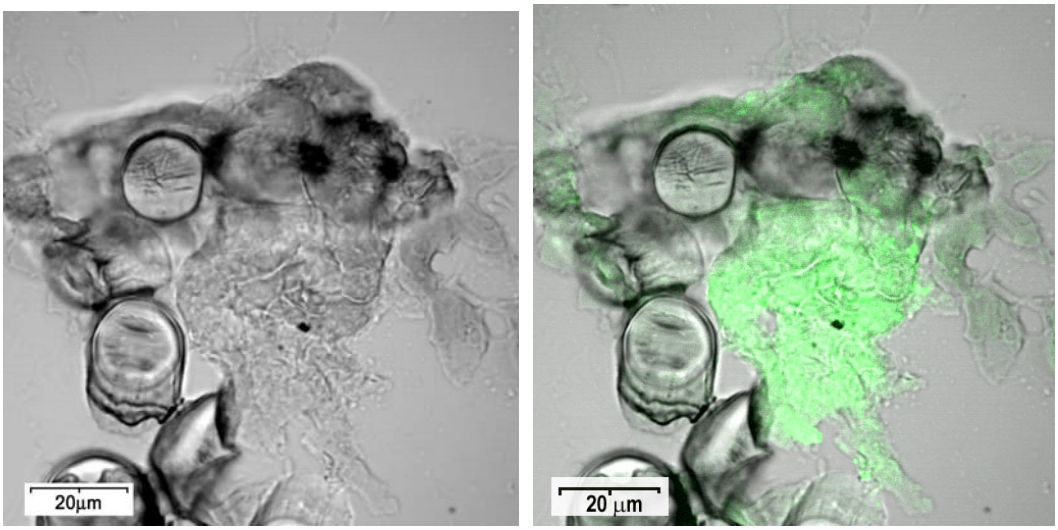

Figure 52 cFDA stained MSCs after 8 weeks' implantation (group III, MSCs and fascia)

Left picture shows section of scaffolds after 8 weeks' implantation. In right picture, fluorescence denotes the cFDA stained MSCs around the scaffolds.

3.3.2 Considerations in scaffold design

Though both Young's modulus and maximal tensile strength were lower than that of normal ACL, both of them could still meet the basic requirements of ACL reconstruction in a 20 week *in vitro* degradation test, partly because biological tissues are subjected to forces ranging from 10% to 25% of their braking loads in normal conditions [261]. Based on previous experiences with knitted scaffolds, diameters of knitted scaffolds will increase with fibroblasts ingrowths when implanted *in vivo* [269]. In the meantime, there was neither increment in the initial cross-sectional area of graft nor tightening of grafts

resulting in superior graft properties, whereas, however, larger grafts would lead to increased cartilage degeneration, osteogenesis, and flexion contractures [270]. On the other aspect, maximal tensile strength of PLLA scaffolds used for ACL reconstruction would be expected to increase with time [37], possibly due to fibroblasts in-growth and subsequent functionality, but unlike what happened *in vitro*, the maximal tensile strength dropped over time due to degradation of polymers [126]. Based on all these knowledge, we tried to employ structures with diameters smaller than normal, to reconstruct ACLs to avoid the consequent increase in diameters, which would inevitablely increase pressure on knee cartilage and deterioration so as to meet the basic requirements for ACL reconstruction. One potential drawback of a knitted structure is that the whole structure will collapse when any one slot breaks. To circumvent it, two independent fine knitted scaffolds were chosen, instead of a larger one, as the scaffolds would not only undergo degradation and mechanical stress *in vivo*, but would also face difficulties going through bone tunnels and being sutured to the periosteum. All these activities would potentially break some of the fibers, even the yarns of scaffolds, which ultimately could cause the collapse of the whole structure.

In our previous study, the knitted PLLA/PGLA scaffolds were found to be non-toxic and had good porosity as well as cell adhesion property. In a 20-week *in vitro* degradation test, both maximal mechanical strength and Young's modulus of the knitted scaffolds could meet the basic requirements of ACL reconstruction. In the design of scaffold for this study, small overall diameter scaffolds were used to reconstruct ACLs instead of larger ones, for the following three reasons: 1) Cummings et al (2002) had

shown that by increasing the initial graft cross-sectional area or having taut grafts will not improve graft mechanical properties, while larger grafts would lead to increased cartilage degeneration, osteogenesis, and flexion contractures [270]; 2) diameters of knitted scaffolds would increase with fibroblast ingrowths when implanted *in vivo* [269]; 3) maximal tensile strength of PLLA scaffolds used for ACL reconstruction would increase with time [37], possibly due to fibroblast in-growth and subsequent functionality [126], but unlike what happened *in vitro*, the maximal tensile strength dropped over time due to degradation of polymers.

When compared with ACL reconstruction using cross-linked collagen in a similar rabbit experiment [271], survival rates of current constructs was higher and they incurred less immuno-response. Though no mature collagen bundle has been reported in tissue engineered ACL research, there are many reports on relatively more mature ACL regeneration, such as formation of collagen fibers, orientations and crimps.[128, 177] Two reasons could be attributed to inferior collagen fiber formation and orientations in the current study; first, PLLA has inferior ability to encourage fibroblasts to attach and function, mainly due to lack of a RGD sequence in collagen [146]; second, the relatively short implantation period impede further maturation of ingrowth fibroblasts and extracellular matrix, when compared with a 48 weeks [177] or one year study [35].

Though PLLA and PGLA have long been regarded as biocompatible biomaterials, the knitted scaffolds made of these biomaterials have to be tested again due to potential contamination from fiber production and knitting procedure. Though results from

tetrazolium-based colorimetric assay (MTT) in previous studies had shown that the knitted structures were free of contamination, further in vivo in situ study was still necessary to examine the host's response.

3.3.3 Histology of tissue engineered ACL

The foreign body reaction to biomaterials is theoretically inevitable, which include foreign body giant cells and the components of granulation tissue: macrophages, fibroblasts and capillaries in varying amounts depending on the form and topography of the implanted materials [272]. Macrophages and capillaries were difficult to find in all of histological samples. Possible explanations were that the PLLA and PGLA used were quite biocompatible and did not induce a significant immune response, as well as knee joints being a special environment lacking conditions for the growth of capillaries.

3.1.3.1 Histology at 4 week

The presence of clear synovial fluid, good topography of cartilage surface and no visible granulation formation around the structures indicated that no strong foreign body reactions and chronic inflammation reactions were caused by knitted scaffolds (Fig 51), while prosthetic ligament inevitably caused synovitis [272]. On the other aspect, no morphologic change of scaffolds could be found. All the results provided good basis for our study to continue.

Figure 53 Frontal view of knee joint 4 weeks after ACL reconstruction with scaffolds

After 4 weeks' implantation, in-growth of fibroblasts and small amount of extracellular matrix could be found around the yarns of scaffolds (Fig 54). There was no difference among different groups, except that there were paralleled fibroblasts and well layered mature extracellular matrix in out-layers of tissue engineered ligament from group III and IV (Fig 55), which came from fascia wrap used.

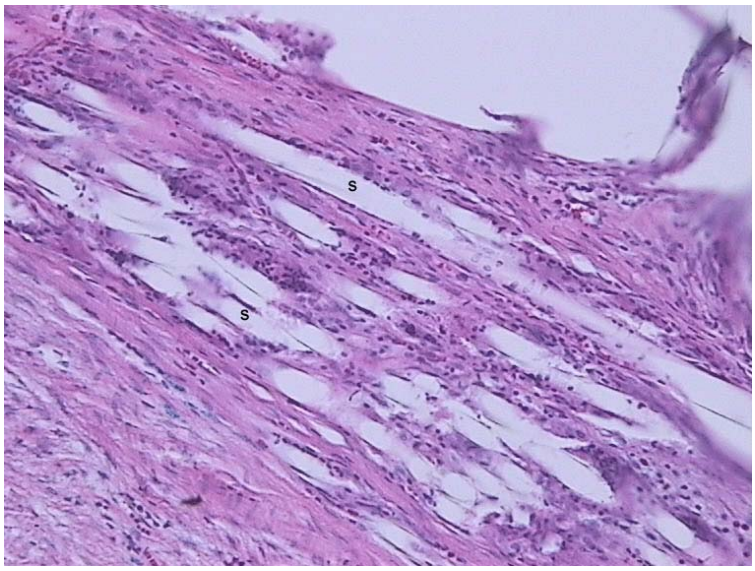

Figure 54 Histology of tissue engineered ligament at 4 weeks (Group I, H&E staining, 100x)

Note: irregular transparent forms (s) were cross-section of yarns of scaffolds

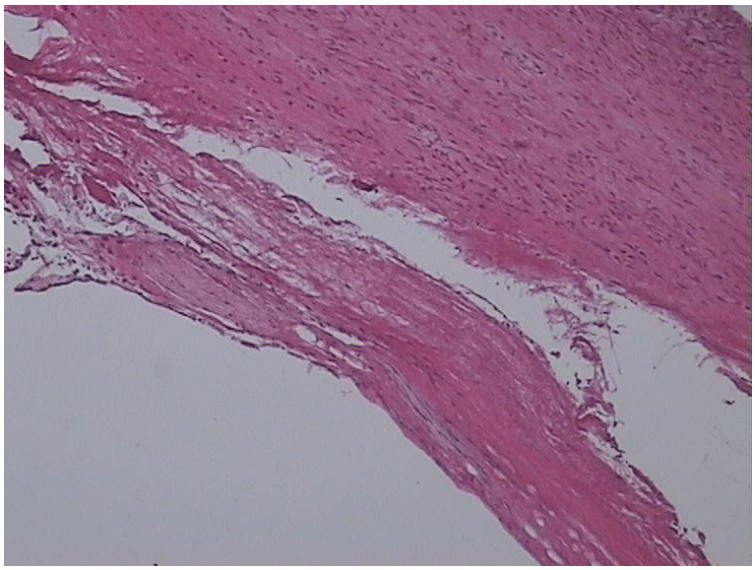

Figure 55 Histology of out-layer of tissue engineered ligament at 4 weeks (Group III, H&E, 100x)

3.1.3.2 Histology at 20 weeks

The rate of degradation of PLLA has been reported to vary from 40 weeks to over 3 years depending on the molecular weight, size and shape of the implant [273]. Polymers in knee joints would usually degrade much faster than in bone tunnels, as a result of greater mechanical stress on the reconstructed ACL caused by multiform motion of the knee joint, which was also supported by the evidence that PLGA fibers in knee joints degraded faster than in bone tunnels. In fact, a 10-month lifespan is enough for ACL regeneration. The risk is that drop in mechanical strength drops before mass loss will affect the whole structure. In our current study, there was no visible sign of PLLA fiber degradation at 20 weeks, in agreement with previous research on braided PLLA scaffolds used for ACL reconstruction [177, 273].

The fibroconnective tissue ingrowth around the PLLA fibers occurred similarly in all four groups. The loose design of the knitted structures seemed to promote and support tissue growth. In contrast, carbon fibers and Dacron induced fibrous-tissue formation only to the outer sheet of the implants [274, 275]. When compared with braided structures, higher porosities of knitted structures could encourage more tissues to grow, though no quantitative comparison has been done between the two structures.

The normal anterior cruciate ligaments are parallel bands of regularly orientated, dense connective tissue connecting the femur and tibia, which are surrounded by a mesentery-like fold of synovium [10]. Fascia was used to wrap the constructs in some groups to mimic the normal structures. Although we are unsure of the actual roles of fascia

covers, we know that they could contribute formation of dense outer layers of tissue engineered ligaments after 20 weeks as well as improve collagen excretion significantly. In microanatomy, the normal ACLs are made up of multiple fascicles (100-250μm in diameter), of which the basic unit is collagen. Parallel and inter-linked fascicles were obvious in normal histology (Fig 56 and 57), but not seen in any experimental group (Fig 58-61), as the collagen fibrils or fibers were not matured to be grouped into fascicles after 20 weeks' implantation. More attention should be paid to promote collagen fiber maturity and functionality.

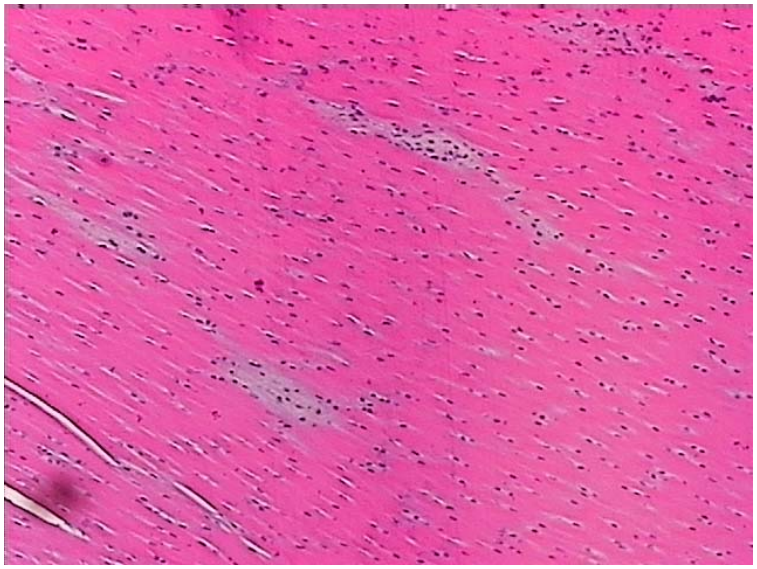

Figure 56 Normal ACL histology (H&E, 100x)

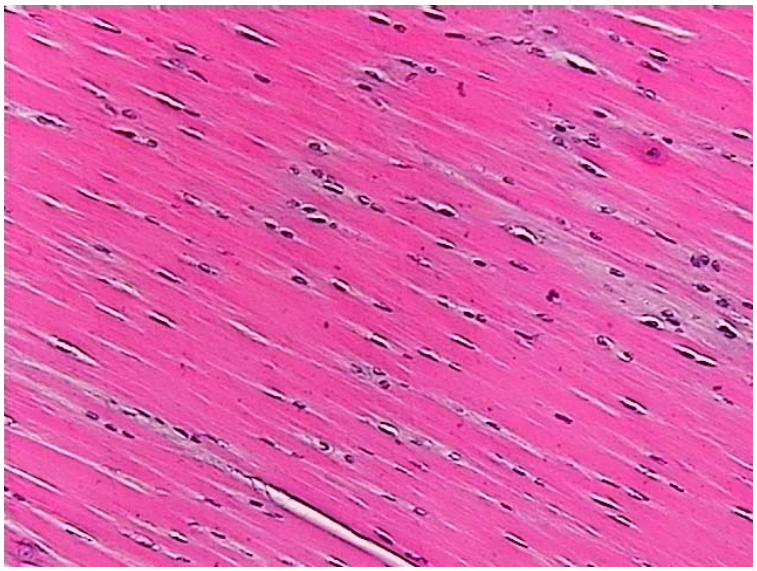

Figure 57 Normal ACL histology (H&E, 200x)

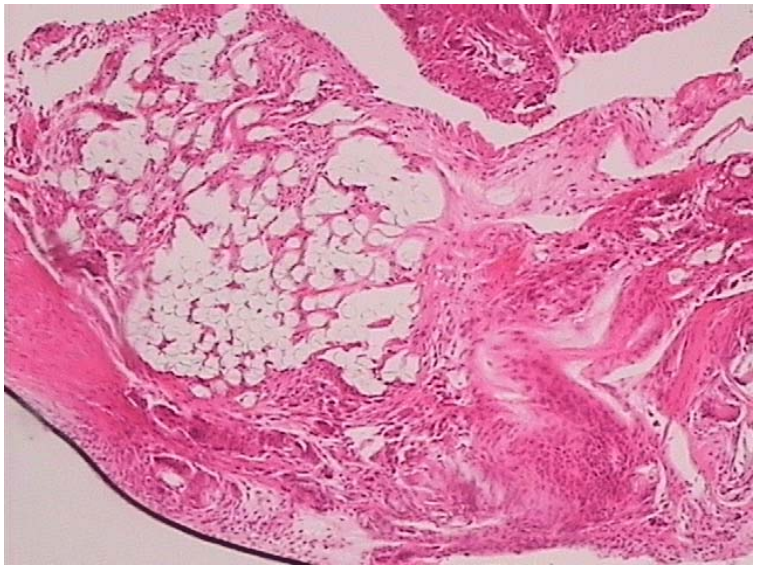

Figure 58 Histology of tissue engineered ACL from group I (H&E, 100x)

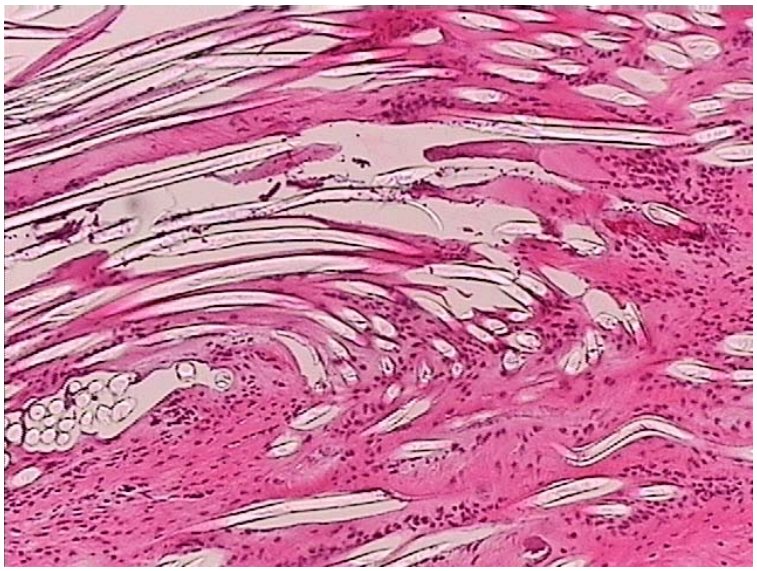

Figure 59 Histology of tissue engineered ACL from group II (H&E, 100x)

Figure 60 Histology of tissue engineered ACL from group III (H&E, 100x)

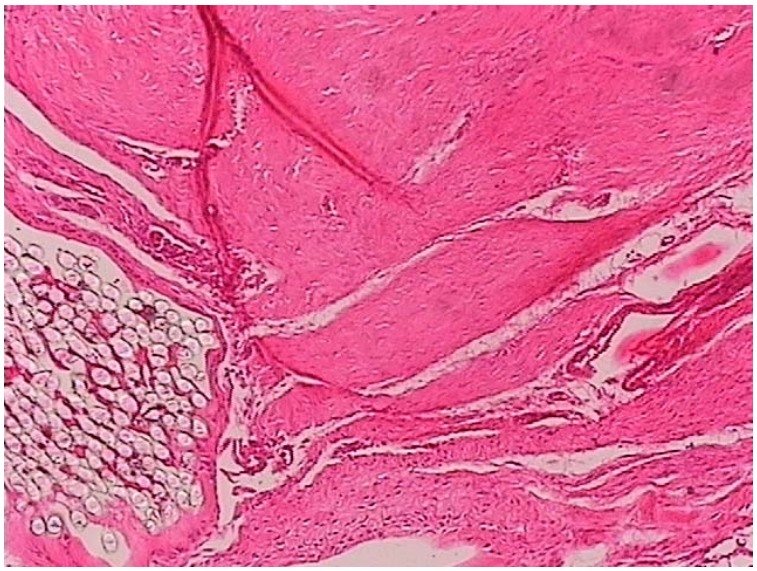

Figure 61 Histology of tissue engineered ACL from group IV (H&E, 100x)

3.3.4 Histology in bone tunnel

The strength of the fixation of the implant at either end of the drill channel is crucial for long-term success, since the interface between a synthetic material and a living tissue is a region of high stress [276]. The normal ACL insertion zone (Fig 62) has material properties that are intermediate between ligament and bone. Its function is to transmit load, distribute and decrease stress concentration at the attachment site [277]. Although the ideal way is to reconstruct the normal transition, conventional tendon transfers are unable to restore this complex anatomy of ACL insertion within the first 6 months [1]. The fibrous tissue formation within the bone tunnel could possibly transforms into a “normal” insertion with the four-zonal structure after a long time [278]. Introduction of large amounts of MSCs to the bone tunnel have shown to improve the healing of tendon to bone at the insertion zone, through formation of fibrocartilagenous attachment at early stages [224]. However, it will be more difficult for tissue engineered ligament, especially

when the number of loading MSCs in our current study was much lower than that reported for tendon healing in the bone tunnel. In all four groups, similar ligament to bone healing was observed with tissue engineered ligaments attached to bone by intermediated fibroblasts (Fig 63). Insufficient integration strength and compliance mismatch with host tissue are possible reasons for scenarios whereby the tissue engineered ligaments were pulled out through the bone tunnel during mechanical tests.

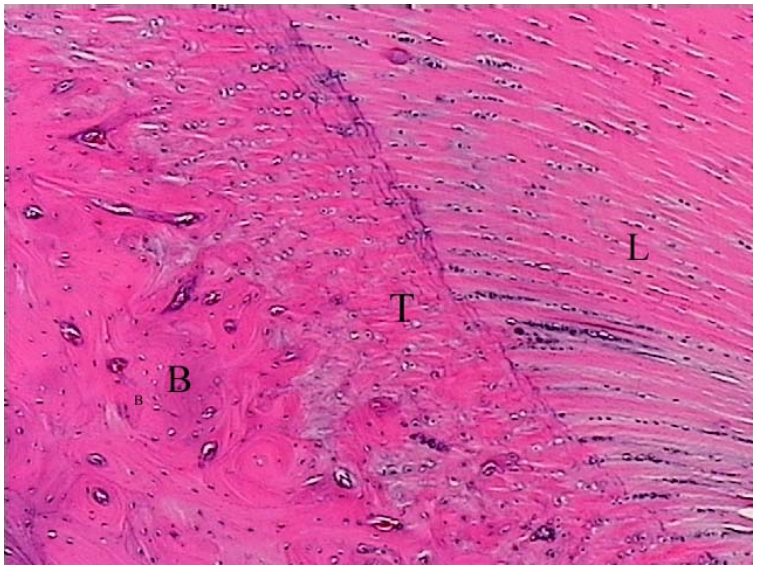

Figure 62 Normal ligament to bone transition (H&E, 100x)

L denotes ligament (ACL); T denotes transition from ligament to bone; B denotes bone.

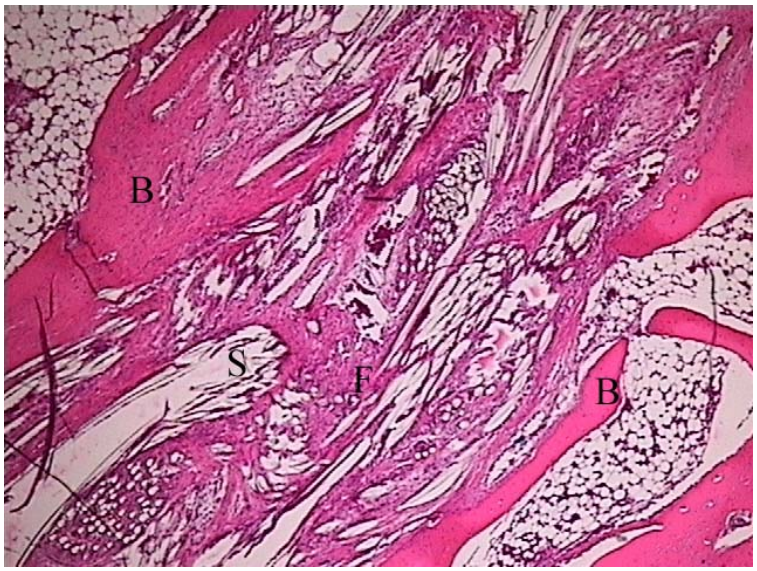

Figure 63 Healing of tissue engineered ligament to bone (H&E, 100x)

S means scaffolds (sectioned from different direction); B means bone; F means fibroblast ingrowth.

3.3.5 Immunohistochemistry

Collagen being a key component in ligaments provides high tensile strength to withstand physiological loads during activities of daily living. It accounts for 70-80% of the tissue dry weight. Type I collagen is about 8 to 9 times far more abundant than type III collagen in ligament tissues, while other collagens such as types V, VI and XII occur in small amounts. The ultimate fibril diameter attained during fibrillogenesis appears to depend on the quantitative ratio in which the type I and type III collagens are secreted during fibril polymerization [238] . Hence, it is important to evaluate the secreted collagen that will be used in ligament repair and regeneration, to determine the existence of type I and type III collagen in the tissue.

In normal ACLs, collagen I staining (Fig 64) was much stronger than that of collagen III (Fig 65). Composition of collagen III will significantly increase during injury [237]. In specimens from experimental group, as collagen III staining significantly increased, there was no significant difference between collagen I (Fig 66) and collagen III staining (Fig 67). This trend was observed across all experimental groups.

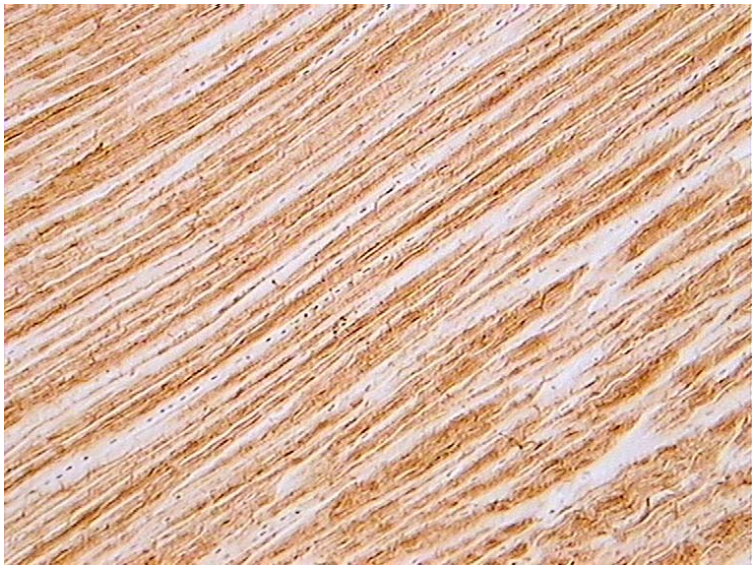

Figure 64 Collagen I staining of normal ACL (100x)

Figure 65 Collagen III staining of normal ACL (100x)

Figure 66 Collagen I staining of tissue engineered ACL (100x)

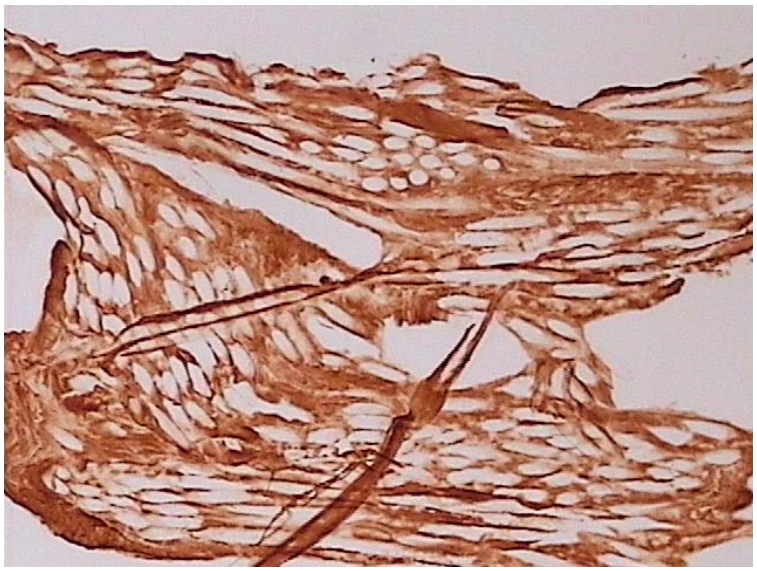

Figure 67 Collagen III staining of tissue engineered ACL (100x)

The white fascicles, cross-section of PLLA yarns, were surrounded by fibroblast ingrowth and ECM which were stained by collagen antibodies.

3.3.6 Western blot analysis

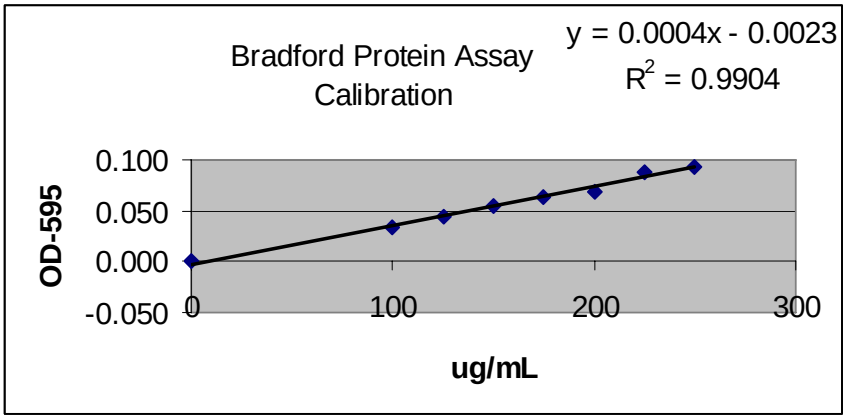

Figure 68 Calibration curve of Bradford protein assay

In four experimental groups and normal control, two bands of collagen type I

were obvious at 210k and 95k respectively, though the densities were different among different groups (Fig 69). The amount of collagen I in group III (146.7%) and IV (163.3%) were higher than in group II (75.1%) and normal control (100%) while there was no significance between group III and IV, as well as between group II and normal control. Collagen I in group I (20.5%) was significantly lower than that in all other groups (Table 16, One-way ANOVA, $P<0.05$) (Fig 70).

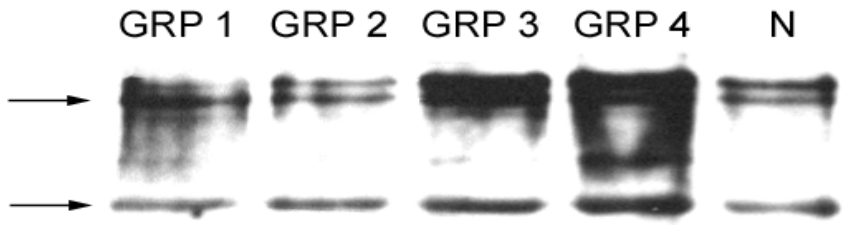

Figure 69 Western blot of collagen I from group I, II, III, IV and normal control

Arrows indicate collagen, Type I detected by α-collagen (I) (Calbiochem) significantly at 95 kDa and 210 kDa.

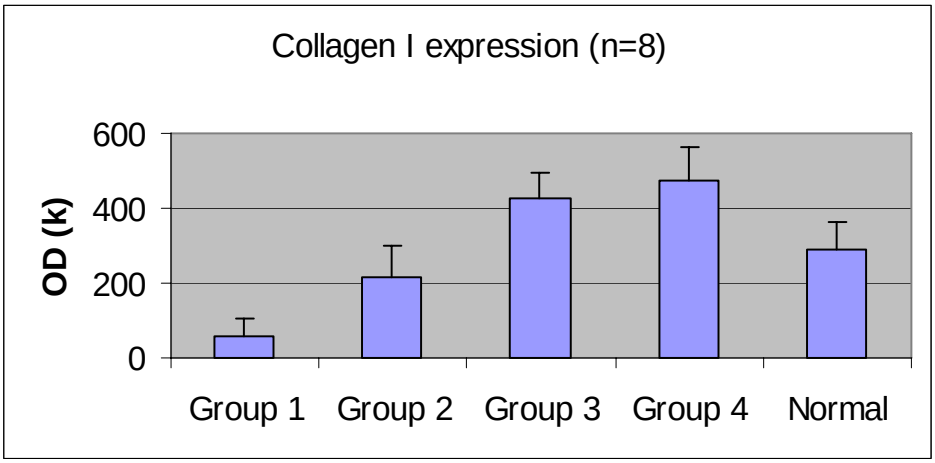

Figure 70 Quantitative expression of collagen I expression in different groups

Table 16 Multiple comparisons of collagen I expressions

Group	Group	Mean Difference	Std. Error	Sig.	95% Confidence Interval	
					Lower Bound	Upper Bound
a. OD in group I (59903)	b	-157206(*)	37211	.000	-232749	-81663
	c	-363793(*)	37211	.000	-439337	-288250
	d	-411990(*)	37211	.000	-487533	-336447
	e	-228814(*)	37211	.000	-304357	-153271
b. OD in group II (217109)	a	157206(*)	37211	.000	81663	232749
	c	-206588(*)	37211	.000	-282131	-131045
	d	-254784(*)	37211	.000	-330327	-179242
	e	-71608	37211	.062	-147151	3935
c. OD in group III (423697)	a	363793(*)	37211	.000	288250	439336
	b	206588(*)	37211	.000	131044	282131
	d	-48197	37211	.204	-123740	27346
	e	134979(*)	37211	.001	59436	210522
d. OD in group IV (471893)	a	411990(*)	37211	.000	336447	487533
	b	254784(*)	37211	.000	179241	330327
	c	48197	37211	.204	-27346	123740
	e	183176(*)	37211	.000	107633	258720
e. normal control (288717)	a	228814(*)	37211	.000	153271	304358
	b	71608	37211	.062	-3935	147151
	c	-134979(*)	37211	.001	-210522	-59436
	d	-183176(*)	37211	.000	-258719	-107633

LSD The mean difference is significant at the .05 level.

In all groups, bands of collagen type III at 110 and 290 kDa were obtained with other minor bands, ranging from 63 kDa to 300 kDa (Fig 71). Collagen III expression in group III (137.1%) and IV (162.9%) were higher than all other groups, while there was no significance between them. Collagen III expression in group II (71.4%) was lower than that in normal control, but higher than group I (20.5%) significantly (Table 17, One-way Anova, $P<0.05$) (Fig 72).

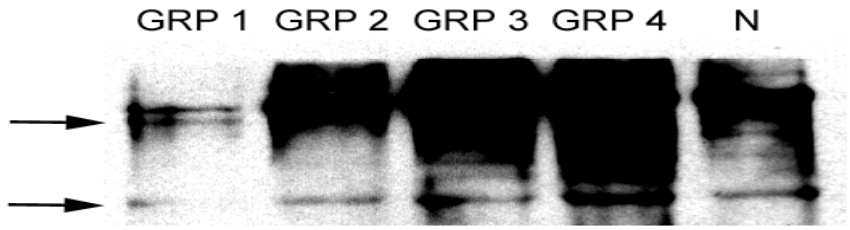

Figure 71 Western blot of collagen III from group I, II, III, IV and normal control

Arrows indicate collagen, Type III detected by α-collagen (III) (Oncogene Research Products) significantly at 110 kDa and 290 kDa.

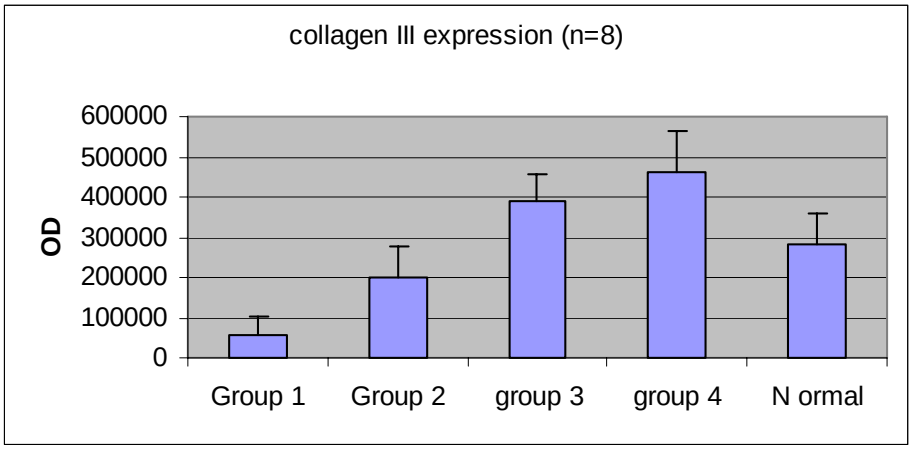

Figure 72 Quantitative expression of collagen III in different groups

Table 17 Multiple comparisons of collagen III expressions

Group	Group	Mean Difference	Std. Error	Sig.	95% Confidence Interval	
					Lower Bound	Upper Bound
a. OD in group I (57867)	b	-144581(*)	37305	.000	-220314	-68849
	c	-330307(*)	37305	.000	-406040	-254574
	d	-403349(*)	37305	.000	-479081	-327616
	e	-225272(*)	37305	.000	-301005	-149539
b. OD in group II (202449)	a	144581(*)	37305	.000	68849	220314
	c	-185726(*)	37305	.000	-261458	-109993
	d	-258767(*)	37305	.000	-334500	-183035
	e	-80691(*)	37305	.037	-156423	-4958
c.OD in group III (388175)	a	330307(*)	37305	.000	254574	406040
	b	185726(*)	37305	.000	109993	261458
	d	-73042	37305	.058	-148774	2691
	e	105035(*)	37305	.008	29302	180768
d. OD in group IV (461216)	a	403349(*)	37305	.000	327616	479081
	b	258767(*)	37305	.000	183035	334500
	c	73042	37305	.058	-2691	148774
	e	178077(*)	37305	.000	102344	253809
e. Normal control (283140)	a	225272(*)	37305	.000	149539	301005
	b	80691(*)	37305	.037	4958	156423
	c	-105035(*)	37305	.008	-180768	-29302
	d	-178077(*)	37305	.000	-253809	-102344

LSD, * The mean difference is significant at the .05 level.

Our results showed that MSC seeding obviously improved excretion of collagen type I and type III. It is postulated that donor cells may help to recruit more progenitor /reparative cells by interacting with host cells, while excreting extracellular matrix [50]. For the authors, it is the first evidence to quantitatively analyze cell seeding effect on *in vivo* protein components for tissue engineering of ACL reconstruction, though many reports on *in vitro* protein analysis have been published [279]. Fascia wrap has been reported to contribute to the formation of well-oriented fibroblasts and extracellular

matrix, as well as improving mechanical properties [37, 177], though it could not provide good mechanical support when used separately [280]. In the current study, fascia wraps did improve protein synthesis and potentially functionality, but it was not clear about the exact ratio of protein which fascia wraps brought to protein synthesis from regeneration. Though fascia wraps have shown stronger effects on collagen excretion than MSC seeding in the current study, further study is necessary when the quantity of fascia wraps and number of seeding cells are well controlled. Longer implantation time and larger animal models are necessary to evaluate their exact roles. The ultimate fibril diameter attained during fibrillogenesis appears to depend on the quantitative ratio in which the type I and type III collagens are secreted during fibril polymerization [238]. In the future, it would be worthwhile to determine the ratio of collagen I and III in the same specimen, and establish their roles in the healing process.

3.3.7 Mechanical properties

3.3.7.1 Maximal tensile loads

Of all the specimens tested, the failure mode of two reconstructed ACLs (one from group II and the other from group IV) was dislodgement from the bone tunnels. In all other cases, the ACL constructs failed in the mid-substance inside the knee joint. However, the exact location of rupture was inconsistent, since multiple ruptures occurred at different places simultaneously. Though sometimes, certain scaffolds seemed intact, rupture of microfibers may have taken place at various spots, causing a drastic drop in tensile load.

---------- *RESULTS AND DISCUSSION* ----------

Maximal tensile loads of tissue engineered ligaments were 9.2%, 9.8%,13.9% and 10.4% of normal in groups I, II, III and IV, respectively (see Table 18), however, there was no significant difference between the different groups (Table 19, One-way ANOVA, $p<0.05$).

Table 18 Maximal tensile loads of tissue engineered ligaments after 20 weeks' implantation

N=5	Maximal tensile load (N)
Group I	14+/- 7.8
Group II	14.9+/- 6.6
Group III	20.9+/-4.5
Group IV	15.8+/- 6.8
Normal control	151.8+/-20.8

Table 19 Multiple comparisons of maximal tensile loads

(I) VAR	(J) VAR	Mean Difference (I-J)	Std. Error	Sig.	95% Confidence Interval	
					Lower Bound	Upper Bound
a. tensile load in group I (14N)	b	-.9	6.9	.902	-15.3	13.6
	c	-6.9	6.9	.331	-21.4	7.6
	d	-1.8	6.9	.798	-16.2	12.7
	e	-137.8 (*)	6.9	.000	-152.2	-123.4
b. tensile load in group II (14.9N)	a	.9	6.9	.902	-13.6	15.3
	c	-6.0	6.9	.394	-20.5	8.4
	d	-.9	6.9	.893	-15.4	13.5
	e	-137.0(*)	6.9	.000	-151.4	-122.5
c. Tensile load in group III (20.9N)	a	6.9	6.9	.331	-7.6	21.4
	b	6.0	6.9	.394	-8.4	20.5
	d	5.1	6.9	.470	-9.4	19.6
	e	-130.9 (*)	6.9	.000	-145.4	-116.5
d. Tensile load in group IV (15.8N)	a	1.8	6.9	.798	-12.7	16.3
	b	.9	6.9	.893	-13.5	15.4
	c	-5.1	6.9	.470	-19.6	9.4
	e	-136.0 (*)	6.9	.000	-150.5	-121.6
e. Normal control (151.8N)	a	137.8 (*)	6.9	.000	123.4	152.3
	b	137.0(*)	6.9	.000	122.5	151.4
	c	131.0(*)	6.9	.000	116.5	145.4
	d	136.0 (*)	6.9	.000	121.6	150.5

LSD, the mean difference is significant at the .05 level.

3.3.7.2 Stiffness

Stiffness of tissue engineered ligaments in groups I, II, III and IV were 9.1%, 18.7%, 16.7% and 13.1% of normal respectively (see Table 20). All of them were significantly lower than the normal value while there was no significant difference in the data between the individual experimental groups (Table 21, one-way ANOVA, $p < 0.05$).

Table 20 Stiffness of tissue engineered ligaments after 20 weeks' implantation

N=5	Stiffness (N/mm)
Group I	8.6+/-2.3
Group II	7.8+/-3.2
Group III	8.4+/-2.2
Group IV	7.4+/-3.4
Normal control	50.4+/-5.3

Table 21 Multiple comparisons of stiffness

(I) VAR	(J) VAR	Mean Difference (I-J)	Std. Error	Sig.	95% Confidence Interval	
					Lower Bound	Upper Bound
a. Stiffness in group I (8.6N/mm)	b	.8	2.2	.711	-3.8	5.4
	c	.2	2.2	.938	-4.4	4.8
	d	1.2	2.2	.595	-3.4	5.8
	e	-41.8(*)	2.2	.000	-46.4	-37.2
b. Stiffness in group II (7.8N/mm)	a	-.8	2.2	.711	-5.4	3.8
	c	-.7	2.2	.770	-5.2	3.9
	d	.4	2.2	.871	-4.2	5.0
	e	-42.6 (*)	2.2	.000	-47.2	-38.0
c. Stiffness in group III (8.4N/mm)	a	-.2	2.2	.938	-4.8	4.4
	b	.7	2.2	.770	-3.9	5.2
	d	1.0	2.2	.650	-3.6	5.6
	e	-42.0(*)	2.2	.000	-46.6	-37.4
d. Stiffness in group IV (7.4N/mm)	a	-1.2	2.2	.595	-5.8	3.4
	b	-.4	2.2	.871	-5.0	4.2
	c	-1.0	2.2	.650	-5.6	3.6
	e	-43.0(*)	2.2	.000	-47.6	-38.4
e.Normal stiffness (50.4N/mm)	a	41.8(*)	2.2	.000	37.2	46.4
	b	42.6 (*)	2.2	.000	38.0	47.2
	c	42.0(*)	2.2	.000	37.4	46.6
	d	43.0(*)	2.2	.000	38.4	47.6

LSD, * The mean difference is significant at the .05 level.

Maximal tensile load and stiffness are important parameters for tissue engineered ACL [281]. Though MSC seeding and fascia wrap are effective to improve collagen excretion and possibly regeneration, none of them could improve maximal tensile load and stiffness of current tissue engineered ligaments significantly. The acquired maximal tensile loads and stiffness were mainly from the partially degraded PLLA fibers, while regenerated tissues were not well oriented and far from functionality. In other words, the excreted collagen still could not form enough collagen fibrils/bundles as well as orientate and cross-link appropriately to undertake mechanical force. So they have shown little effect on maximal tensile load and stiffness at the current stage.

3.3.7.3 Strain and Cross-section

The cross section areas of tissue engineered ligaments from group 1, 2, 3, and 4 were 48.9%, 106.4%, 68.1% and 14.9% respectively (Fig 73). Though the crosssectional areas of cell loading groups (Group 2 and 3) were higher than cell free groups (Group 1 and 4), there was no significance between them due to a relatively high variation (Table 22 and 23). Possibly the loading cells could promote more regeneration due to more chemotoxin excreted, when compared with cell free groups. More results are necessary to evaluate and draw conclusions.

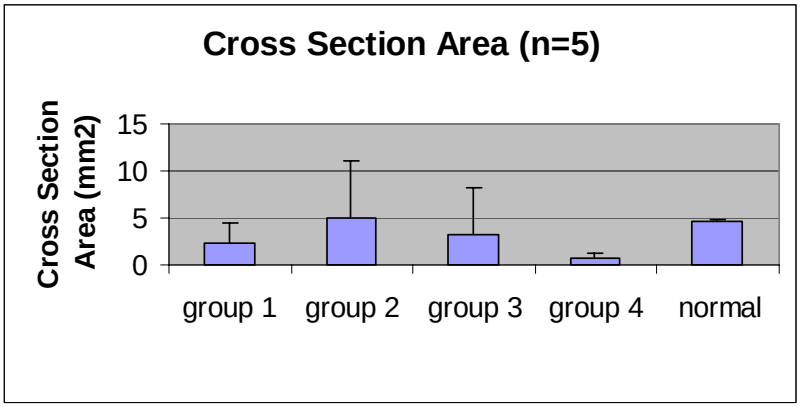

Figure 73 Cross section areas of tissue engineered ligaments

Table 22 Cross-sectional areas of tissue engineered ACL

Cross-section (mm^2)	Specimen 1	Specimen 2	Specimen 3	Specimen 4	Specimen 5
group 1	2.0	2.0	0.8	5.9	0.7
group 2	3.5	2.8	3.2	0.2	15.5
group 3	1.3	0.3	11.9	2.5	0.2
group 4	0.3	1.8	0.6	0.2	0.4
normal	4.8	4.3	4.8	4.6	4.8

Table 23 Multiple comparisons of cross-sectional areas

(I) VAR	(J) VAR	Mean Difference (I-J)	Std. Error	Sig.	95% Confidence Interval	
					Lower Bound	Upper Bound
a. areas in group I ($2.3mm^2$)	b	-2.8	2.3	.241	-7.5	2.0
	c	-1.0	2.3	.679	-5.7	3.8
	d	1.6	2.3	.486	-3.1	6.4
	e	-2.4	2.3	.310	-7.1	2.4
b. areas in group II ($5.0\ mm^{2)}$)	a	2.8	2.3	.241	-2.0	7.5
	c	1.8	2.3	.440	-3.0	6.6
	d	4.4	2.3	.069	-.4	9.1
	e	.4	2.3	.869	-4.4	5.1
c. areas in group III ($3.2\ mm^{2)}$)	a	1.0	2.3	.679	-3.8	5.7
	b	-1.8	2.3	.440	-6.6	3.0
	d	2.6	2.3	.272	-2.2	7.3
	e	-1.4	2.3	.541	-6.2	3.3
d. areas in group IV ($0.7\ mm^{2)}$)	a	-1.6	2.3	.486	-6.4	3.1
	b	-4.4	2.3	.069	-9.1	.4
	c	-2.6	2.3	.272	-7.3	2.2
	e	-4.0	2.3	.095	-8.8	.8
e. areas in normal ACL ($4.7\ mm^{2)}$)	a	2.4	2.3	.310	-2.4	7.1
	b	-.4	2.3	.869	-5.1	4.4
	c	1.4	2.3	.541	-3.3	6.2
	d	4.0	2.3	.095	-.8	8.8

Though ACLs are viscoelastic, more than 6% of strain will not recover fully and lead to elongation and loss of functionalities [65]. Hence, it is necessary for tissue engineered ligaments to exactly match the viscoelastic properties of ACLs. In current clinical practice, autografts are often used, which will undergo elongation possibly due to enzymatic degradation *in vivo* [262]. The viscoelastic properties of tissue engineered ligaments came from both knitted structures and PLLA polymer chains [282]. It was noticeable that gauge lengths from two cell loading groups, group 2 and 3, were less than the other two experimental groups (Fig 74). There was no significance between either one from

group 1, 2, 3, 4 and normal ACLs (Table 24), though there was significance between group 1 and 2, between group 2 and 4, as well as between group 3 and 4 (Table 25). In general, the gauge lengths were acceptable in all experimental groups, as there was no significance between individual experimental group and normal control.

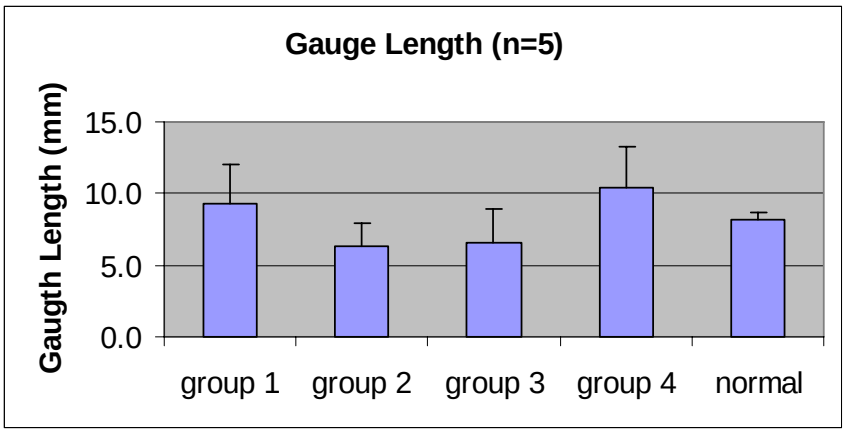

Figure 74 Gauge lengths of tissue engineered ligaments

Table 24 Gauge length of tissue engineered ligaments

mm	Specimen 1	Specimen 2	Specimen 3	Specimen 4	Specimen 5
group 1	12.0	10.6	10.6	8.0	5.2
group 2	8.2	4.6	7.8	6.0	4.8
group 3	8.8	9.3	5.3	4.4	5.3
group 4	7.9	10.8	9.2	9.0	15.2
normal	8.8	7.9	7.9	8.4	8.1

Table 25 Multiple comparisons of gauge lengths

(I) VAR	(J) VAR	Mean Difference (I-J)	Std. Error	Sig.	95% Confidence Interval	
					Lower Bound	Upper Bound
a. Length in group I (9.3mm)	b	3.0(*)	1.4	.041	.1	5.9
	c	2.7	1.4	.067	-.2	5.5
	4	-1.1	1.4	.416	-4.0	1.7
	e	1.1	1.4	.449	-1.8	3.9
b. Length in group II (6.3mm)	a	-3.0(*)	1.4	.041	-5.9	-.1
	c	-.3	1.4	.807	-3.2	2.5
	d	-4.1(*)	1.4	.007	-7.0	-1.3
	e	-1.9	1.4	.173	-4.8	.9
c. Length in group III (6.6mm)	a	-2.7	1.4	.067	-5.5	.2
	b	.3	1.4	.807	-2.5	3.2
	d	-3.8(*)	1.4	.012	-6.7	-.9
	e	-1.6	1.4	.257	-4.5	1.3
d. Length in group IV (10.4mm)	a	1.1	1.4	.416	-1.7	4.0
	b	4.1(*)	1.4	.007	1.3	7.0
	c	3.8(*)	1.4	.012	.9	6.7
	e	2.2	1.4	.124	-.7	5.1
e. Length in Normal ACL (8.1mm)	a	-1.1	1.4	.449	-3.9	1.8
	b	1.9	1.4	.173	-.9	4.8
	c	1.6	1.4	.257	-1.3	4.5
	d	-2.2	1.4	.124	-5.1	.7

LSD, the mean difference is significant at the .05 level.

The knitted scaffolds could support tissue in-growth and improved structures with greater maximal load will potentially serve as good tissue engineered ligaments. Ultimately, a longer implantation course is necessary for denser fibroblast ingrowth as well as for the extracellular matrix to mature and function well.

4 Conclusion and future direction

Mesenchymal stem cells were found to be a better cell source than ACL and MCL fibroblasts in this study, with regards to proliferation, collagen excretion as well as collagen expression profiles (Collagen I, collagen III and alpha smooth muscle actin). The Young's modulus of knitted scaffolds could possibly meet the minimal requirements for ACL reconstruction in the first twenty weeks. The knitted scaffolds could survive after 20 weeks' implantation when used in ACL reconstruction. Mesenchymal stem cells and fascia lata covers could possibly promote ligament regeneration, with regards to mechanical strength, cross-sectional areas and histology. Fibroblasts were not well oriented and there was no collagen bundle formation. In general, fascia wrap and MSCs were found to have potential for ligament tissue engineering. However, in consideration of the challenge and complexity of ligament tissue engineering, more techniques and understanding of ligament regeneration would be necessary for future success in making functional tissue engineered ligaments.

4.1 Growth factors, bioreactors and gene therapy

Ligament healing is a complex and highly-regulated process that is initiated, sustained and eventually terminated by a variety of molecules. Growth factors represent one of the most important biomolecules involved in healing. IGF-I, TGF-beta, vascular VEGF, PDGF, and bFGF have been reported to be markedly up-regulated following ligament injury and are active at multiple stages of the healing process. They are involved in the proliferation and

migration of fibroblasts and/or to subsequently leading to increase collagen production, and/or angiogenesis, and/or the production of other growth factors [283].

As the lack of blood supply after ACL ruptures is one of the main reasons to block subsequent ligament regeneration, controlled angiogenesis should theoretically be beneficial. As VEGF has long been regarded to have strong influence on blood supply, it may be beneficial to introduce it at both bone tunnels as well as mid-substance of tissue engineered ligaments [283, 284].

As well-controlled mechanical and biochemical parameters are essential for potential ligament regeneration both *in vivo* and *in vitro*, bioreactors are sure to contribute [76]. More knowledge about exact roles, effective pathways, necessary duration of growth factors, optimized parameters of mechanical stimuli, as well as/or controlled gene regulation, is necessary for future progress. Side effects from gene therapy, growth factor controlled delivery and bioreactor should be avoided while all these procedures should be simplified and done with good quality control.

4.2 *In vivo* collagen cross-link

Collagen V which increased after ligament injuries has been reported to possibly inhibit the larger collagen bundle formation and further functionality [285]. After more understanding about the exact role of collagen V in ligament regeneration, its role would be well controlled. Except for growth factor delivery, more attention would be paid to

promote the maturity of excreted extracellular matrix to allow collagen bundle formation and cross-link between them before they can be functional [144, 286-288].

4.3 Inhibit harsh environment

There were significant changes in cytokine profiles after ACL injuries, which could lead to the difficulties of ACL regeneration [38]. Unfortunately until now the exact roles and pathway of each cytokine are not clear. It has been hypothesized that ACL regeneration is better accomplished if we have better ways to control these cytokines.

4.4 Larger animal models and stronger scaffolds

Although large amount of ligament relevant research have been done using rabbit model, there are still lots of limitations on broad usage of rabbit models. Their relatively small knee joint size restricts accurate drilling, which is essential for functional reconstruction [289]. Their knee joints could not really mimic normal mechanics in human beings, who can extend their knee joints further. Goat or pig model should be adopted while more accurate bone tunnel drilling techniques could be used, such as computer-assisted surgery.

Ideal tissue engineered ACL prostheses should match normal ACLs in maximal tensile strength, Young's Modulus, viscoelastic properties and diameters. Stronger scaffolds should be used, possibly with the incorporation of braided cord to improve maximal load. It will mimic normal knee joint physiology by using a prosthesis, which has same mechanical properties of a normal ACL, to reconstruct at initial time. Notchplasty could be done just like in human cases if necessary. To further improve cell-attaching

surface in the scaffolds and potentially improve micro-environments for ingrowth cells' proliferation and differentiation, electrospun nanofibers could be used [290]

4.5 Proposed design improvement of scaffold for ligament tissue engineering

As mentioned above, no satisfactory results have been reported on a scaffold with good initial mechanical properties, controlled degradation and biocompatibility when used for *in vivo* ACL reconstruction. Currently, it is postulated that an ideal structure to meet the basic requirements should be a dual structure (Fig 75). The two ends of the dual structure should be induced for osteogenesis and integrated with host bone after implantation, while the middle part of it should have host tissue ingrowth and achieve subsequent functionality with time.

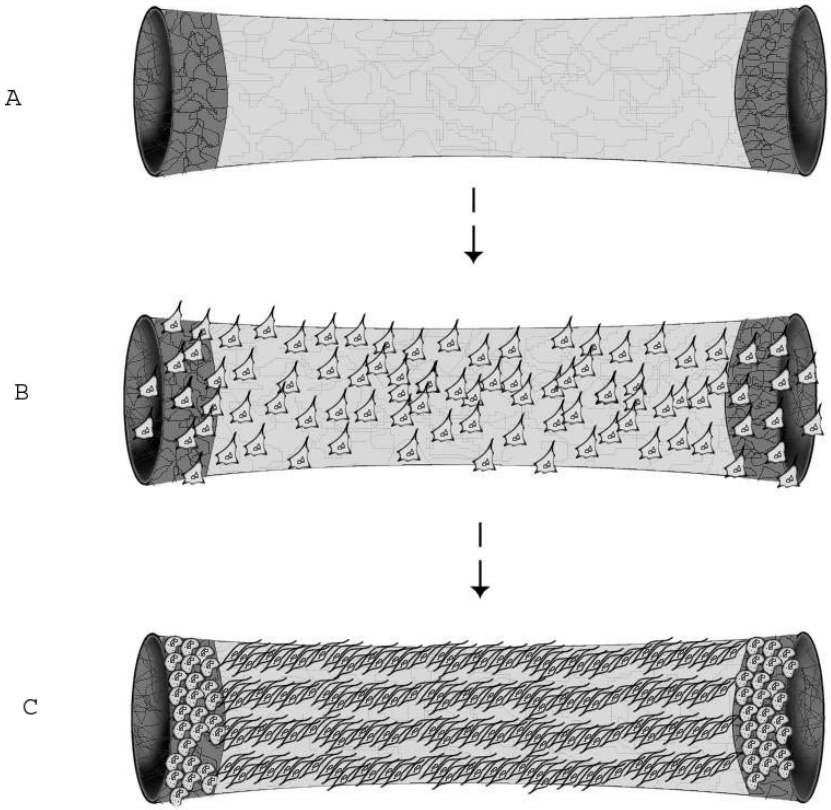

Figure 75 Schematic structure of composite scaffold for ACL reconstruction

A: Composite structure biodegradable scaffold, with both ends being osteo-inductive and the middle portion having potential for ligament/tendon tissue formation/regeneration.
B: Cell-seeded composite scaffold with proliferative potential and/or reparative cells recruited into the scaffold with regenerative potential.
C: Cells in two ends will be induced to form bone and integrate with host bone, while cells in middle part will express extracellular matrix (ECM).

From a cross-sectional view, it could be a multiple layered structure while individual layers take on different functions as well as degrade at different rates (Fig 76). At initial stage (A), the outlayer of the structure is a biomembrane which could block the inflammatory cytokines and other macromolecules from knee joints while allowing nutrient ion exchange. The middle layer is a loose structure to provide a good micro-environment for tissue ingrowth as well as subsequent functionality. The growth factors originally kept in the middle layer will be released to promote faster tissue ingrowth. The core of the ideal structure is made of multiple intact layers, which would take the necessary mechanical strength for ACL reconstruction and degrade layer by layer. The changes of mechanical properties would be moderate and be offset by functionality in the middle layer. Thus, the general mechanical properties of the structure will remain stable during degradation and match that of the ACL. The growth factors which are kept inside the core of the ideal structure, mainly to promote blood supply and tissue functionality,

will be released at a later stage at a stable rate. This improved design of scaffold for ligament tissue engineering has been filed for patent application.

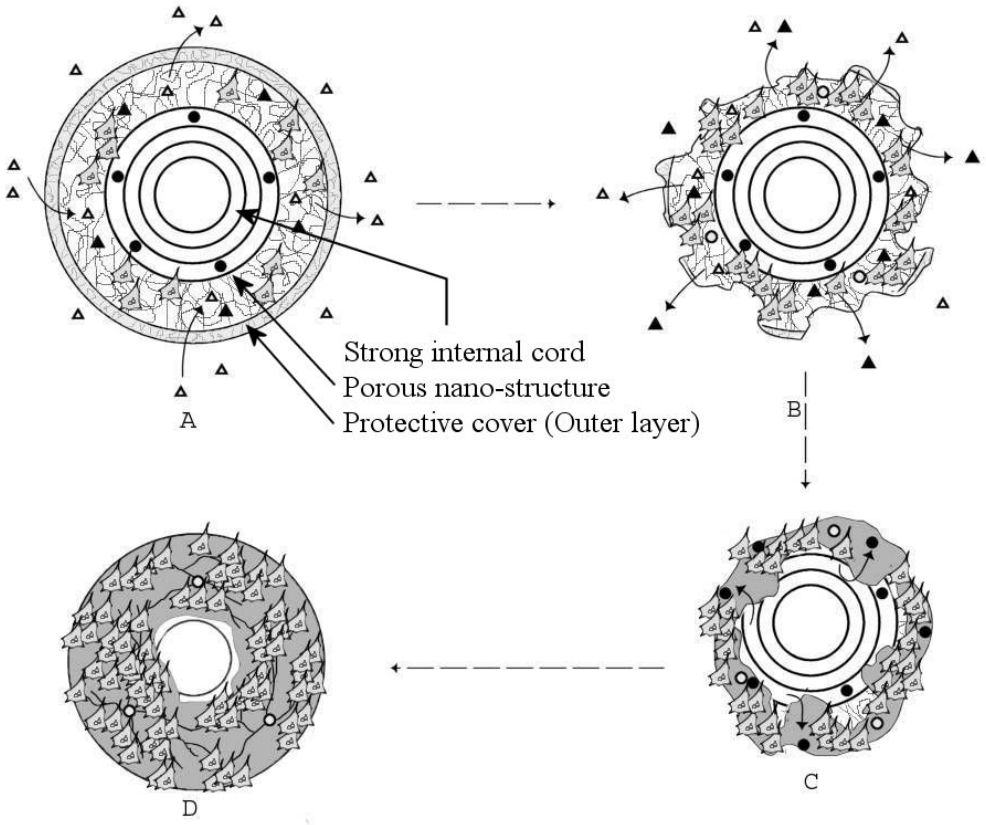

Figure 76 Cross-sectional view of composite structure for ACL reconstruction

The cross-sectional views of the three individual layers in the composite scaffold are shown in degradation. They are (1) protective cover (outlayer); (2) porous nano-structures and (3) strong internal cord. The irregularly-shaped structures found within the porous nano-structural region are the transplanted and/or reparative cells. Growth factor molecules shown here in "open triangle" on porous nanostructures will be released at early stage. Growth factor molecules (closed circle) encapsulated in the internal cord will be released while internal cord degrades in later stage.

4.6 Innervations of tissue engineered ligaments

Stretch-sensitive mechanoreceptors in the ligaments of the knee trigger muscle contractions that protect the knee from extremes of motion [39]. Reconstructive procedures may restore the structural role of ligaments, but traumatic loss of proprioception is most likely permanent under current therapy. In future, a functional ACL should have normal reflex arcs to protect the human knee.

5 References

1. Fu FH, Bennett CH, Lattermann C, Ma CB. Current trends in anterior cruciate ligament reconstruction. Part 1: Biology and biomechanics of reconstruction. Am J Sports Med 1999;27:821-830.
2. Pennisi E. Tending tender tendons. Science 2002;295:1011
3. Vunjak-Novakovic G, Altman G, Horan R, Kaplan DL. Tissue engineering of ligaments. Annu Rev Biomed Eng 2004;6:1-26.
4. Woo SLY, Hildebrand K, Watanabe N, Fenwck JA, Papageorgiou CD, Wang JHC. Tissue Engineering of Ligament and Tendon Healing. Clin Ortho 1999;367s:312-321.
5. Simonian.P.T., Harriso SD, Cooley VJ. Assessment of morbidity of semitendinosus and gracilis tendon harvest for ACL reconstruction. Am J Knee Surg 197;10:54-59.
6. Amiel D, Kleiner JB, Roux RD. The phenomenon of "ligamentization": Anterior cruciate ligament reconstruction with autogenous patellar tendon. J Orthop Res 1986;4:162-172.
7. Miller RH. Knee injuries; In: Canale ST, Ed. Campbell's Operative Orthopaedics, Mosby, 2003, vol, pp. 2274-2275.
8. Wilson SA, Vigorita VJ, Scott WN. Anatomy; In: Scott WN, Ed. The knee, Mosby, St Louis, 1994, vol 2, pp. 15-54.
9. Muller W. Kinematics of the cruciate ligaments; In: Feagin JA, Ed. The Crucial ligaments: diagnosis and treatment of ligamentous injuries about the knee, Churchill Livingstone, New York, 1994, vol 6, pp. 289-305.

10. Arnoczky SP, Warren RF. Anatomy of the cruciate ligaments; In: Feagin JA, Ed. The Crucial ligaments: diagnosis and treatment of ligamentous injuries about the knee, Churchill Livingstone, New York, 1994, vol 5, pp. 269-287.
11. Jackson RW. The torn ACL: Natural history of untreated lesions andrationale fo selectuve treatment; In: Feagin JA, Ed. The Crucial ligaments: diagnosis and treatment of ligamentous injuries about the knee, Churchill Livingstone, New York, 1994, vol, pp. 485-493.
12. Danylchuk KD, Finlay JB, Krcek JP. Microstructural organization of human and bovine cruciate ligaments. Clin Ortho 1978;131:294-298.
13. Akeson WH, Woo SLY, amiel D, Frank CB. The chemical basis of tissue repair: ligament biology; In: Hunter LY, Funk FJ, Eds. Rehabilitation of the injured knee, CV Mosby, St Louis, 2004, vol, p. 92.
14. Cooper RR, Misol S. Tendon and ligament insertion. A light and election microscopic study. J Bone Joint Surg 1970;52A:1-20.
15. Arnoczky SP. Blood supply to the anterior curciate ligament andsupporting structures. Orthop Clin North Am 1985;16:15-28.
16. Kennedy JC, Alexander IJ, Hayes KC. Nerve supply of the juman knee and its functional importance. Am J Sports Med 1982;10:329-335.
17. Chen EH, Black J. Materials design analysis of the prosthetic anterior cruciate ligament. J Biomed Mater Res 1980;14:567-586.
18. Noyes FR, Grood ES. The strength of the anterior cruciate ligament in humans and Rhesus monkeys. J Bone Joint Surg Am 1976;58:1074-1082.
19. Woo SL-Y, Hollis JM, Adams DJ. Tensile properties of the human femur-

anterior cruciate ligament-tibia complex. The effects of specimen age and orientation. Am J Sports Med 1991;19:217-234.

20. Martin RB, Burr DB, Sharkey NA. Mechanical Properties of Ligament and Tendon; In:Skeletal Tissue Mechanics, Springer-Verlag, New York. 1998; : 309-346., 1998, vol 8, pp. 309-349.
21. Nichols C, Johnson RJ. Anterior cruciate ligament injuries; In: Scott N, Ed. The knee, Mosby-year book, St. Louis, 1994, vol 39, pp. 723-744.
22. Shelburne KD, Klootwyk TE, Wilchens JH. Ligament stability two to six years after anterior cruciate ligament reconstruction with autogenous patellar tendon graft and participation in accelerated rehabilitation program. Am J Sport Med 1995;23:575-579.
23. Koski JA, Ibarra C, Rodeo SA. Tissue-engineered Ligament. Ortho Clin North Am 2000;31:437-451.
24. Frank CB, Jackson DW. The science of reconstruction of the anterior cruciate ligament. J Bone Joint Surg Am 1997;79:1556-1576.
25. Rittmeister M, Noble PC, Lintner DM, Alexander JW, Conditt M, Kohl III. The effect of strand configuration on the tensile properties of quadrupled tendon grafts. Arthroscopy 2002;18:194-200.
26. Altman GH, Horan RL, Lu HH, Moreau J, Martin I, Richmond JC, Kaplan DL. Silk matrix for tissue engineered anterior cruciate ligaments. Biomaterials 2002;23:4131-4141.
27. Dunn MG. Anterior cruciate ligament prostheses; In: Fahey T, Ed. Encyclopedia of Sports Medicine and Science, http://www.sportsci.org/encyc/index.html,

2004, vol.

28. Langer R, Vacanti JP. Tissue engineering. Science 1993;260:920-926.
29. Chaignaud BE, Langer RS, Vacanti JP. The history of tissue engineering using synthetic biodegradable polymer scaffolds and cells; In: Atala A, Mooney D, Eds. Synthetic biodegradable polymer scaffolds, Birkhauser, Boston, 1997, vol, pp. 1-14.
30. Butler DL, Goldstein SA, Guilak F. Functional tissue engineering: the role of biomechanics. J Biomech Eng 2000;122:570-575.
31. Schmidt CE, Leach JB. Neural tissue engineering: strategies for repair and regeneration. Annu Rev Biomed Eng 2003;5:293-347.
32. Ibarra C, Cao Y, Vacanti JP. Tissue engineering Ligaments. Surg Forum 1996;47:612-615.
33. Dunn MG, Tria AJ, Kato YP, Bechler JR, Ochner RS, Zawadsky JP, Silver FH. Anterior cruciate ligament reconstruction using a composite collagenous prosthesis. A biomechanical and histologic study in rabbits. Am J Sports Med 1992;20:507-515.
34. Dunn MG, Bellincampi LD, Tria AJ, Zawadsky JP. Prelliminary Development of a Collagen-PLA Composite for ACL Reconstruction. J Appl Polym Sci 1995;63:1423-1428.
35. Jackson DW, Simon TM, Lowery W, Gendler EI. Biologic remodeling after Anterior Cruciate Ligament Reconstruction using a Collagen Matrix Derived from Demineralized Bone. Am J Sport Med 1996;24:405-414.
36. Chvapil M, Speer DP, Holubec H, Chvapil TA, King DH. Collagen fibers as a

temporary scaffold for replacement of ACL in goats. J Biomed Mater Res 1993;27:313-325.

37. Laitinen O, Pohjonen T, TÖrmälä P, Saarelainen K, Vasenius J, Rokkanen P, Vainionpää S. Mechanical properties of biodegradable poly-L-lactide ligament augmentation device in experimental anterior cruciate ligament reconstruction. Arch Orthop Trauma Surg 1993;112:270-274.
38. Cameron ML, Fu FH, Paessler HH, Schneider M, Evans CH. Synovial fluid cytokine concentrations as possible prognostic indicators in the ACL-deficient knee. Knee Surg Sports Traumatol Arthrosc 1994;2:38-44.
39. Borsa PA, Lephart SM, Irrgang JJ, Safran MR, Fu FH. The effects of joint position and direction of joint motion on proprioceptive sensibility in anterior cruciate ligament-deficient athletes. Am J Sports Med 1997;25:336-340.
40. Lin VS, Lee MC, O'neal S, McKean J, Sung KLP. Ligament tissue engineering using synthetic biodegradable fiber scaffolds. Tissue Eng 1999;5:443-451.
41. McLaren A. Ethical and social considerations of stem cell research. Nature 2001;414:129-131.
42. Donovan PJ, Gearhart J. The end of the beginning for pluripotent stem cells. Nature 2001;414:92-97.
43. Pittenger MF, Mackay AM, eck SC, Jaiswal RK, Douglas R, Mosca JD, Moorman MA, Simonetti DW, Craig S, Marshak DR. Multipineage potentials of adult human mesenchymal stem cells. Science 1999;284:143-147.
44. Colter DC, Class R, DiGirolamo CM, Prockop D. Rapid expansion of recycling stem cells in cultures of plastic-adherent cells from human bone marrow. Proc

Nat Aca Sci 2000;97:3213-3218.

45. Jiang Y, Jahagirdar BN, Reinhardt RL, Schwartz RE, Keene CD, Ortiz-Gonzalez SR, Reyes M, Lenvik T, Lund T, Blackstad M, Du J, Aldrich S, Lisherg A, Low WC, Pargaespada DA, Verfaillle CM. Pluripotency of mesenchymal stem cells derived from adult marrow. Nature 2002;418:41-49.
46. Awad HA, Butler DL, Boivin GP, Smith FN, Malaviya P, Huibregtse B, Caplan AI. Autologous mesenchymal stem cell-mediated repair of tendon. Tissue Eng 1999;5:267-271.
47. Bruder SP, Jaiswal N, Ricalton NS, Mosca JD, Kraus KH, Kadiyala S. Mesenchymal stem cells in osteobiology and applied bone regeneration. Clin Orthop 1998;355:247-256.
48. Wu GD, Nolta JA, Jin YS, Barr ML, Yu H, Starnes VA, Cramer DV. Migration of mesenchymal stem cells to heart allografts during chronic rejection. Transplantation 2003;75:679-685.
49. Woo SL, Hildebrand K, Watanabe N, Fenwick JA, Papageorgiou CD, Wang JH. Tissue engineering of ligament and tendon healing. Clin Orthop 1999;367:312-323.
50. Hilldebrand KA, Jia F, Woo SL. Response of donor and recipient cells after transplantation of cells to the ligament and tendon. Microscopy research and technique 2002;58:34-38.
51. Caplan AI. Mesenchymal stem cells. J Orthop Res 1991;9:641-650.
52. Young HE, Mancini ML, Wright RP, Smith JC, Black AC, Jr., Reagan CR, Lucas PA. Mesenchymal stem cells reside within the connective tissues of many organs. Dev Dyn 1995;202:137-144.

53. Friedenstein AJ, Gorskaja JF, Kulagina NN. Fibroblast precursors in normal and irradiated mouse hematopoietic organs. Exp Hematol 1976;4:267-274.

54. Nathan S, Das DS, Thambyah A, Fen C, Goh J, Lee EH. Cell-based therapy in the repair of osteochondral defects: a novel use for adipose tissue. Tissue Eng 2003;9:733-744.

55. Huibregtse BA, Johnstone B, Goldberg VM, Caplan AI. Effect of age and sampling site on the chondro-osteogenic potential of rabbit marrow-derived mesenchymal progenitor cells. J Orthop Res 2000;18:18-24.

56. Mets T, Verdonk G. Variations in the stromal cell population of human bone marrow during aging. Mech Ageing Dev 1981;15:41-49.

57. Song L, Tuan RS. Transdifferentiation potential of human mesenchymal stem cells derived from bone marrow. FASEB J 2004;18:980-982.

58. Anderson DJ, Gage FH, Weissman IL. Can stem cells cross lineage boundaries? Nat Med 2001;7:393-395.

59. Krampera M, Glennie S, Dyson J, Scott D, Laylor R, Simpson E, Dazzi F. Bone marrow mesenchymal stem cells inhibit the response of naive and memory antigen-specific T cells to their cognate peptide. Blood 2003;101:3722-3729.

60. Horwitz EM, Gordon PL, Koo WK, Marx JC, Neel MD, McNall RY, Muul L, Hofmann T. Isolated allogeneic bone marrow-derived mesenchymal cells engraft and stimulate growth in children with osteogenesis imperfecta: Implications for cell therapy of bone. Proc Natl Acad Sci U S A 2002;99:8932-8937.

61. Hutmacher DW. Scaffolds in tissue engineering bone and cartilage. Biomaterials 2000;21:2529-2543.

62. Myllyharju J. Molecular biology and biosynthesis of collagens; In: Massaro EJ, Rogers JM, Eds. The Skeleton: Biochemical, Genetic, and Molecular Intractions in Development and Homeostasis, Humana Press, Totowa, New Jersey, 2004, vol 1.5, pp. 77-88.

63. Hutmacher DW, Goh JC, Teoh SH. An introduction to biodegradable materials for tissue engineering applications. Ann Acad Med Singapore 2001;30:183-191.

64. McDougall JJ, Bray RC. Animal models of ligament repair; In: An HY, Friedman RJ, Eds. Animal models in orthopaedic research, CRC press, New York, 1999, vol 24, pp. 461-490.

65. Haut RC. The mechanical and viscoelastic properties of the anterior cruciate ligement and of ACLfascicles; In: Jackson DW, Arnoczky SP, Frank CB, Woo SL-Y, Simon TM, Eds. The anterior cruciate ligament: current an future concepts, Raven Press, New York, 1993, vol, p. 63.

66. Dunn MG, Tria AJ, Kato YP, Bechler JR, Ochner RS, Zawadsky JP, Silver FH. Anterior cruciate ligament reconstruction using a composite collagenous prosthesis. A biomechanical and histologic study in rabbits. Am J Sports Med 1992;20:507-515.

67. Young RG, Butler DL, Weber W, Caplan AI, Gordon SL, Fink DJ. Use of mesenchymal stem cells in a collagen matrix for Achilles tendon repair. J Orthop Res 1998;16:406-413.

68. Salthouse TN. Cellular enzyme activity at the polymer-tissue interface: a review. J Biomed Mater Res 1976;10:197-229.

69. Lee CH, Singla A, Lee Y. Biomedical applications of collagen. Int J Pharm

2001;221:1-22.

70. Friess W. Collagen--biomaterial for drug delivery. Eur J Pharm Biopharm 1998;45:113-136.
71. Kaplan DI *et al.* Silk; In: McGrath K, Kaplan DI, Eds. Protein based materials, Birkhauser, boston, 1997, vol 4, pp. 103-131.
72. Altman GH, Diaz F, Jakuba C, Calabro T, Horan RL, Chen J, Lu H, Richmond J, Kaplan DL. Silk-based biomaterials. Biomaterials 2003;24:401-416.
73. Bucknall TE, Teare L, Ellis H. The choice of a suture to close abdominal incisions. Eur Surg Res 1983;15:59-66.
74. Greenwald D, Shumway S, Albear P, Gottlieb L. Mechanical comparison of 10 suture materials before and after in vivo incubation. J Surg Res 1994;56:372-377.
75. Salthouse TN, Matlaga BF, Wykoff MH. Comparative tissue response to six suture materials in rabbit cornea, sclera, and ocular muscle. Am J Ophthalmol 1977;84:224-233.
76. Altman GH, Lu HH, Horan RL, Calabro T, Ryder D, Kaplan DL, Stark P, Martin I, Richmond JC, Vunjak-Novakovic G. Advanced bioreactor with controlled application of multi-dimensional strain for tissue engineering. J Biomech Eng 2002;124:742-749.
77. Wen CM, Ye ST, Zhou LX, Yu Y. Silk-induced asthma in children: a report of 64 cases. Ann Allergy 1990;65:375-378.
78. Soong HK, Kenyon KR. Adverse reactions to virgin silk sutures in cataract surgery. Ophthalmology 1984;91:479-483.
79. Dewair M, Baur X, Ziegler K. Use of immunoblot technique for detection of

human IgE and IgG antibodies to individual silk proteins. J Allergy Clin Immunol 1985;76:537-542.

80. Campoccia D, Doherty P, Radice M, Brun P, Abatangelo G, Williams DF. Semisynthetic resorbable materials from hyaluronan esterification. Biomaterials 1998;19:2101-2127.
81. Skaugrud O, Hagen A, Borgersen B, Dornish M. Biomedical and pharmaceutical applications of alginate and chitosan. Biotechnol Genet Eng Rev 1999;16:23-40.
82. Oerther S, Payan E, Lapicque F, Presle N, Hubert P, Muller S, Netter P. Hyaluronate-alginate combination for the preparation of new biomaterials: investigation of the behaviour in aqueous solutions. Biochim Biophys Acta 1999;1426:185-194.
83. De VP, De Haan BJ, Wolters GH, Strubbe JH, Van SR. Improved biocompatibility but limited graft survival after purification of alginate for microencapsulation of pancreatic islets. Diabetologia 1997;40:262-270.
84. Miyoshi Y, Date I, Ono T, Imaoka T, Asari S, Ohmoto T, Iwata H. [Encapsulated dopamine-secreting cells transplanted into the brain: a possible therapy for Parkinson's disease]. No Shinkei Geka 1996;24:35-39.
85. Chowdhury TT, Bader DL, Shelton JC, Lee DA. Temporal regulation of chondrocyte metabolism in agarose constructs subjected to dynamic compression. Arch Biochem Biophys 2003;417:105-111.
86. Saris DB, Mukherjee N, Berglund LJ, Schultz FM, An KN, O'Driscoll SW. Dynamic pressure transmission through agarose gels. Tissue Eng 2000;6:531-537.
87. Hung CT, Mauck RL, Wang CC, Lima EG, Ateshian GA. A paradigm for

functional tissue engineering of articular cartilage via applied physiologic deformational loading. Ann Biomed Eng 2004;32:35-49.

88. Mauck RL, Seyhan SL, Ateshian GA, Hung CT. Influence of seeding density and dynamic deformational loading on the developing structure/function relationships of chondrocyte-seeded agarose hydrogels. Ann Biomed Eng 2002;30:1046-1056.
89. Lee DA, Bader DL. Compressive strains at physiological frequencies influence the metabolism of chondrocytes seeded in agarose. J Orthop Res 1997;15:181-188.
90. Roberts DAF, *Chitin chemistry* (The Macmillan Press, Hong Kong, 1992), pp. 1-6.
91. Itoh M, Izumi S, Uemura M, Baba N, Suyama K, Kuga Y, Mizuno A, Nakane PK, Koji T. Prevention of death of axotomized hypoglossal neurones and promotion of regeneration by chitin grafting. Cell Mol Neurobiol 2000;20:529-540.
92. Abe M, Takahashi M, Tokura S, Tamura H, Nagano A. Cartilage-scaffold composites produced by bioresorbable beta-chitin sponge with cultured rabbit chondrocytes. Tissue Eng 2004;10:585-594.
93. Ge Z, Baguenard S, Lim LY, Wee A, Khor E. Hydroxyapatite-chitin materials as potential tissue engineered bone substitutes. Biomaterials 2004;25:1049-1058.
94. Mi FL, Shyu SS, Lin YM, Wu YB, Peng CK, Tsai YH. Chitin/PLGA blend microspheres as a biodegradable drug delivery system: a new delivery system for protein. Biomaterials 2003;24:5023-5036.
95. Paluch D, Szosland L, Staniszewska-Kus J, Solski L, Szymonowicz M, Gebarowska E. The biological assessment of the chitin fibres. Polim Med 2000;30:3-31.
96. Nakajima M, Atsumi K, Kifune K, Miura K, Kanamaru H. Chitin is an

effective material for sutures. Jpn J Surg 1986;16:418-424.

97. Tachibana M, Yaita A, Taniura H, Fukasawa K, Nagasue N, Nakamura T. The use of chitin as a new absorbable suture material--an experimental study. Jpn J Surg 1988;18:533-539.
98. Sato M, Maeda M, Kurosawa H, Inoue Y, Yamauchi Y, Iwase H. Reconstruction of rabbit Achilles tendon with three bioabsorbable materials: histological and biomechanical studies. J Orthop Sci 2000;5:256-267.
99. Wang L, Khor E, Wee A, Lim LY. Chitosan-alginate PEC membrane as a wound dressing: Assessment of incisional wound healing. J Biomed Mater Res 2002;63:610-618.
100. Shu XZ, Zhu KJ, Song W. Novel pH-sensitive citrate cross-linked chitosan film for drug controlled release. Int J Pharm 2001;212:19-28.
101. Singla AK, Chawla M. Chitosan: some pharmaceutical and biological aspects--an update. J Pharm Pharmacol 2001;53:1047-1067.
102. Vila A, Sanchez A, Tobio M, Calvo P, Alonso MJ. Design of biodegradable particles for protein delivery. J Control Release 2002;78:15-24.
103. Itoh S, Yamaguchi I, Suzuki M, Ichinose S, Takakuda K, Kobayashi H, Shinomiya K, Tanaka J. Hydroxyapatite-coated tendon chitosan tubes with adsorbed laminin peptides facilitate nerve regeneration in vivo. Brain Res 2003;993:111-123.
104. Alini M, Roughley PJ, Antoniou J, Stoll T, Aebi M. A biological approach to treating disc degeneration: not for today, but maybe for tomorrow. Eur Spine J 2002;11 Suppl 2:S215-S220.
105. Wang X, Ma J, Wang Y, He B. Structural characterization of phosphorylated

chitosan and their applications as effective additives of calcium phosphate cements. Biomaterials 2001;22:2247-2255.

106. Subramanian A, Lin HY, Vu D, Larsen G. Synthesis and evaluation of scaffolds prepared from chitosan fibers for potential use in cartilage tissue engineering. Biomed Sci Instrum 2004;40:117-122.

107. Iwasaki N, Yamane ST, Majima T, Kasahara Y, Minami A, Harada K, Nonaka S, Maekawa N, Tamura H, Tokura S, Shiono M, Monde K, Nishimura S. Feasibility of polysaccharide hybrid materials for scaffolds in cartilage tissue engineering: evaluation of chondrocyte adhesion to polyion complex fibers prepared from alginate and chitosan. Biomacromolecules 2004;5:828-833.

108. Elder SH, Nettles DL, Bumgardner JD. Synthesis and characterization of chitosan scaffolds for cartilage-tissue engineering. Methods Mol Biol 2004;238:41-48.

109. Liu H, Mao J, Yao K, Yang G, Cui L, Cao Y. A study on a chitosan-gelatin-hyaluronic acid scaffold as artificial skin in vitro and its tissue engineering applications. J Biomater Sci Polym Ed 2004;15:25-40.

110. Qin Y. A comparison of alginate and chitosan fibres. Med Device Technol 2004;15:34-37.

111. Mercier NR, Costantino HR, Tracy MA, Bonassar LJ. A novel injectable approach for cartilage formation in vivo using PLG microspheres. Ann Biomed Eng 2004;32:418-429.

112. Nettles DL, Vail TP, Morgan MT, Grinstaff MW, Setton LA. Photocrosslinkable hyaluronan as a scaffold for articular cartilage repair. Ann Biomed Eng 2004;32:391-397.

113. Solchaga LA, Gao J, Dennis JE, Awadallah A, Lundberg M, Caplan AI, Goldberg VM. Treatment of osteochondral defects with autologous bone marrow in a hyaluronan-based delivery vehicle. Tissue Eng 2002;8:333-347.

114. Radice M, Brun P, Cortivo R, Scapinelli R, Battaliard C, Abatangelo G. Hyaluronan-based biopolymers as delivery vehicles for bone-marrow-derived mesenchymal progenitors. J Biomed Mater Res 2000;50:101-109.

115. Widmer MS, Mikos AG. Fabrication of biodegradable polymer scaffolds for tissue engineering; In: Patrick CW, Mikos AG, Mcintire LV, Eds. Frontiers in tissue engineering, Pergamon, New York, 1998, vol 2, pp. 107-120.

116. Engelberg I, Kohn J. Physico-mechanical properties of degradable polymers used in medical applications: a comparative study. Biomaterials 1991;12:292-304.

117. Miller RA, Brady JM, Cutright DE. Degradation rates of oral resorbable implants (polylactates and polyglycolates): rate modification with changes in PLA/PGA copolymer ratios. J Biomed Mater Res 1977;11:711-719.

118. Chu CC. An in-vitro study of the effect of buffer on the degradation of poly(glycolic acid) sutures. J Biomed Mater Res 1981;15:19-27.

119. Freed LE, Vunjak-Novakovic G, Biron RJ, Eagles DB, Lesnoy DC, Barlow SK, Langer R. Biodegradable polymer scaffolds for tissue engineering. Biotechnology (N Y) 1994;12:689-693.

120. Saldanha V, Grande DA. Extracellular matrix protein gene expression of bovine chondrocytes cultured on resorbable scaffolds. Biomaterials 2000;21:2427-2431.

121. Mooney DJ, Mazzoni CL, Breuer C, McNamara K, Hern D, Vacanti JP, Langer R. Stabilized polyglycolic acid fibre-based tubes for tissue engineering.

Biomaterials 1996;17:115-124.

122. Sittinger M, Reitzel D, Dauner M, Hierlemann H, Hammer C, Kastenbauer E, Planck H, Burmester GR, Bujia J. Resorbable polyesters in cartilage engineering: affinity and biocompatibility of polymer fiber structures to chondrocytes. J Biomed Mater Res 1996;33:57-63.

123. Chu CR, Coutts RD, Yoshioka M, Harwood FL, Monosov AZ, amiel D. Articular cartilage repair using allogeneic perichondrocyte-seeded biodegradable porous polylactic acid (PLA): a tissue-engineering study. J Biomed Mater Res 1995;29:1147-1154.

124. El-Amin SF, Attawia M, Lu HH, Shah AK, Chang R, Hickok NJ, Tuan RS, Laurencin CT. Integrin expression by human osteoblasts cultured on degradable polymeric materials applicable for tissue engineered bone. J Orthop Res 2002;20:20-28.

125. Parker JA, Brunner G, Walboomers XF, Von den Hoff JW, Maltha JC, Jansen JA. Release of bioactive transforming growth factor beta(3) from microtextured polymer surfaces in vitro and in vivo. Tissue Eng 2002;8:853-861.

126. Laitinen O, Tormala P, Taurio R, Skutnabb K, Saarelainen K, Iivonen T, Vainionpaa S. Mechanical properties of biodegradable ligament augmentation device of poly(L-lactide) in vitro and in vivo. Biomaterials 1992;13:1012-1016.

127. Cui YL, Hou X, Qi AD, Wang XH, Wang H, Cai KY, Ji YY, De YK. Biomimetic surface modification of poly (L-lactic acid) with gelatin and its effects on articular chondrocytes in vitro. J Biomed Mater Res 2003;66A:770-778.

128. Dunn MG, Tria AJ, Kato P, Bechler JR, Ochner RS, Zawadsky JP, Silver FH.

Anterior cruciate Ligament reconstruction using a composite collagenous prosthesis. Am J Sport Med 1992;20:507-515.

129. Sinha VR, Bansal K, Kaushik R, Kumria R, Trehan A. Poly-epsilon-caprolactone microspheres and nanospheres: an overview. Int J Pharm 2004;278:1-23.
130. Cao T, Ho KH, Teoh SH. Scaffold design and in vitro study of osteochondral coculture in a three-dimensional porous polycaprolactone scaffold fabricated by fused deposition modeling. Tissue Eng 2003;9 Suppl 1:S103-S112.
131. Huang Q, Goh JC, Hutmacher DW, Lee EH. In vivo mesenchymal cell recruitment by a scaffold loaded with transforming growth factor beta1 and the potential for in situ chondrogenesis. Tissue Eng 2002;8:469-482.
132. Shin M, Yoshimoto H, Vacanti JP. In vivo bone tissue engineering using mesenchymal stem cells on a novel electrospun nanofibrous scaffold. Tissue Eng 2004;10:33-41.
133. Kikuchi M, Koyama Y, Yamada T, Imamura Y, Okada T, Shirahama N, Akita K, Takakuda K, Tanaka J. Development of guided bone regeneration membrane composed of tricalcium phosphate and poly (l-lactide-co-glycolide-co -caprolactone) composites. Biomaterials 2004;25:5979-5986.
134. Barber FA, Click JN. The effect of inflammatory synovial fluid on the breaking strength of new "long lasting" absorbable sutures. Arthroscopy 1992;8:437-441.
135. Gisselfalt K, Edberg B, Flodin P. Synthesis and properties of degradable poly(urethane urea)s to be used for ligament reconstructions. Biomacromolecules 2002;3:951-958.
136. Eglin D, Ali SA, Perry CC. Comparative study of the in vitro apatite-forming

ability of poly(epsilon-caprolactone)-silica sol-gels using three osteoconductivity tests (static, dynamic, and alternate soaking process). J Biomed Mater Res 2004;69A:718-727.

137. Kim HW, Knowles JC, Kim HE. Hydroxyapatite/poly(epsilon-caprolactone) composite coatings on hydroxyapatite porous bone scaffold for drug delivery. Biomaterials 2004;25:1279-1287.
138. Liu H, Yin Y, Yao K, Ma D, Cui L, Cao Y. Influence of the concentrations of hyaluronic acid on the properties and biocompatibility of Cs-Gel-HA membranes. Biomaterials 2004;25:3523-3530.
139. Mao JS, Liu HF, Yin YJ, Yao KD. The properties of chitosan-gelatin membranes and scaffolds modified with hyaluronic acid by different methods. Biomaterials 2003;24:1621-1629.
140. Cai K, Yao K, Lin S, Yang Z, Li X, Xie H, Qing T, Gao L. Poly(D,L-lactic acid) surfaces modified by silk fibroin: effects on the culture of osteoblast in vitro. Biomaterials 2002;23:1153-1160.
141. Park JB, Lakes RS, *Biomaterials: An introduction* (Plenum, New York, ed. 2, 1992), pp. 1-6.
142. Dee KC, Puleo DA, Bigirs R, *In introduction to tissue-biomaterial interactions* (Wiley, New Jersy, 2002), p. 174.
143. Lamba NMK, Baumgartner JA, Cooper SL. Cell-synthetic surface interactions; In: Patrick CW, Mikos AG, Mcintire LV, Eds. Frontiers in tissue engineering, Pergamon, New York, 1998, vol 2.6, pp. 121-137.
144. Mosher DF. Adhesive proteins and their cellular receptors. Cardiovascular

Pathology 1993;2:149s-155s.

145. Bongrand P. Intermolecular forces; In: Bongrand P, Ed. Physical basis of cell-cell adhesion, CRC press, Boca Raton, 1988, vol, pp. 1-37.
146. Hynes RO. Integrins: a family of cell surface receptors. Cell 1987;48:549-554.
147. Hautanen A, Gailit J, Mann DM, Ruoslahti E. Effects of modifications of the RGD sequence and its context on recognition by the fibronectin receptor. J Biol Chem 1989;264:1437-1442.
148. Massia SP, Hubbell JA. covalently attached GRGD on polymer surfaces promotes biospecific adhesion of mammalian cells.; In: Goldstein D, DiBiasio D, Pedersen H, Eds. Annals of the New YorkAcademy of Science, New York, 1900, vol, pp. 261-270.
149. Park KD, Mosher DF, Cooper SL. Acute surface-induced thrombosis inthe canine ex vivo model:importance ofprotein concentration of the initial monolayer and platelet activation. J Biomed Mater Res 1986;20:589-612.
150. Domotor E, Sipos I, Kittel A, Abbott NJ, dam-Vizi V. Improved growth of cultured brain microvascular endothelial cells on glass coated with a biological matrix. Neurochem Int 1998;33:473-478.
151. Zhang M, James SP, King R, Beauregard G. Surface modification of UHMWPE for use in total joint replacements. Biomed Sci Instrum 2004;40:13-17.
152. Pavesio A, Renier D, Cassinelli C, Morra M. Anti-adhesive surfaces through hyaluronan coatings. Med Device Technol 1997;8:20-27.
153. Arnold MP, Blankevoort L, ten Ham A, Verdonschot N, van Kampen A. Twist and its effect on ACL graft force. J Orthop Res 2004;22:963-969.

154. Cooper JA, Lu HH, Ko FK, Freeman JW, Laurencin CT. Fiber-based tissue-engineered scaffold for ligament replacement: design considerations and in vitro evaluation. Biomaterials 2005;26:1523-1532.

155. Barrett GR, Line Jr LL, Shelton WR, Manning JO, Phelps R. The Dacron ligament prosthesis in anterior cruciate ligament reconstruction. A four-year review. Am J Sports Med 1993;21:367-373.

156. Thomson RC, Shung AK, Yaszemski MJ, Mikos AG. Polymer Scaffold Processing; In: Lanza RP, Langer R, Vacanti JP, Eds. Principles of Tissue Engineering, Academic Press, San Diego, 2000, vol 21, pp. 251-261.

157. Wintermantel E, Mayer J, Blum J, Eckert K-L, Luscher P, Mathey M. Tissue engineering scaffolds using superstructures. Biomaterials 1996;17:83-91.

158. Scardino F. An Introduction to Textile Structures and their Behavior; In: Chou T-W, Ko FK, Eds. Textile structure composites, Elsevier, Amsterdam, 1989, vol 1, pp. 1-26.

159. Rowland JRJ, Tsukazaki S, Kikuchi T, Fujikawa K, Kearney J, Lomas R, Wood E, Seedhom BB. Radiofrequency-generated glow discharge treatment: potential benefits for polyester ligaments. Journal of Orthopaedic Science 2003;8:198-206.

160. Murray AW, Macnicol MF. 10-16 year results of Leeds-Keio anterior cruciate ligament reconstruction. The Knee 2004;11:9-14.

161. Cameron M, Fu FH. Prosthetic ligaments in ACL reconstruction. Bulletin on the Rheumatic Diseases 1994;43:4-6.

162. Kumar K, Maffulli N. The ligament augmentation device: An historical perspective. Arthroscopy 1999;15:422-432.

163. van Heerwaarden RJ, Stellinga D, Frudiger AJ. Effect of pretension in reconstructions of the anterior cruciate ligament with a Dacron prosthesis. A retrospective study. Knee Surgery, Sports Traumatology, Arthroscopy: Official Journal Of The ESSKA 1996;3:202-208.

164. Ouyang HW, Goh JC, Thambyah A, Teoh SH, Lee EH. Knitted poly-lactide-co-glycolide scaffold loaded with bone marrow stromal cells in repair and regeneration of rabbit Achilles tendon. Tissue Eng 2003;9:431-439.

165. Roolker W, Patt TW, van Dijk CN, Vegter M, Marti RK. The Gore-Tex prosthetic ligament as a salvage procedure in deficient knees. Knee Surgery, Sports Traumatology, Arthroscopy: Official Journal Of The ESSKA 2000;8:20-25.

166. Laurencin CT, Ambrosio AMA, Borden MD, Cooper Jr JA. Tissue engineering: orthopedic applications. Annu Rev Biomed Eng 1999;01:19-46.

167. Cooper JA, Lu HH, Ko FK, Freeman JW, Laurencin CT. Fiber-based tissue-engineered scaffold for ligament replacement: design considerations and in vitro evaluation. Biomaterials 2005;26:1523-1532.

168. Mikos AG, Bao Y, Cima LG, Ingber DE, Vacanti JP, Langer R. Preparation of poly(glycolic acid) bonded fiber structures for cell attachment and transplantation. J Biomed Mater Res 1993;27:183-189.

169. Lee CH, Shin HJ, Cho IH, Kang Y-M, Kim IA, Park K-D, Shin J-W. Nanofiber alignment and direction of mechanical strain affect the ECM production of human ACL fibroblast. Biomaterials 2005;26:1261-1270.

170. Barrett GR, Field LD. Comparison of patella tendon versus patella tendon/Kennedy ligament augmentation device for anterior cruciate ligament

reconstruction: study of results, morbidity, and complications. Arthroscopy 1993;9:624-632.

171. Amiel D, Frank C, Harwood F, Fronek J, Akeson W. Tendons and ligaments: a morphological and biochemical comparison. J Orthop Res 1984;1:257-265.

172. Amiel D, Billings E, Aksson WH. Ligament structure, chemistry, and physiology; In: Daniel D, Akeson W, O'connor J, Eds. Knee ligaments: structure, function, unjury, and repair, Raven press, New York, 1990, vol 5, pp. 77-91.

173. Nakamura N, Hart DA, Boorman RS, Kaneda Y, Shrive NG, Marchuk LL, Shino K, Ochi T, Frank CB. Decorin antisense gene therapy improves functional healing of early rabbit ligament scar with enhanced collagen fibrillogenesis in vivo. J Orthop Res 2000;18:517-523.

174. Frank C, Shrive N, Hiraoka H, Nakamura N, Kaneda Y, Hart D. Optimisation of the biology of soft tissue repair. J Sci Med Sport 1999;2:190-210.

175. Shimomura T, Jia F, Niyibizi C, Woo SL. Antisense oligonucleotides reduce synthesis of procollagen alpha1 (V) chain in human patellar tendon fibroblasts: potential application in healing ligaments and tendons. Connect Tissue Res 2003;44:167-172.

176. Chvapil M, Speer DP, Holubec H, Chvapil TA, King DH. Collagen fibers as a temporary scaffold for replacement of ACL in goats. J Biomed Mater Res 1993;27:313-325.

177. Laitinen O, Alitalo I, Toivonen T, Vasenius J, Tormala P, Vainionpaa S. Tissue response to a braided poly-L-lactide implant in an experimental reconstruction of anterior cruciate ligament. J Mater Sci Mater Med 1993;4:547-554.

178. Goh JC, Ouyang HW, Teoh SH, Chan CK, Lee EH. Tissue-engineering approach to the repair and regeneration of tendons and ligaments. Tissue Eng 2003;9 Suppl 1:S31-S44.

179. Vunjak-Novakovic G, Obradovic B, Martin I, Freed LE. Bioreactor studies of native and tissue engineered cartilage. Biorheology 2002;39:259-268.

180. Goulet F, Rancourt R, Cloutier R. Tendon and ligaments; In: Lanza R, Langer R, Chick W, Eds. Principles of tissue engineering, Academic Press, San Diego, 2000, vol 50, pp. 711-723.

181. Toyoda T, Matsumoto H, Fujikawa K, Saito S, Inoue K. Tensile load and the metabolism of anterior cruciate ligament cells. Clin Orthop 1998;353:247-255.

182. Carrier RL, Papadaki M, Rupnick M, Schoen FJ, Bursac N, Langer R, Freed LE, Vunjak-Novakovic G. Cardiac tissue engineering: cell seeding, cultivation parameters, and tissue construct characterization. Biotechnol Bioeng 1999;64:580-589.

183. Carrier RL, Rupnick M, Langer R, Schoen FJ, Freed LE, Vunjak-Novakovic G. Effects of oxygen on engineered cardiac muscle. Biotechnol Bioeng 2002;78:617-625.

184. Obradovic B, Carrier RL, Vunjak-Novakovic G, Freed LE. Gas exchange is essential for bioreactor cultivation of tissue engineered cartilage. Biotechnol Bioeng 1999;63:197-205.

185. Fermor B, Urban J, Murray D, Pocock A, Lim E, Francis M, Gage J. Proliferation and collagen synthesis of human anterior cruciate ligament cells in vitro: effects of ascorbate-2-phosphate, dexamethasone and oxygen tension. Cell Biol Int

1998;22:635-640.

186. Tseng SC, Lee PC, Ells PF, Bissell DM, Smuckler EA, Stern R. Collagen production by rat hepatocytes and sinusoidal cells in primary monolayer culture. Hepatology 1982;2:13-18.

187. Vogel Z, Daniels MP, Chen T, Xi ZY, Bachar E, Ben-David L, Rosenberg N, Krause M, Duksin D, Kalcheim C. Ascorbate-like factor from embryonic brain. Role in collagen formation, basement membrane deposition, and acetylcholine receptor aggregation by muscle cells. Ann N Y Acad Sci 1987;498:13-27.

188. Lee SJ. Cytokine delivery and tissue engineering. Yonsei Med J 2000;41:704-719.

189. Spindler KP, Imro AK, Mayes CE, Davidson JM. Patellar tendon and anterior cruciate ligament have different mitogenic responses to platelet-derived growth factor and transforming growth factor beta. J Orthop Res 1996;14:542-546.

190. Attisano L, Wrana JL. Signal transduction by the TGF-beta superfamily. Science 2002;296:1646-1647.

191. Blakesley VA, Scrimgeour A, Esposito D, Le RD. Signaling via the insulin-like growth factor-I receptor: does it differ from insulin receptor signaling? Cytokine Growth Factor Rev 1996;7:153-159.

192. Deie M, Marui T, Allen CR, Hildebrand KA, Georgescu HI, Niyibizi C, Woo SL. The effects of age on rabbit MCL fibroblast matrix synthesis in response to TGF-beta 1 or EGF. Mech Ageing Dev 1997;97:121-130.

193. Lo IK, Marchuk L, Hart DA, Frank CB. Messenger ribonucleic acid levels in disrupted human anterior cruciate ligaments. Clin Orthop 2003249-258.

194. Marui T, Niyibizi C, Georgescu HI, Cao M, Kavalkovich KW, Levine RE,

Woo SL. Effect of growth factors on matrix synthesis by ligament fibroblasts. J Orthop Res 1997;15:18-23.

195. Ross SM, Joshi R, Frank CB. Establishment and comparison of fibroblast cell lines from the medial collateral and anterior cruciate ligaments of the rabbit. In Vitro Cell Dev Biol 1990;26:579-584.

196. Sakai T, Yasuda K, Tohyama H, Azuma H, Nagumo A, Majima T, Frank CB. Effects of combined administration of transforming growth factor-beta1 and epidermal growth factor on properties of the in situ frozen anterior cruciate ligament in rabbits. J Orthop Res 2002;20:1345-1351.

197. Jin HJ, Chen J, Karageorgiou V, Altman GH, Kaplan DL. Human bone marrow stromal cell responses on electrospun silk fibroin mats. Biomaterials 2004;25:1039-1047.

198. Scherping SC, Jr., Schmidt CC, Georgescu HI, Kwoh CK, Evans CH, Woo SL. Effect of growth factors on the proliferation of ligament fibroblasts from skeletally mature rabbits. Connect Tissue Res 1997;36:1-8.

199. Hildebrand KA, Woo SL, Smith DW, Allen CR, Deie M, Taylor BJ, Schmidt CC. The effects of platelet-derived growth factor-BB on healing of the rabbit medial collateral ligament. An in vivo study. Am J Sports Med 1998;26:549-554.

200. Letson AK, Dahners LE. The effect of combinations of growth factors on ligament healing. Clin Orthop 1994207-212.

201. Forslund C, Aspenberg P. Tendon healing stimulated by injected CDMP-2. Med Sci Sports Exerc 2001;33:685-687.

202. Aspenberg P, Forslund C. Enhanced tendon healing with GDF 5 and 6. Acta

Orthop Scand 1999;70:51-54.

203. Fu SC, Wong YP, Chan BP, Pau HM, Cheuk YC, Lee KM, Chan KM. The roles of bone morphogenetic protein (BMP) 12 in stimulating the proliferation and matrix production of human patellar tendon fibroblasts. Life Sci 2003;72:2965-2974.

204. Lou J, Tu Y, Burns M, Silva MJ, Manske P. BMP-12 gene transfer augmentation of lacerated tendon repair. J Orthop Res 2001;19:1199-1202.

205. Lo H, Kadiyala S, Guggino SE, Leong KW. Poly(L-lactic acid) foams with cell seeding and controlled-release capacity. J Biomed Mater Res 1996;30:475-484.

206. Whang K, Tsai DC, Nam EK, Aitken M, Sprague SM, Patel PK, Healy KE. Ectopic bone formation via rhBMP-2 delivery from porous bioabsorbable polymer scaffolds. J Biomed Mater Res 1998;42:491-499.

207. Tabata Y, Nagano A, Ikada Y. Biodegradation of hydrogel carrier incorporating fibroblast growth factor. Tissue Eng 1999;5:127-138.

208. Salyapongse AN, Billiar TR, Edington H. Gene therapy and tissue engineering. Clin Plast Surg 1999;26:663-76, x.

209. Orlans FB. Animal rights and animal welfare. Hastings Cent Rep 1979;9:45

210. An HY. Methods of evaluation in orthopaedic animal research; In: An HY, Friedman RJ, Eds. Animal models in orthopaedic research, CRC press, New York, 1999, vol, pp. 3-14.

211. An HY, Friedman RJ. Animal selectins in orthopaedic research; In: An HY, Friedman RJ, Eds. Animal models in orthopaedic research, CRC press, New York, 1999, vol 3, pp. 39-58.

212. Jackson DW, Grood ES, Arnoczky SP, Butler DL, Simon TM. Cruciate reconstruction using freeze dried anterior cruciate ligament allograft and a ligament augmentation device (LAD). An experimental study in a goat model. Am J Sports Med 1987;15:528-538.

213. Jackson DW, Grood ES, Arnoczky SP, Butler DL, Simon TM. Freeze dried anterior cruciate ligament allografts. Preliminary studies in a goat model. Am J Sports Med 1987;15:295-303.

214. Kobayashi K, Healey RM, Sah RL, Clark JJ, Tu BP, Gooner WH, Aheson WH, Moriya H, Amiel D. Novel Method for the Quantitative Assessment of Cell Migration: A Study on the Motility of Rabbit Anterior Cruciate (ACL) and Medial Collateral Ligament (MCL) Cells. Tissue Eng, 2000;6:29-39.

215. Nagineni CN, amiel D, Green MH, Berchuck M, Akeson WH. Characterization of the Intrinsic Properties of the Anterior Cruciate and Medical Collateral Ligament Cells: An In Vitro Cell Culture Study. J Orthop Res 1992;10:465-475.

216. Freshney RI. Quantitation; In:Culture of Animal Cells. A manual of basic technique., Wiley-Liss, New Jersy, 2005, vol 21, pp. 345-347.

217. Salacinski HJ, Goldner S, Giudiceandrea A, Hamilton G, Seifalian AM, Edwards A, Carson RJ. The mechanical behavior of vascular grafts: a review. J Biomater Appl 2001;15:241-278.

218. Hunt TK. The physiology of wound healing. Ann Emerg Med 1988;17:1265-1273.

219. Nakahara H, Goldberg VM, Caplan AI. Culture-expanded human periosteal-derived cells exhibit osteochondral potentials in vivo. J Orthop Res 1991;9:465-476.

220. Nathanson MA, Hay ED. Analysis of cartilage differentiation from skeletal muscle grown on bone matrix II. Chondroitin sulfate synthesis and reaction to exogenous glycosaminoglycans. Dev Biol 1980;78:332-351.

221. Zuk PA, Zhu M, Mizuno H, Huang J, Futrell JW, Katz AJ, Benhaim P, Lorenz HP, Hedrick MH. Multilineage cells from human adipose tissue: implications for cell-based therapies. Tissue Engineering 2001;7:211-228.

222. Joyner CJ, Bennett A, Triffitt JTI. Identification and enrichment of human osteoprogenitor by differentiation stage-specific monoclonal antibody. Bone 1997;21:1-6.

223. Haynesworth SE, Goshima J, Goldberg VM, Caplan AI. Characterization of cells with osteogenic potential from human marrow. Bone 1992;13:81-90.

224. Ouyang HW, Goh JC, Lee EH. Use of bone marrow stromal cells for tendon graft-to-bone healing: histological and immunohistochemical studies in a rabbit model. Am J Sports Med 2004;32:321-327.

225. Solchaga LA, Johnstone B, Yoo JU, Goldberg VM, Caplan AI. High variability in rabbit bone marrow-derived mesenchymal cell preparations. Cell transplantation 1999;8:511-519.

226. Neurath MF, Printz H, Stofft E. Cellular ultrastructure of the ruptured anterior cruciate ligament. Acta Orthop scand 1994;65:71-76.

227. Franc C, Woo SLY, Amiel D, Harwood F, Gomez M, Akeson W. Medial collateral ligament healing: a multidisciplinary assessment in rabbits. Am J Sports Med 1983;11:379-389.

228. Woo SL, Inoue M, McGuire-Burleson E, Gomez MA. Treatment of medical

collateral ligament injury. II, Structure and function of canine knees in response to differing treatment regimens. Am J Sports Med 1987;15:22-29.

229. Alberts B *et al.* Cell junctions, cell adhesion, and the extracellular matrix; In:Molecular Biology of the Cell, Garland Science, USA, 2002, vol, pp. 1090-1104.

230. Cabral WA, Mertts MV, Makareeva E, Colige A, Tekin M, Pandya A, Leikin S, Marini JC. Type I collagen Triplet Duplication Mutation in Lethal Osteogenesis Imperfecta Shifts Register of a Chain thoroughout the Helox and Disrupts Incorporation of Mutant Helices into Fibrils and Extracellular Matrix. J Biol Chem 2003;278:10006-10012.

231. Knuutinen A, Kokkonen N, Risteli J, Vähäkangas K, Kallioinen M, Salo T, Oikarinen A. Smoking affects collagen synthesis and extracellular matrix turnover in human skin. Bri J Derm 2002;146:588-594.

232. Oikarinen A, Untio P, Kiistala U, Risteli L, Risteli J. A new method to measure type I and III collagen synthesis in human skin in vivo: Demonstratin of decreased collagen synthesis after topical glucocorticoid treatment. J Invest Dermatol 1992;98:220-225.

233. Krampera M, Glennie S, Dyson J, Scott D, Laylor R, Simpson E, Dazzi F. Bone marrow mesenchymal stem cells inhibit the response of naive and memory antigen-specific T cells to their cognate peptide. Blood 2003;101:3722-3729.

234. Jackson DW, Simon TM. Donor cell survival and repopulation after intraarticular transplantation of tendon and ligament allografts. Microscopy research and technique 2002;58:25-33.

235. Watanabe N, Takai S, Morita N, Kawata M, Hirasawa Y. A method of tracking donor cells after simulated autologous transplantation: a study using synovial cells of transgenic rats. Cell Tissue Res 1999;298:519-525.

236. Bellincampi LD, Closkey RF, Prasad R, Zawadsky JP, Dunn MG. Viability of fibroblast-seeded ligament analogs after autogenous implantation. J Ortho Res 1998;16:414-420.

237. Huiskey R, Blankevoort L. Anatomy and Biomechanics of the Anterior Cruciate Ligament: A Three-Dimensional Problem; In: Jakob RP, Staubli HU, Eds. The Knee and the cruciate ligaments : anatomy, biomechanics, clinical aspects, reconstruction, complications, rehabilitation, Springer-Verlag, Berlin, 1992, vol, pp. 92-110.

238. Hunziker EB. Structural molecules in articular cartilage, tendons, and ligaments; In: Jakob RP, Staubli HU, Eds. The Knee and the cruciate ligaments : anatomy, biomechanics, clinical aspects, reconstruction, complications, rehabilitation, Springer-Verlag, New York, 1992, vol, pp. 62-77.

239. McCulloch CAG, Melcher AH. Cell density and cell generation in the periodontal ligament of mice. Am J Anat 1983;167:43-48.

240. Arora PD, McCulloch CAG. Dependence of collagen remodeling on a-smooth muscle actin expression by fibroblasts. J Cell Physio 1994;159:161-175.

241. Faryniarz DA, Chaponnier C, Gabbiani G, Yannas IV, Spector M. Myofibroblasts in the healing lapine medial collateral ligament: possible mechanisms of contraction. J Ortho Res 1996;14:228-237.

242. Murray MM, Spector M. Fibroblast distribution in the anteromedial bundle of

the human anterior cruciate ligament: the presence of a-smooth muscle actin-Positive cells. J Ortho Res 1999;17:18-27.

243. Cai D, Marty-Roix R, Hsu HP, Spector M. Lapine and canine bone marrow stromal cells contain smooth muscle actin and contract a collagen-glycosaminoglycan matrix. Tissue Eng 2001;7:829-841.

244. Peled A, Zipori D, Abramsky O. Expression of alpha-smooth muscle actin in murine bone marrow stromal cells. Blood 1991;78:304-312.

245. Bonanno E, Ercoli L, Missori P, Rocchi G, Spagnoli LG. Homogeneous stromal cell population from normal human adult bone marrow expressing alpha-smooth muscle actin filaments. Lab Invest 1994;71:308-315.

246. Galmiche MC, Koteliansky VE, Briere J, Herve P, Charbord P. Stromal cells from human long-term marrow cultures are mesenchymal cells that differentiate following a vascular smooth muscle differentiation pathway. Blood 1993;82:66-76.

247. Schakenraad IM. Cells: their surfaces an interactions with materials; In: Rather BD, Hoffman AS, Schoen FJ, Lemon JE, Eds. Biomaterials science: an introduction to materails in medicine, Academic Press, San diego, 1996, vol, pp. 141-142.

248. Ouyang HW, Goh J, Lee EH. Characterization of anterior cruciate ligament cells and bone marrow stromal cells on various biodegradable polymeric films. Mater Sci&Eng C 2002;20:63-69.

249. Kim BS, Mooney DJ. Development of biocompatible synthetic extracellular matrices for tissue engineering. TIBTECH Trends Biotechnl 1996;16:115-124.

250. Hasirci V. Biodegradable biomedical polymers: Review of degradation of and in vivo responses to polylactides and polyhydroxyalkanoates; In: Wise DC, Ed.

Biomaterials and bioengineering handbook, Marcel Dekker, New York, 2000, vol, pp. 141-155.

251. James MJ, Cleland LG, Rofe AM, Leslie AL. Intraarticular pressure and the relationship between synovial perfusion and metabolic demand. J Rheumatol 1990;17:521-527.

252. Vert M, Li S, Garreau H. More about the degradation of LA/GA-derived matrices in aqueous media. J Contr Rel 1991;16:15-26.

253. Widmer MS, Gupta PK, Lu L, Meszlenyi RK, Evans GR, Brandt K, Savel T, Gurlek A, Patrick CW, Jr., Mikos AG. Manufacture of porous biodegradable polymer conduits by an extrusion process for guided tissue regeneration. Biomaterials 1998;19:1945-1955.

254. Yuan X, Mak AFT, Yao K. Surface degradation of poly (L-lactic acid) fibres in a concentrated alkaline solution. Polymer degradation and stability 2003;79:45-52.

255. Perego G, Demenico G, Bastilio C. Effect of molecular weight and crystallinity on poly(lactic acid) mechanical properties. Journal of Applied Polymer Science 1996;59:37-43.

256. Greenwald SE, Berry CL. Improving vascular grafts: the importance of mechanical and haemodynamic properties. J Pathol 2000;190:292-299.

257. Shah JS, Jayson MI, Hampson WG. Low tension studies of collagen fibres from ligaments of the human spine. Ann Rheum Dis 1977;36:139-145.

258. Butler DL, Kay MD, Stouffer DC. Comparison of material properties in fascicle-bone units from human patellar tendon and knee ligaments. J Biomech 1986;19:425-432.

259. Noyes FR, DeLucas JL, Torvik PJ. Biomechanics of anterior cruciate ligament failure: an analysis of strain-rate sensitivity and mechanisms of failure in primates. J Bone Joint Surg Am 1974;56:236-253.

260. Noyes FR, Keller CS, Grood ES, Butler DL. Advances in the understanding of knee ligament injury, repair, and rehabilitation. Med Sci Sports Exerc 1984;16:427-443.

261. Noyes FR, Butler DL, Grood ES, Zernicke RF, Hefzy MS. Biomechanical analysis of human ligament grafts used in knee-ligament repairs and reconstructions. J Bone Joint Surg Am 1984;66:344-352.

262. Boorman RS, Thornton GM, Shrive NG, Frank CB. Ligament grafts become more susceptible to creep within days after surgery: evidence for early enzymatic degradation of a ligament graft in a rabbit model. Acta Orthop Scand 2002;73:568-574.

263. Donahue TLH, Gregersen C, Hull ML, Howell SM. Comparison of Viscoelastic, Structural, and Material Properties of Double-Looped Anterior Cruciate Ligament Grafts Made From Bovine Digital Extensor and Human Hamstring Tendons. Transactions of the ASME 2001;123:162-169.

264. Chapekar MS. Tissue engineering: challenges and opportunities. J Biomed Mater Res 2000;53:617-620.

265. EI-Badri NS, Wang BY, Good RA. Osteoblasts promote engraftment of allogeneic hematopoietic stem cells. Exp Hematol 1998;26:110-116.

266. Klyushnenkova E, Mosca JD, McIntosh KR. Human mesenchymal stem cells suppress allogeneic T cell responses in vitro: Implication for allogeniec

transplantation. Blood 1998;92:642a

267. Tria AJ, Alicea JA. Ligament and capsular structures; In: AJ T, Ed. Ligaments of the knee, Churchill Livingstone, New York, 1995, vol, p. 20.

268. Menovsky T, De Vries J, Van Den Bergh WM, Grotenhuis JA. Stability of fibrin sealant in cerebrospinal fluid: an in-vitro study. Neurosurgery 2002;51:1453-1456.

269. Ouyang HW, Goh JC, Thambyah A, Teoh SH, Lee EH. Knitted poly-lactide-co-glycolide scaffold loaded with bone marrow stromal cells in repair and regeneration of rabbit Achilles tendon. Tissue Eng 2003;9:431-439.

270. Cummings JF, Grood ES, Levy MS, Korvick DL, Wyatt R, Noyes FR. The effects of graft width and graft laxity on the outcome of caprine anterior cruciate ligament reconstruction. J Orthop Res 2002;20:338-345.

271. Dunn MG, Tria AJ, Kato YP, Bechler JR, Ochner RS, Zawadsky JP, Silver FH. Anterior cruciate ligament reconstruction using a composite collagenous prosthesis. A biomechanical and histologic study in rabbits. Am J Sports Med 1992;20:507-515.

272. Thomas NP, Turner IG, Jones CB. Prosthetic anterior cruciate ligaments in the rabbit. A comparison of four types of replacement. J Bone Joint Surg Br 1987;69:312-316.

273. Bos RR, Rozema FR, Boering G, Nijenhuis AJ, Pennings AJ, Verwey AB, Nieuwenhuis P, Jansen HW. Degradation of and tissue reaction to biodegradable poly(L-lactide) for use as internal fixation of fractures: a study in rats. Biomaterials 1991;12:32-36.

274. McPherson GK, Mendenhall HV, Gibbons DF, Plenk H, Rottmann W,

Sanford JB, Kennedy JC, Roth JH. Experimental mechanical and histologic evaluation of the Kennedy ligament augmentation device. Clin Orthop 1985186-195.

275. Turner IG, Thomas NP. Comparative analysis of four types of synthetic anterior cruciate ligament replacement in the goat: in vivo histological and mechanical findings. biomaterials 1990;11:321-329.

276. Aragona J, Parsons JR, Alexander H, Weiss AB. Soft tissue attachment of a filamentous carbon-absorbable polymer tendon and ligament replacement. Clin Orthop 1981268-278.

277. Benjamin M, Evans EJ, Copp L. The histology of tendon attachments to bone in man. J Anat 1986;149:89-100.

278. Shino K, Kawasaki T, Hirose H, Gotoh I, Inoue M, Ono K. Replacement of the anterior cruciate ligament by an allogeneic tendon graft. An experimental study in the dog. J Bone Joint Surg Br 1984;66:672-681.

279. Van EF, Saris DB, Riesle J, Willems WJ, Van Blitterswijk CA, Verbout AJ, Dhert WJ. Tissue engineering of ligaments: a comparison of bone marrow stromal cells, anterior cruciate ligament, and skin fibroblasts as cell source. Tissue Eng 2004;10:893-903.

280. Holden JP, Grood ES, Butler DL, Noyes FR, Mendenhall HV, Van Kampen CL, Neidich RL. Biomechanics of fascia lata ligament replacements: early postoperative changes in the goat. J Orthop Res 1988;6:639-647.

281. Suggs J, Wang C, Li G. The effect of graft stiffness on knee joint biomechanics after ACL reconstruction--a 3D computational simulation. Clin Biomech

(Bristol , Avon) 2003;18:35-43.

282. Bercovy M, Goutallier D, Voisin MC, Geiger D, Blanquaert D, Gaudichet A, Patte D. Carbon-PGLA prostheses for ligament reconstruction. Experimental basis and short-term results in man. Clin Orthop 1985159-168.

283. Molloy T, Wang Y, Murrell G. The roles of growth factors in tendon and ligament healing. Sports Med 2003;33:381-394.

284. Petersen W, Unterhauser F, Pufe T, Zantop T, Sudkamp NP, Weiler A. The angiogenic peptide vascular endothelial growth factor (VEGF) is expressed during the remodeling of free tendon grafts in sheep. Arch Orthop Trauma Surg 2003;123:168-174.

285. Niyibizi C, Kavalkovich K, Yamaji T, Woo SL. Type V collagen is increased during rabbit medial collateral ligament healing. Knee Surg Sports Traumatol Arthrosc 2000;8:281-285.

286. Mosher DF, Proctor RA. Binding and factor XIIIa-mediated cross-linking of a 27-kilodalton fragment of fibronectin to Staphylococcus aureus. Science 1980;209:927-929.

287. Mosher DF, Schad PE, Vann JM. Cross-linking of collagen and fibronectin by factor XIIIa. Localization of participating glutaminyl residues to a tryptic fragment of fibronectin. J Biol Chem 1980;255:1181-1188.

288. Mosher DF. Fibronectin. Prog Hemost Thromb 1980;5:111-151.

289. Musahl V, Burkart A, Debski RE, Van SA, Fu FH, Woo SL. Anterior cruciate ligament tunnel placement: Comparison of insertion site anatomy with the guidelines of a computer-assisted surgical system. Arthroscopy 2003;19:154-

160.

290. Li WJ, Laurencin CT, Caterson EJ, Tuan RS, Ko FK. Electrospun nanofibrous structure: a novel scaffold for tissue engineering. J Biomed Mater Res 2002;60:613-621.

6. Publications from current research

1. Zigang Ge, Lishan Wang, Eunice PS Tan, James CH Goh, Eng Hin Lee. Knitted Poly-L-lactic acid structures for potential ligament reconstruction. *J Biomaterials Science Polymer Edition, 16(9):1179-1192 (2005).*
2. Zigang Ge, James CH Goh, Eng Hin Lee. Selection of cell sources for ligament tissue engineering. *Cell tranplantation, 14(12):1247-1258 (2005).*
3. Zigang Ge, James CH Goh, Eng Hin Lee. The Effects of Bone Marrow-derived Mesenchymal Stem Cells and Fascia Wrap Application to Anterior Cruciate Ligament Tissue Engineering. *Cell transplantation (In Press).*
4. Zigang Ge, Fang Yang, James C. H. Goh, Seeram Ramakrishna, Eng Hin Lee. Biomaterials for ligament tissue engineering. *Journal of Biomedical Material Research (In Press).*

7. Conference papers

1. Ge Zigang, Goh Cho Hong, James, Lee Eng Hin. Characterization of mesenchymal stem cells, anterior cruciate ligament fibroblasts and medial collateral ligament fibroblasts. 5th Asia-Pacific Conference on Medical & Biological Engineering and 11th International Conference on Biomedical Engineering (4th - 7th December 2002, Singapore). Oral Presentation, p87.
2. GE Zigang, Goh J.C.H and E.H. Lee. Characterization of Cells for Use in Ligament Tissue Engineering. 2003 Summer Bioengineering Conference, Florida, USA.

3. Ge Zigang, Goh JCH and Lee EH. Selection of Cell Sources for Ligament Tissue Engineering. 7Th NUS-NUH Annual Scientific Meeting, Oct 2-4, 2003, Singapore.
4. Goh, JCH; Ge, ZG; Lee, EH. Bi-phasic composite scaffold for ligament tissue engineering, 13th International Conference on Mechanics in Medicine and Biology, Nov 12-15, 2003, Tainan, Taiwan.
5. Ge Zigang, Goh JCH and Lee EH. Poly-L-Lactic acid based tissue engineered anterior cruciate ligament. 1st International Conference of Epithelial Technology and Tissue Enginneering, 4th to 6th December 2003, Singapore.
6. Ge Zigang, Goh JCH and Lee EH. Selection of cell source for ligament tissue engineering. 1st International Conference of Epithelial Technology and Tissue Engineering, 4th to 6th December 2003, Singapore.
7. Ge Zigang, Goh JCH and Lee EH. Poly-L-Lactic Acid Based Tissue Engineered Anterior Cruciate Ligament. Sixth Annual TESI International Conference and Exposition, December 11-13, 2003, USA.
8. Ge Zigang, Goh JCH and Lee EH. Selection of Cell Sources for Ligament Tissue Engineering. Sixth Annual TESI International Conference and Exposition, December 11-13, 2003, USA
9. Goh, JCH; Ge, ZG; Lee, EH. Bi-phasic knitted polymeric scaffold for anterior cruciate ligament tissue engineering. 50th Annual Meeting of Orthopedic Research Society, San Francisco, March 7 - 10, 2004.
10. Ge Zigang, Goh JCH and Lee EH. 14th Triennial Congress of Aisa Pacific Orthopedic Association, Sep 05-10, 2004, Kuala Lumpur, Malaysia.

8. Invention Disclosure

James C.H. Goh, Zigang Ge, Siew Lok Toh. Composite scaffolds for ligament reconstruction. *(submitted to INTRO for patent application).*